TR - O -0061

40

Quasi-Optic Electrooptic Modulator on $LiNbo_3$

Elisabeth Penard

1993.7.23.

ATR光電波通信研究所

Just a few words to thank you very much all of you from the Optical and Radio Communications Laboratories. As you know this was my first time in Japan, and although communication was not always easy, I think we managed pretty well Thank you very much to Dr Habara for his always very kind encouragements, and to the very active Dr Furuhama, he always beats at tennis (6/0,6/0) but, honestly, who can beat him ? Thank you also to Dr E Ogawa always free for discussions. Should I be gratefull to H Ogawa, always very enthousiastic, who gave me this funny project, which almost sent me to psychiatric hospital when I was trying to line up a super tiny fiber with a super tiny optical waveguide? actually I enjoyed it, and I thank him very much. This is a very special thank you to K Matsui, he helped me lot dealing with experiments and communicating with other companies, without him I was lost.

Thank you also to professor Kitazawa from Ibaraki University for his assistance in theoretical calculations. I enjoyed working with the engineers from Sumitomo Cement, especielly Mr Sugamata and Mr Shimotsu , I was very impressed by their efficiency. And lastly I wish good luck to Imai san and all his team, to succeed in their project to build a millimeter wave fiber optic link.

1 INTRODUCTION

This research was conducted within the frame of the Millimeter wave fiber optic links project, now under development at the ATR Optical and Radio Communications laboratories. Optic fibers provide, due to the low transmission loss and the very high bandwith capacity, new facilities for routing high data rate information and for the development of wireless communications. The feasibility of such systems implies to master both the technology of optic fiber and millimeter wave, but moreover these new techniques will emerged if we are able to provide simple, and low cost transducers for converting a millimeter wave signal into an optical signal, and vice versa. Figure 1-a below shows a simplified architecture of an millimeter wave optical link. On the up link data are transfered on a fiber from the central station to the remote base station, the simplest system architecture requires to develop high frequency optical modulators, and also high frequency photodetectors. On the down link data are sent from the remote base station to the central station, the microwave signal received by the antenna modulates the optical sub-carrier, there are in that case two alternative the first one is to down convert and then directly modulate a laser diode , but then a mixer is needed in the base station which increases the cost and complexity of the receiver, the second one (Figure 1-b) is to use an external modulator for direct modulation of the optical subcarrier at millimeter wave frequency.

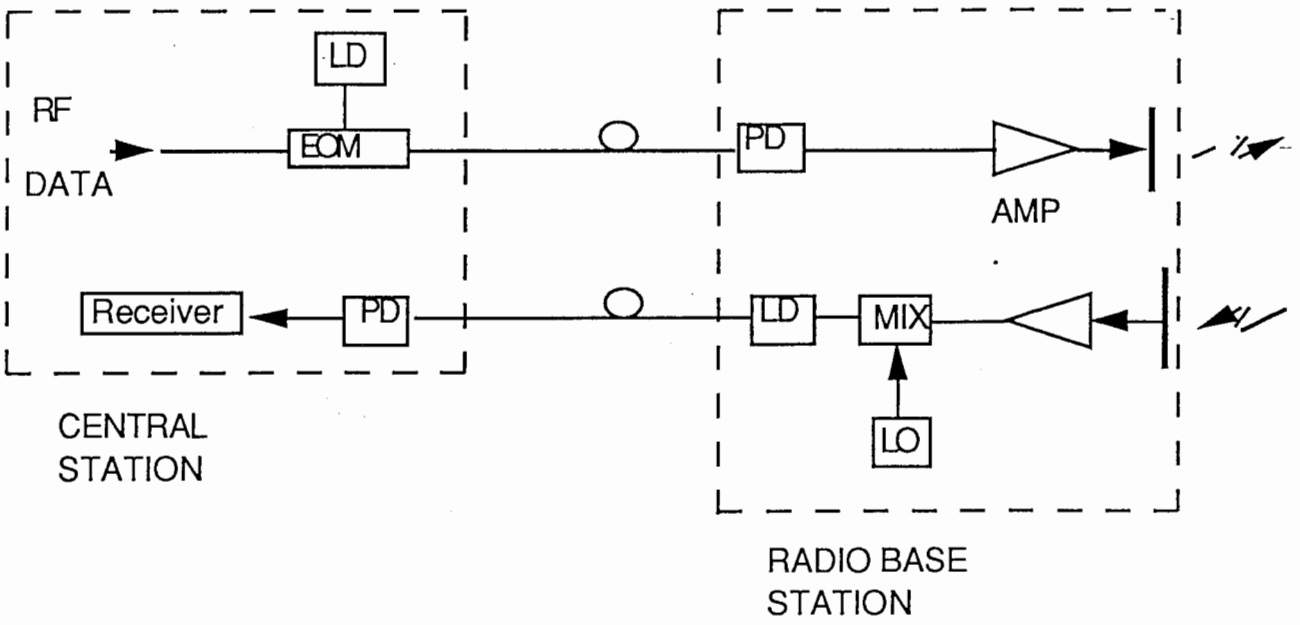

Figure 1 -a Basic Millimeter wave optical link

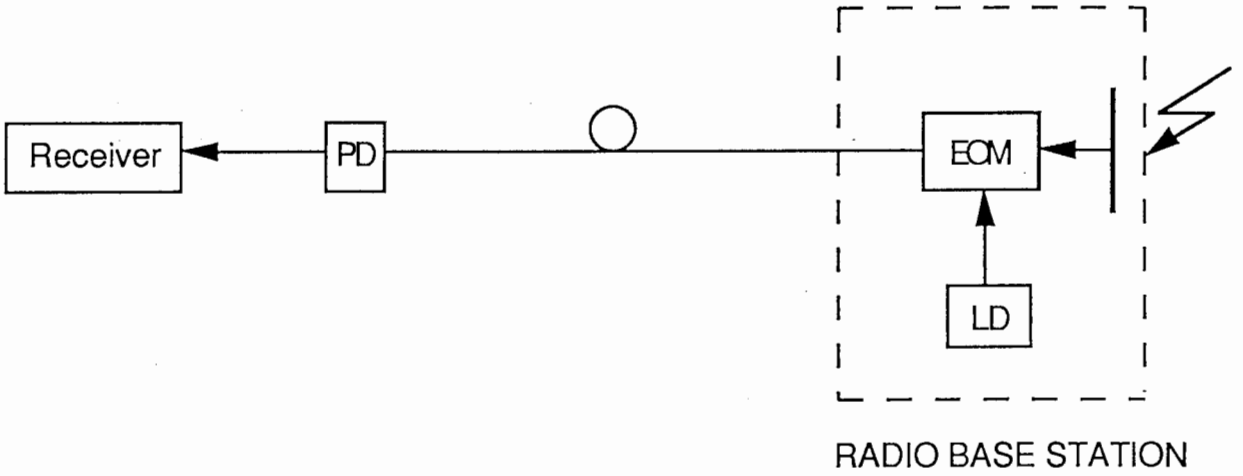

Figure 1- b Direct modulation at millimeter wave

D Polifko [7] and [8] have demonstrated that it is possible to design electro-optic modulator on LiNbO3 up to 40GHz. One step further in the simplification is to integrate the receiving antenna directly on

the same substrate as the modulator, as shown on figure 1-c. The incident electric field on the printed antenna directly couples to the optical wave guides and then it results a modulation of the optical subcarrier due to the electrooptic effect (Pockels effect) . This has been demonstrated for sensing applications [4], and also at 60GHz and 94GHz [9], but in that last case the signal feed to the modulator had to distribute the power from the end of a waveguide to the antenna. So far no experience of free space coupling at millimeter wave frequency has been reported.

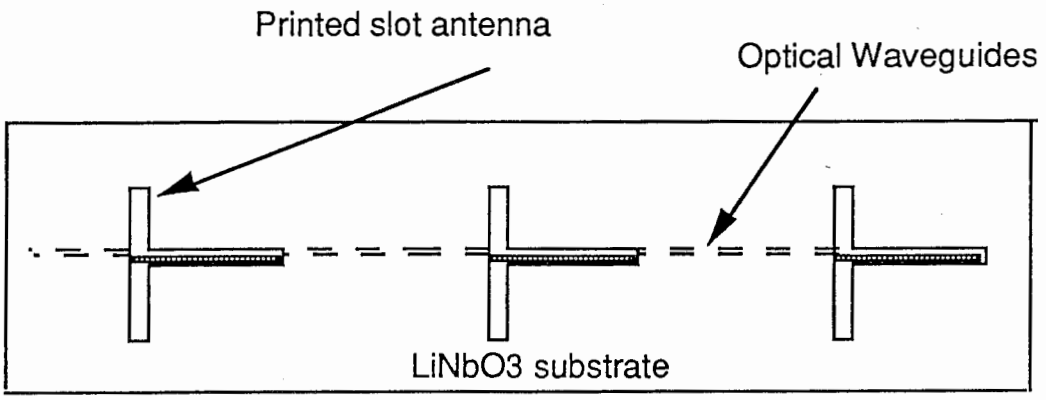

Figure 1-c Conceptual drawing of a quasi-optic modulator

The aim of our project was to design such quasi-optic modulator in order to check its feasibility.
This report covers 6 months work, this is very short for the total completion of the project, nevertheless we managed to design a quasi optic intensity modulators at 20GHz and 25GHz and do some first measurements.

The main problems to be considered were:

1) The design of printed antennas
LiNbO3 substrate has optical anisotropy, and has a very high dielectric constant, so the accurate design of printed antenna on such substrate is a major difficulty. We designed and measured radiation properties of some slot antennas on alumina. We also measured

impedances on the probe station of about 20 different type of slot antennas on LiNbO3.

2) The coupling of the incident electric field to the optical waveguides and then the design of the modulator electrodes.

Finally we designed 8 different modulators at 1.3µm.

2) ELECTROOPTIC MODULATOR ON LINBO3

1) Background

2-1 Electrooptic effect

To fabricate dielectric waveguides the refractive index of the guiding region must be higher than the index of the host substrate. For electrooptic crystal like LiNbO3 dielectric waveguides are made by diffusion of Ti.

At 1.3µm, the waveguide width is 6-7µm

The linear electrooptic effect provides a change in the refractive index proportional to an applied electric field. Voltage V applied to the electrodes placed alongside the waveguides creates an internal field
E/G where G is the electrodes gap. For an applied field along z axis (vertical axis) , the electrooptically induced index change for light polarized along z direction is (Figure 2-1) :

$$\Delta n_e = -n_e^3 \, r33 \, E_z / 2$$

where r33 is the electrooptic coefficient, n_e is the extraordinary index. For LiNbO3 : $n^3 \, r33 = 320 \, 10^{-12}$ m/v

So the induced index change can be expressed in function of the applied voltage:

$$\Delta n(V) = -n^3 r V \Gamma / G / 2$$

Γ is the overlap integral between the applied electric field and the optical field, it is a measure of the optic/electric coupling efficiency.

So to obtain high variation of the index, a large electrooptic coefficient is required, as well as a small spacing between the electrodes. For coplanar electrodes , the spacing is typically 25µm

The variation of the refractive index results in a phase shift which cumulates along the electrodes of length L.

The total phase shift is then:

$$\Delta\Phi = -2\pi \Delta n(v) L/\lambda = -\pi n^3 r \Gamma V L / G / \lambda$$

λ is the optical wavelength

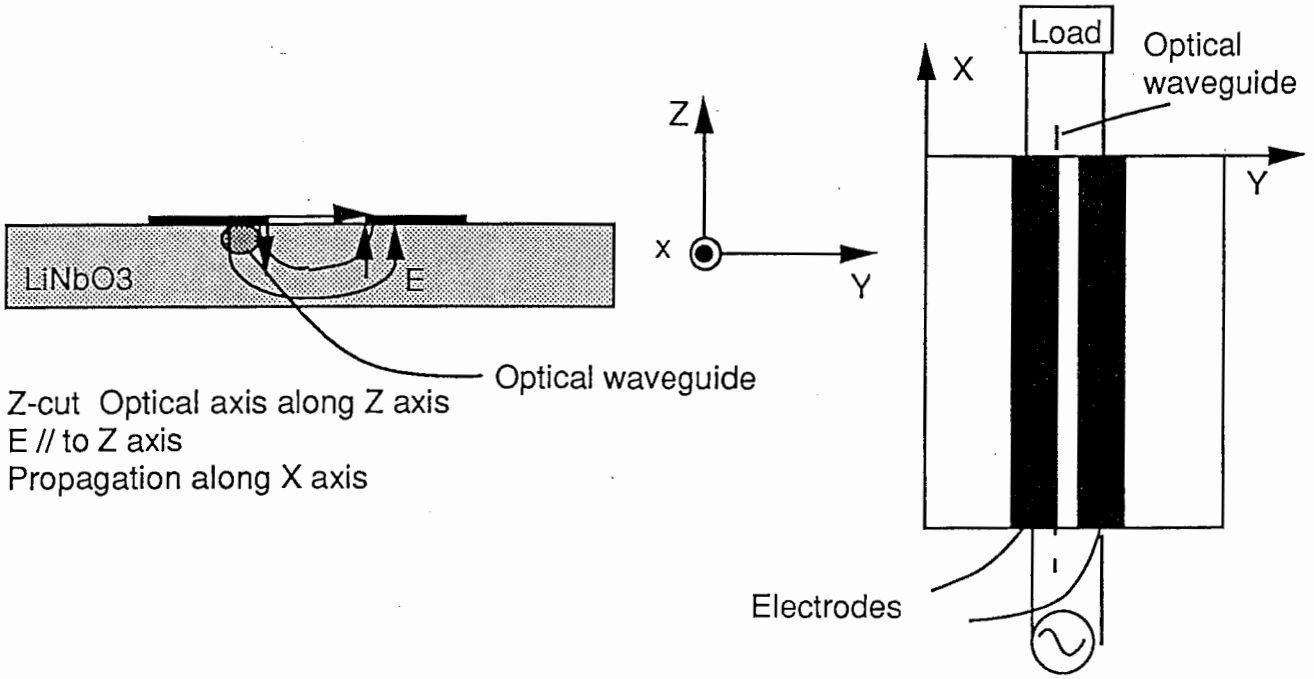

FIGURE 2-1 Typical phase modulator

2-3 Intensity modulator (Mach-Zender)

Intensity modulator are based on the interferometer principle as shown on figure 2.2 By applying a voltage Vo into the two electrodes The guided modes are phase shifted by $+\Delta\phi$ and $-\Delta\phi$ in the lower and upper arms, respectively. The output light is then modulated in response to the phase difference between the two guided modes.

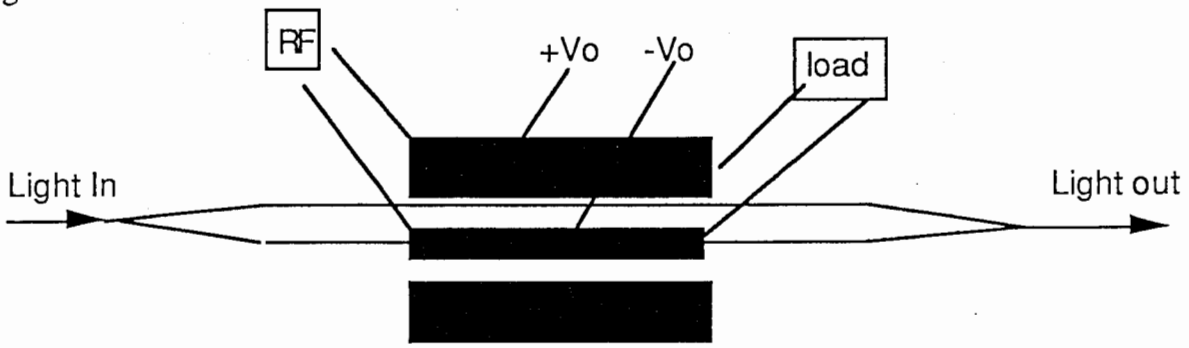

Figure 2-2 Intensity modulator

So if the beamsplitters divide the optical power equally the transmitted optical intensity I_{out} is related to the optical input intensity Iin by :

$$Iout=Iin \cos^2 (\Delta\Phi/2)$$

The parameter $V\pi$ the half-wave voltage, is the applied voltage at which the phase shift changes by π (figure2-3). $V\pi$ is an important parameter, it depends on the material, on the length and separation of the electrodes, and on the optical wavelength. Typically $V\pi$ is around 8V for L=1cm and G=25µm.

$$V\pi=G \lambda / L / n^3 r$$

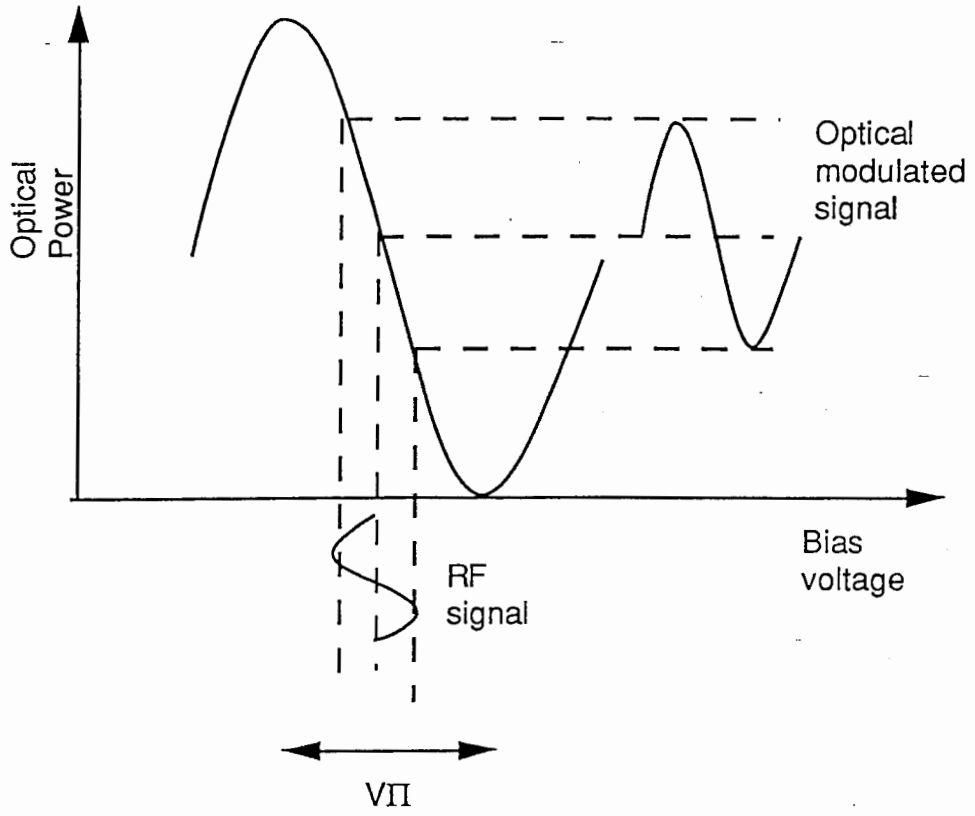

Figure 2-3 Intensity modulation

2-4) Frequency response

It would be too simple (and may be, we would be out of job) if electrooptic modulators had no frequency limitations. The main limitation is due to the mismatch between the optical and the microwave velocity, and also to the RF connection and to the electric loss into the electrodes.
The optical refractive index is about 2.3 for LiNbO3 substrate while the microwave refractive index is around 4.2 for coplanar electrodes. We could make the analogy with microwave couplers where it is important to equalize the velocity of the ood mode with that of the even mode if order to achieve a wide bandwidth. As we will see, this mismatch factor is critical as the length of the

electrodes is increased, because then, the phase shift induced by electrooptic effect does not add up constructively along the electrodes.
We will also show that in our case, that problem is almost overcome.

Lets write the equations .

First we consider the case of one the phase modulation.

No is the optical refractive index
Nm is the microwave refractive index, $Nm=\varepsilon_{eff}^{1/2}$
c is the speed of light in free space
f is the microwave frequency and $\omega=2\pi f$
α : electric loss

An optical signal which enters the modulator at z=0 and t=to reaches point z at t=to +No z / c

The RF voltage which produces a phase change in the optical signal via an induced change in the index of refraction in the optical waveguide is, in the case of a travelling wave electrode:

$$V(z,to) = Vo \exp(-j \omega Nm\, z / c + j\omega to + j \omega No\, z / c) \exp(-\alpha z)$$

or

$$V(z,to) = Vo \exp(-j \omega(Nm\, \delta\, z / c - to)) \exp (-\alpha z)$$

whith $\delta = 1 - No / Nm$, δ is the velocity mismatch factor.

So the total induced phase shift for photons incident at t=to and electrodes of length L is:

$$\Delta\Phi(to)=-\int_0^L \Delta\beta_o\, V(z,to)\, dz$$

$$\Delta\beta_o = -\pi n^3\, r\Gamma\, /\lambda\, /G$$

$$\Delta\Phi(to) = \Delta\beta o\ Vo\ L\ sh(T/2) / (T/2)\ \exp(j\omega to - T/2)$$

with $T = (j\omega Nm\ \delta / c + \alpha) L$

Lets consider a real case:

- $LiNbO_3$ is anisotropic $\varepsilon r = 43$ in the perpendicular direction, and $\varepsilon r = 28$ is the parallel direction.
- Electrodes are formed by the strips of a coplanar wave guide.
- For $Z = 50\Omega$, $w = 7\mu m$, $g = 25\mu m$
- Optical index $No = 2.14$
- frequency=20Ghz
- An SiO_2 layer is used as a buffer layer between the metal and the dielectric waveguide. The thickness of this buffer, as well as the metallization thickness can be adjusted in order to decrease the microwave index.

We consider a lossless substrate.

In figure 2-5a is plotted the total induced phased shift along the electrodes versus the length for different values of Nm. We can observe that the pic value varies very rapidly in function of the mismatch between No and Nm, and that the period is smaller as Nm increase (the mismatch increases). In the case of Nm=4.0 , the optimum length is $.25\lambda o$, and for Nm=2.5 the optimum length is $1.3\lambda o$. The frequency response is also plotted on figure 2-5-b. for L=1.5cm and for different value of Nm. The bandwidth varies inversely with the microwave index and with the modulator length. For the given case of figure 2-5-c, N=2.5, the 3 db bandwidth is 20GHz for 1cm long electrode, it drops to 10Ghz for a 2cm long electrode.

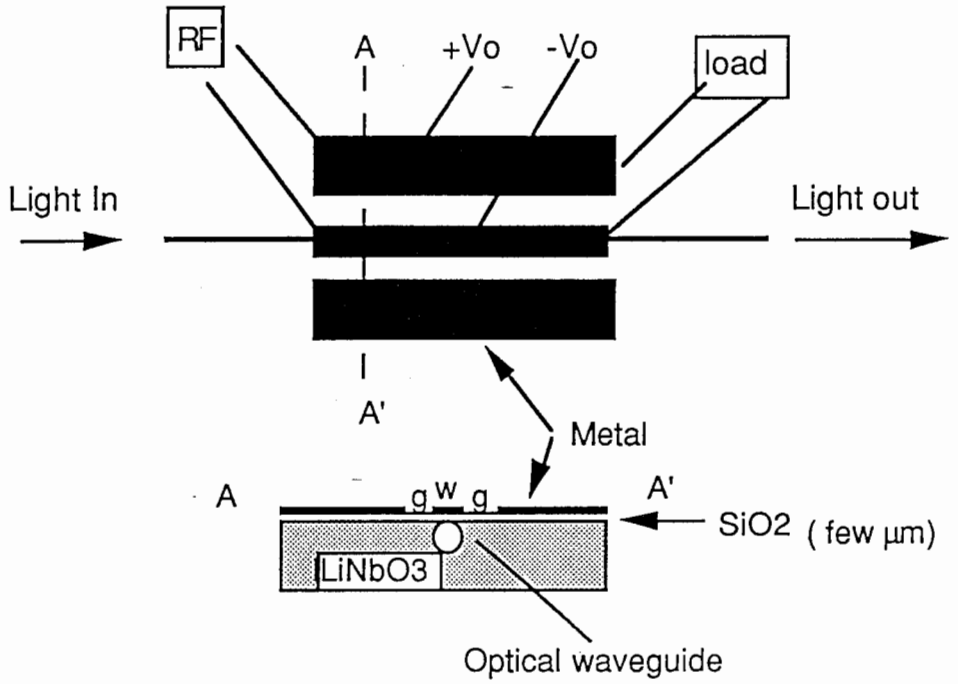

Figure 2-4 phase modulator

2-5) Velocity matching techniques [2], [6], [10]

The fisrt technique reported is to decrease the microwave index, by optimizing the buffer layer thickness and the metallization thickness [11].
The magnitude of the phase shift along the modulator begins to degrade when the phase difference between the optical and microwave signal differs by more than 180^{o} as illustrated on the figure 2-6-a below. (this corresponds to zeros in plot of figure 2.5 a.
One technique is to periodically reverse the phase on the electrodes to compensate for the polarity reversal due to the velocity mismatch, note that if we had no phase reversal the integral of V(z,to) over one period would be zero. The second is to remove the electrodes from the waveguide when the velocity mismatch results in polarity reversal of the applied field. (figure 2-6-b).

2-6) State of art

Modulators have been designed up to 40GHz with good performances. NTT [8] reports a straigth electrode modulator at 1.5µm with a 3dB bandwidth of 40Ghz. A shielding plane is put on top of the electrodes for velocity matching, and the LiNbO3 is etched between the electrodes. Another straight electrode modulator with 40GHz bandwidth is demonstrated at 1.3µm [14], in that case the optical-microwave matching is achieved by thick coplanar electrodes.
As mentioned earlier, modulators which use radiation coupling have been designed at 60GHz and 94Ghz [9].

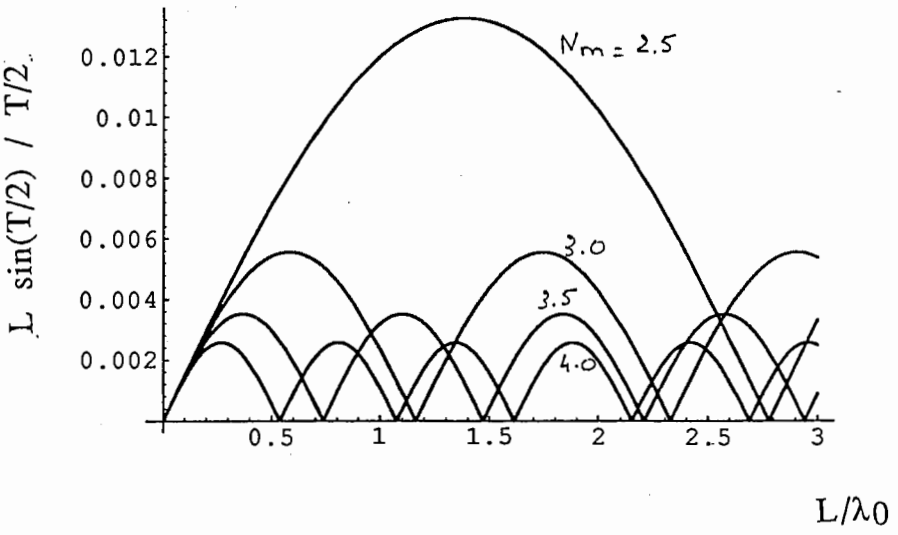

Figure 2-5-a Amplitude versus length for different Nm, $N_o = 2.15$

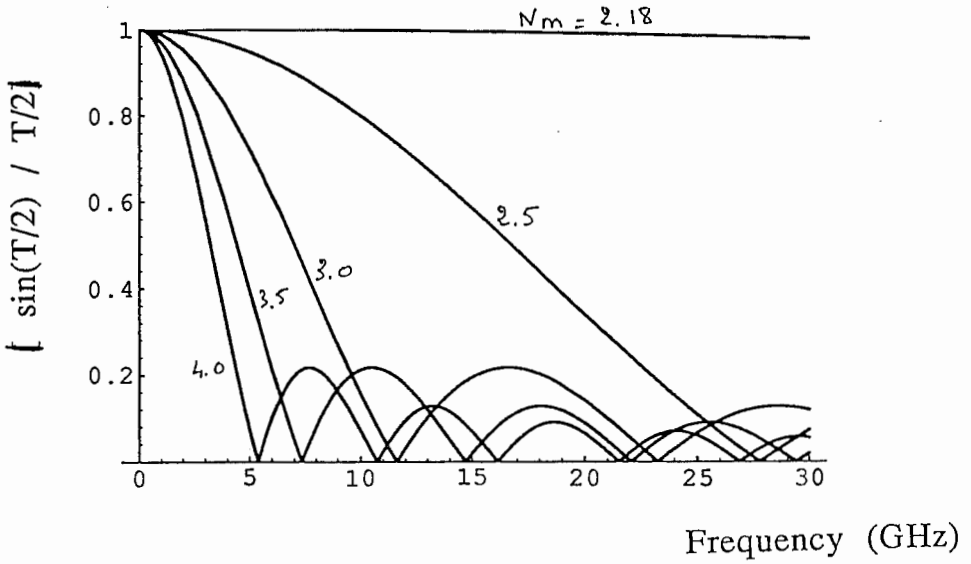

Figure 2-5-b Frequency response for different Nm, $N_o = 2.15$, $L = 1.5$ cm

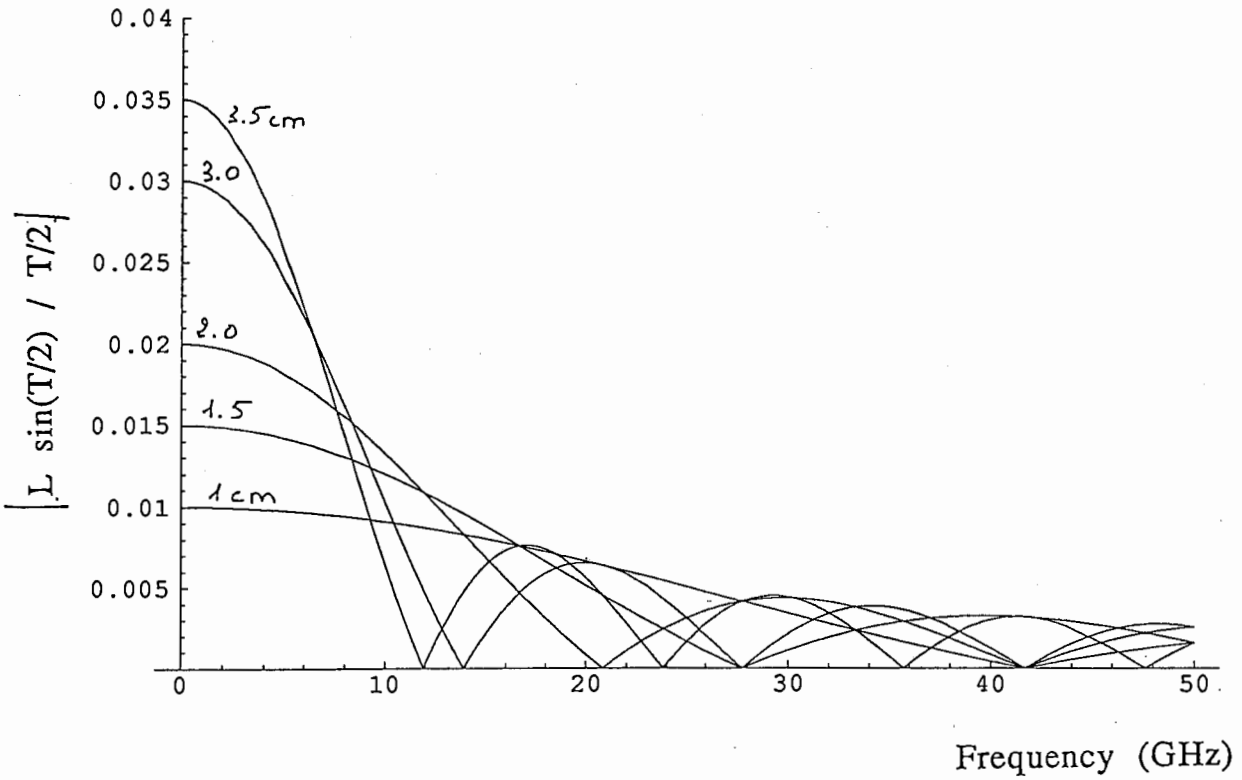

Figure 2-5-c Frequency response for different length of electrodes. Nm=2.5, No=2.15

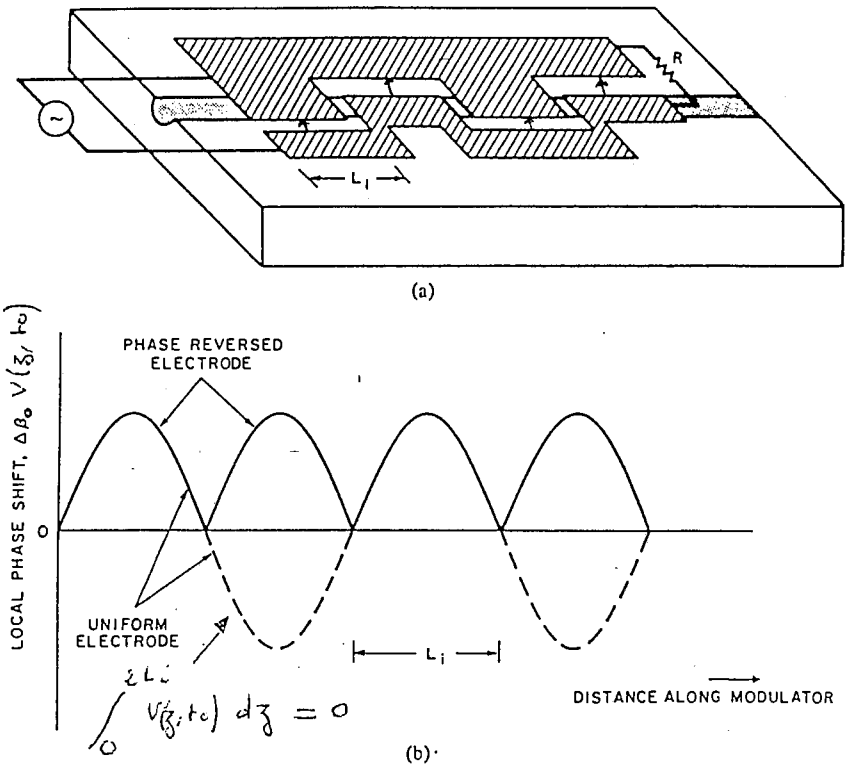

Figure 2-6-a Phase reversal technique

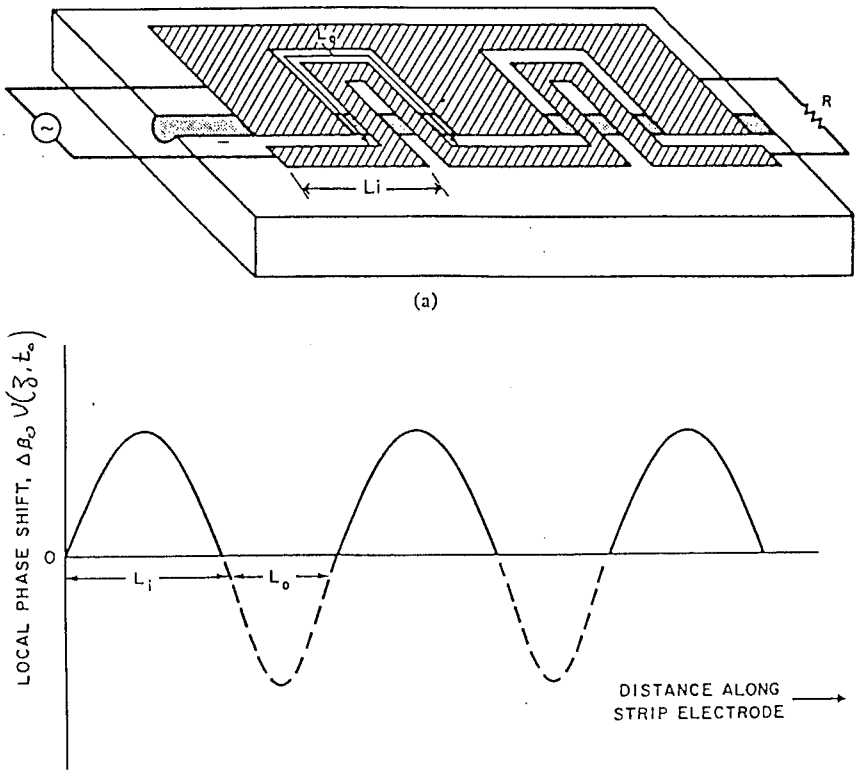

Figure 2-6-b Intermittent interaction technique

3 QUASI-OPTIC MODULATOR

The lay out of the modulator is shown in appendix 2-a and a photo of the wafer is given Figure 3-1. We have designed 8 different structures, and also 17 single slot antennas which were tested on the probe station.

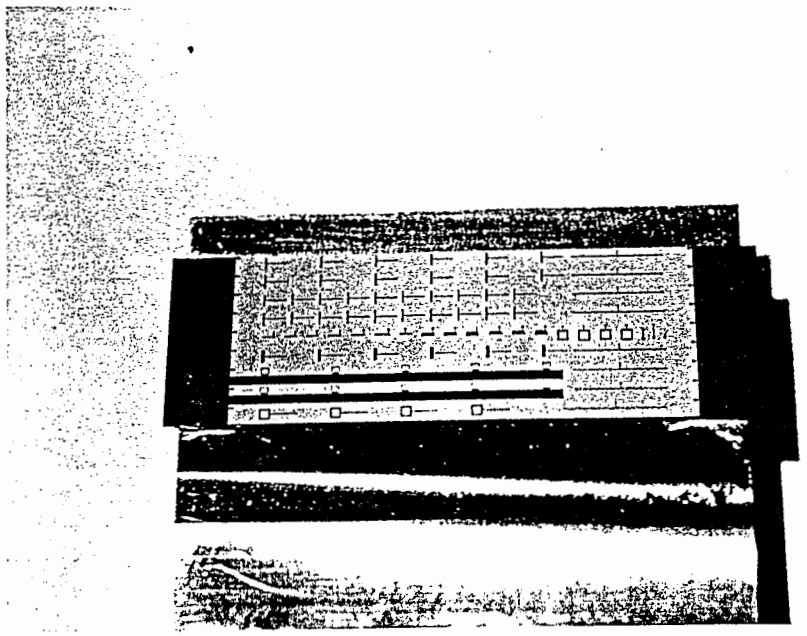

Figure 3-1 Quasi-optic modulator on LiNbO3

Many short intensity modulators are operated simultaneously, the RF signal is coupled to the electrodes by a printed antenna. The RF signal is radiated into free space and received by an array of these antennas. The advantage of such structure is that there is almost no average mismatch along the modulator, there is a mismatch at each electrode but the length is kept so short that the bandwidth is very large (see Figure 2-5). However, the bandwidth at each element is limited by the coupling antenna.
The distance between each interaction section is such that the optical signal is in phase on each electrode element.
We have also used the phase reversal technique in order to increase the number of interaction sections.
It is worth mentioning that there is no need for direct electric connection which is usually another limitation at millimeter wave frequencies.

3-1 Choice of the antenna structure

The type of electrodes that are currently used are usually slot lines or different version of coplanar wave guides (figure 3-2). The

choice of one or another is dictated the type of LiNbO3 crystal : Z cut or Y cut. Z cut and Y cut are illustrated on figure 3-3.
Briefly, for a Z-cut crystal the wave guide propagates a TM mode and the vertical component of the electric field couples to the optical field, while for a Y-cut the wave guide propagates a TE mode and the Y component of the electric field couples to the optical field. Slot lines are well suited for Y-cut substrate while coplanar wave guides are better in the case of Z-cut substrate.

Our modulator is manufactured by Sumitomo Cement on Z-cut LiNbO3.
Dipole antennas or slot antennas are well compatible with coplanar wave guides electrodes. [3] have used dipoles connected to twin lines to achieve a phase modulator at 60Ghz and 94GHz. It has been shown that dipole antennas printed on a very high dielectric constant radiates more power into the substrate than in air, slot antennas seem to be slightly better (I said sightly). So for the above raisons, we chose to use slot antennas fed by a coplanar waveguide.

3-2 Substrate characteristics

We used the commercially available process. Dimensions are given in figure 3-4 .

- For LiNbO3:

$\varepsilon//=28$

$\varepsilon\perp=43$

- For Si02:

$\varepsilon=4.4$

- Optical wave guides

width 7µm
separation 32µm
optical index No=2.14

- Coplanar wave guide

w=7µm
g=25µm
Zc=50Ω

$\varepsilon eff=8.46$, Microwave index Nm=2.91

Professor Kitazawa from Ibaraki university calculated the characteristics of slot lines, coplanar strips and coplanar waveguides on LiNbO3.

Slot lines : w= 50μm and w=100μm
Coplanar strips for g=25μm and w=7μm and w=15μm
Coplanar waveguides g=25μm, w=7μm

Geometry of the different lines is described figure 3-5a, εeff and Zc are plotted versus frequency figures 3-5b,c.

3-3 Antennas design

Accurate softwares to design slot antennas on very high dielectric constant and anisotropic substrates were not available at the time of this project, so we had no tools to calculate the antenna characteristics. At the beginning of the project, we had planned to do first some measurement of antennas on alumina substrate, but time ran out very fast and we had to provide the modulator lay-out before we received the antennas on alumina. For more details on slot antennas, please refer to section 4.
All the slot antennas are connected to a modulator section of 1/2 λg
We designed 3 main types of antennas. (see appendix 2b for all drawing and dimensions).

a)1/2 λg slot antenna at 25GHz (LINSLOT)
width w=100μm
Length L= λg/2- h/2 so at 25GHz L=1.190mm
h is the LiNbO3 thickness

b) Coupled slots antenna. (CPSLOT)
The purpose of this design is to increase the bandwidth. 3 slots of different dimensions separated by very small gap should resonate at different frequency and it should result in a wider bandwidth.

We made the central slot resonate at 25Ghz, the separation between slots is arbitrarily 7μm. Slots width is100μm
Slot 1 is connected to the modulator section : L=1.140mm
Slot 2, central slot : L=1.190mm
Slot 3: L=1.240mm

c) Square slot antenna (SQSLOT1)
The design frequency is 20GHz.

Total length of the square slot is one guided wavelength.
The width is 100μm
we have short-circuited the slot at 0.25 λg, from the feed point where the electric field is null for the mode we are considering, this will cancel out high order modes.

d) Square slot antenna (SQSLOT2)
It is a modified version of the above square slot. One side of the square slot is also a modulator section. The optical wave guides are located under both edges of one of the horizontal slots. But as we have shown above, slot lines are not good electrodes for z-cut substrate, so in order to increase the vertical component of the electric field in the substrate, we have reduced the width of the ground plane of that slot and etched a window in the central ground of the square slot. The interaction section is then equivalent to two coplanar strips 15μm wide. The slot width is also reduced to 25μm to accommodate the optical wave guides.

3-4 Modulator design

3-4-1 Theory

Lets consider an array of N modulator elements.

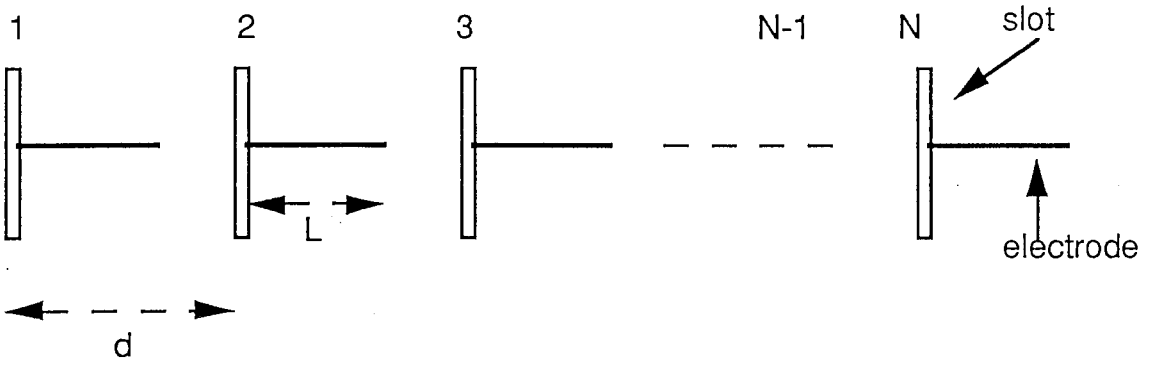

d is the distance between modulator elements
L is the interaction length
The model uses the basic equations described in section 2-4, except that we have now two terms, one for the forward propagating wave at the modulating frequency and one for the reflected wave from the open circuit at the end of the modulator electrodes.
If we assume no loss, the voltage seen by an optical signal at t=to and at z on electrode N°1 is :

$$Vo(e^{-j\omega Nmz/c}e^{j\omega t_o}e^{j\omega Noz/c}+e^{j\omega Nmz/c}e^{j\omega t_o}e^{j\omega Noz/c})$$

At electrode N° n

$$Vo(e^{-j\omega Nmz/c}e^{j\omega t_o}e^{j\omega No((n-1)d+z)/c}+e^{j\omega Nmz/c}e^{j\omega t_o}e^{j\omega No((n-1)d+z)/c})$$

The phase shift induced on each electrodes should add up along the different electrodes. Each radiating element "sees" an equi-phase" front wave, so the optical signal should also be in phase on each electrode. The inter-element distance is then given by the condition:

$\omega Nod/c=2p\pi$ so that $d/\lambda_o=1/No$

The total electrooptically induced phase shift is given by:

$$\Delta\phi=kVo\,e^{j\omega t_o}\sum_{n=1}^{N}.\int_0^L(E^+ + E^-).dz$$

where

$$E^+=Vo\,e^{-j\omega Nmz/c}e^{j\omega t_o}e^{j\omega No((n-1)d+z)/c}$$

$$E^-=Vo\,e^{j\omega Nmz/c}e^{j\omega t_o}e^{j\omega No((n-1)d+z)/c}$$

And finally we get:

$$\Delta\phi=kVoL[e^{j\omega(N-1)Nod/c/2}\sin(NP/2)/\sin(P/2)].$$
$$[e^{j(\omega t_o-T^+/2)}.\sin(T^+/2)/(T^+/2)+e^{j(\omega t_o-T^-/2)}.\sin(T^-/2)/(T^-/2)$$

with:

$P=\omega Nod/c$

$$T^{+} = \frac{\omega}{c} Nm(1 - \frac{No}{Nm})L$$

$$T^{-} = \frac{\omega}{c} Nm(1 + \frac{No}{Nm})L$$

$$k = \pi . N_o^3 . r_{33} . \Gamma / g / \lambda_{opt}$$

No is the effective optical index
Nm is the microwave index
λopt=1.3μm is the optical wavelength
r33 is the electrooptic coefficient
g is the gap between the electrodes.

The first bracket term is a phase locking term that describes the additive effect of the N sections of the modulator, it depends on the period. As shown in figure 3-6-a, it has a bandwidth limitation. For 25Ghz central frequency, d=5.6mm, N=6 the 3dB bandwidth is 20%. The amplitude term (second bracket term) is only dependant on the length of the electrodes, and do not depend on the number of electrodes, the bandwidth is then given by the bandwidth of one modulator element. Each electrode being very small (2mm) the bandwidth is then very wide. The amplitude term versus frequency is plotted in figure 3-6-b. The total frequency response is also given figure 3-6-c . The modulator works also at even harmonics, as can be seen on the graph.

But the modulator bandwidth depends also strongly on the antennas characteristics, impedance, effective area.

The antenna receives a power:

$$P_r = P_{inc} A_e$$

where Pinc is the incident power:

$$P_{inc} = P_t G_t \frac{1}{4\pi R^2}$$

and Ae is effective area: $A_e = \frac{\lambda^2}{4\pi} G$

The impedance of the slot antenna is :

$$Za = R + jX$$

then the total input impedance is

$Z = Z_a // (-jZo\cot g(\theta))$ where Zo is the characteristic impedance of the electrodes of length θ.

So the voltage on the electrodes is :

$$Vo = \frac{Zo.\cos(\theta)\sqrt{P_r R}}{\sqrt{(R^2 \sin^2(\theta) + (X\sin(\theta) - Zo\cos(\theta))^2}}$$

and for 0.5λg electrodes: $Vo = \sqrt{P_r R}$

We deduce from the above equation, that in order to get the maximun voltage, the slot antenna should have a high impedance. The received power depends on the gain of the antenna, it will also depends on the angle of incidence. Radiation patterns for 6 radiating elements with a spacing of 0.466λo and for 11 elements with a spacing of 0.233λo (case of phase reversal technique) are given figure 3-7-a,b. The 3 dB beamwidth is about 25°.

Conclusion
Unless we can design antenna with at least 20% bandwidth, which is very difficult to achieve on a high dielectric constant, the bandwidth of the modulator will be mainly limited by the antenna bandwidth.

3-3 Wafer lay-out

The wafer was divided in two parts, the first part was dedicated to optical probe measurements and to the impedance measurement of different designs of slot antenna, the second half duplicates the first part for packaging. Only half of the wafer is shown in the appendix.

We used a separate biasing electrode, which does not disturb the antenna. The length is 9mm, this should give Vπ#10v (Vπ.L=9v.cm) For LINSLOT3 and LINSLOT2 we have used a phase reversal technique. As explained in section 2, the spacing between the antennas is now such that the optical phase differs by 180° at each

element. In order to add up the electrooptically induced phase shift on each modulateur section, the RF phase is also reversed. This is explained on Figure 3-8. The advantage is that the number of modulator elements is increased, and so the sensitivity should be higher.

a) modulators

A summary of the different modulator designs is given is the table below

Name	Design freq GHz	length µm	spacing µm	Number of element	
LINSLOT1	25	1190	5600	6	
LINSLOT2	23	1300	5600	6	
LINSLOT3	25	1190	2800	11	Phase reversal
LINSLOT4	23	1300	2800	11	Phase reversal
SQSLOT1	20	926/side	7000	5	with short circuits
CPSLOT	25	1140 1190 1240	5600	6	
SQSLOT3	20		5600	6	
SQSLOT4	20		5600	6	with short circuits

b) Antennas for RF probe measurements. See lay-out appendix 2-a

We have 17 antennas different dimensions. We were expecting a very high input impedance , so we moved the feed point toward the slot edge where the input impedance is smaller. This is described in section 4.
We also included a calibration Kit for TRL measurements.

3-4 measurements

We were planning to do measurements with different ground planes at the back of the LiNbO3, and no ground plane at all. The reason for the ground plane is that first it is is easier to assemble and second the slot antennas should be more directive. In fact as we will see on the antenna impedance measurements, it seems that some modes are propagating in the substrate.

Wafer 1: the LiNbO3 substrate is glued on aluminium
- Distance from antenna to reflector plane is 0.25λg at 25GHz

Wafer 2: the LiNbO3 substrate is glued on quartz 800µm thick, and the quartz substrate is glued on aluminium.
- Distance from antenna to reflector plane is 0.38λg

3-4-1 Impedance measurements

Measurements are made on the CASCADE probe station, with a TRL calibration.
The reference plane is at the junction of the coplanar wave guide and the slot antenna.

Loss in the coplanar wave guide is 0.2dB/mm.

All impedance measurements for wafer 1 and wafer 2 are given in in appendix 2-c. On each page we give results for wafer 1 and wafer 2.

	Ls µm	Le µm
LINSLOT1	1190	50
LINSLOT2	1190	100
LINSLOT3	1190	150
LINSLOT4	1300	100
LINSLOT5	1400	100
LINSLOT6	1500	100
LINSLOT7	1190	595

	LS1 µm	LS2 µm	LS3 µm	e µm	Le µm
CPSLOT1	1140	1190	1240	7	100
CPSLOT2	1140	1190	1240	15	100
CPSLOT3	1140	1190	1240	50	100
CPSLOT4	1090	1190	1240	7	100
CPSLOT5	1090	1190	1290	15	100
CPSLOT6	1090	1190	1290	50	100

	La=wa	Lb=wb
SQSLOT11	1026	826
SQSLOT12	1100	900

SQSLOT21: same as SQSLOT11 but with short circuits to decrease impedance
SQSLOT22: same as SQSLOT12 " " " " " "

For wafer 2 add '2' before antenna names.

They are many data that need to be deciphered.
we can just mention here very important points:

• The impedances are smaller than expected, this is probably due to high loss in the substrate.

• The results are very different for wafer 1 and wafer 2. This might be caused by modes propagating in the substrate and especially in the quartz slab.
This is illustrated in figure 3-9-a where are compared LINSLOT7 (same dimensions as for the modulator) on wafer 1 and wafer 2. There is an inductive effect in the case of wafer 1, wafer 2 has a more "normal " impedance locus. But, for both the resonant frequency is centered around 25GHz.

On figure 3-9-b We compare impedance in the case of LINSLOT on wafer 1 for different dimensions but the same feed position, a variation of 100µm changes the resonant frequency by about 350MHz to 500MHz.

• CPSLOT seems to provide a wider bandwidth, it is very dependent on the spacing between the slot strips , and the strips length. On wafer 1 , we get the optimum bandwidth for CPSLOT6, with a separation of 50µm and 100µm difference in length between strips, but once again results are very different on wafer 2. Figure 3-9-c

Conclusion on the antenna measurements.

We used a very accurate method of calibration, so we can assume that measurements are correct. The influence of a reflector plane and of a dielectric slab at the back of the antenna is very important.

we think that more measurements must be done, and especially without metallic plane.

•A theoretical model must be developed in order to design antennas with a good precision, these first results can be used as a data base to check the theory.
Loss in the substrate seem to be high, probably because of high order modes, the wafer thickness must be decreased, a 300µm process should soon be available at Sumitomo Cement.

3-4-2 Modulator measurements.

As we mentioned earlier we did not have enough time to test all the different modulators.
We measured LINSLOT1, LINSLOT3 (phase reversal) and CPSLOT.

The experimental set up for the optical probe measurements is described figure 3-10.

We use a laser from lightwave at 1.3µm, and a 40Ghz bandwidth photodetector from Newfocus, data sheets are given in appendix 3.
The optical probes were designed at ATR, they have only 3 axes: X,Y,Z.
Optical probes, and a DC probe were mounted on the probe station.

The polarization of the optical signal at the wave guide input must be a TM mode, usually a polarization maintaining fiber (PM fiber) and a chip polarizer is used, it is then easy to adjust the polarization for the maximum output optical signal. Unfortunately it was too difficult for us to equip the probes with a PM fiber, and we did not have any chip polarizer on the wafer. So we had to use a single mode fiber and an external polarizer.

Measurement procedure

1) line up the fiber with the optical wave guide.
First we use a laser at 0.633µm and try to align visually the red beam with the wave guide input and output.

2) then connect the 1.3µm laser and adjust the optical probes to get the maximum output optical power;

3) adjust the polarization, and check if it is a TM mode by measuring the DC response of the modulator in function of bias voltage, we expect a nice sinusoid.

With this procedure we could not get better than -8db optical insertion loss fiber to fiber, and an on/off ratio of 15 to 20 dB. For a modulator assembled by Sumitomo we can get -4.5dB insertion loss and an on/off ratio of 30dB.

4) finally set the horn antenna above the sample, and readjust the optical probe to compensate for the weight on the probe station table (we could loose up to 10dB!!!!!)

Results

For a transmitted power of 23dBm and a distance from horn to antenna of about 35cm and if we assume that the printed slot has a gain of 2dB (this is optimistic), the received power by one radiating element is -3dBm, and for an array of 6 elements it is about 7dBm
We had to use a long fiber to avoid a direct coupling of the radiated power to the photodiode.

The input optical power on the wave guide was about 10dBm, and the modulator biased in the linear region.

The RF power detected by the photodetector , and for the 3 designs mentioned above, is given figure 3-11.
The measured level is around -80/-90dBm, it is low but it very interesting to note that the coupled slots modulator is 10dB above the linear slot modulators. The difference between LINSLOT1 and LINSLOT3 (with phase reversal) is very little.

Conclusion on the modulator measurements

It is difficult at this point to draw an objective conclusion

a) the experimental conditions were not very good. The modulators were not in the horn far field, we had a lot of reflections on the probe station.

b) It was difficult to line up the fiber, and get a good TM polarization.
c) As we have seen in the previous section, the antenna a " strange" impedance characteristic.

d) So we decided to assembled all the modulators in a package, with PM fiber and chip polarizer, and we also machined away the bottom of the package, so the slot antennas do not have any reflector plane. All measurements will be made in the anechoic chamber.

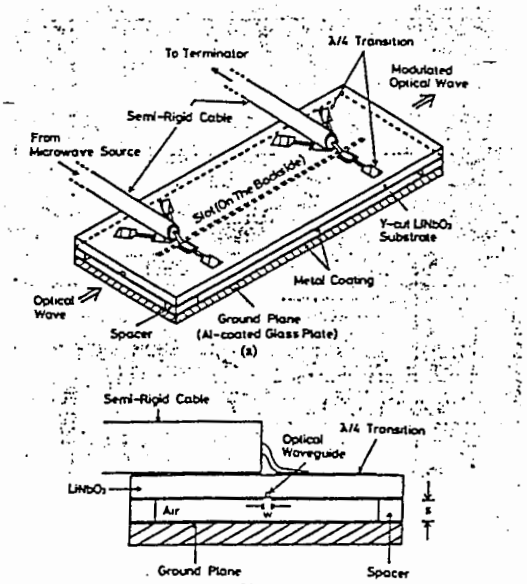

Fig. 1.

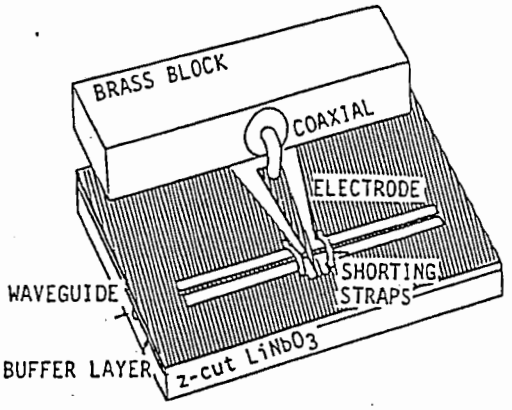

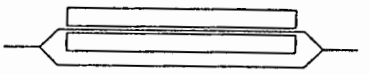

(a) Y-CUT , TWIN-ELECTRODE

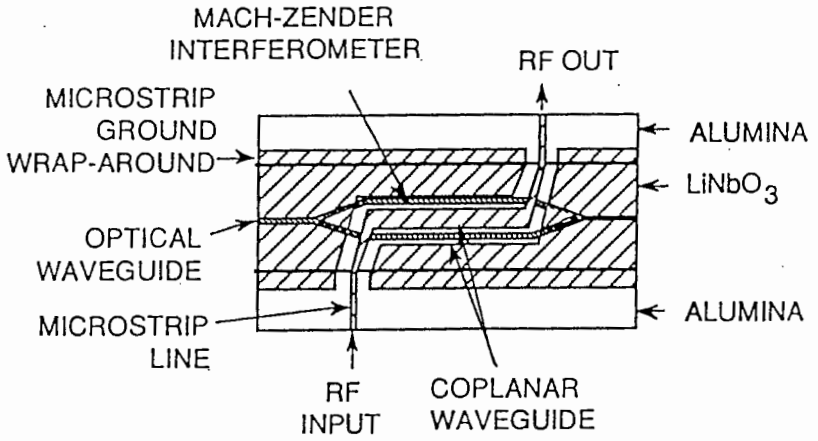

Figure 1. Schematic of an integrated optic modulator with a coplanar waveguide travelling wave electrode.

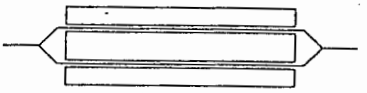

(b) Y-CUT , TRI-ELECTRODE

Figure 1 The schematic diagram of symmetric electrodes

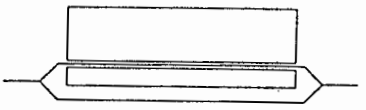

(a) Y-CUT , TWIN-ELECTRODE

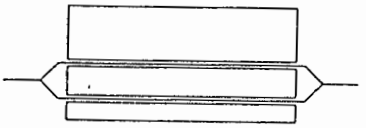

(b) Y-CUT , TRI-ELECTRODE

The schematic diagram of asymmetric electrodes

Figure 3-2 different types of electrodes

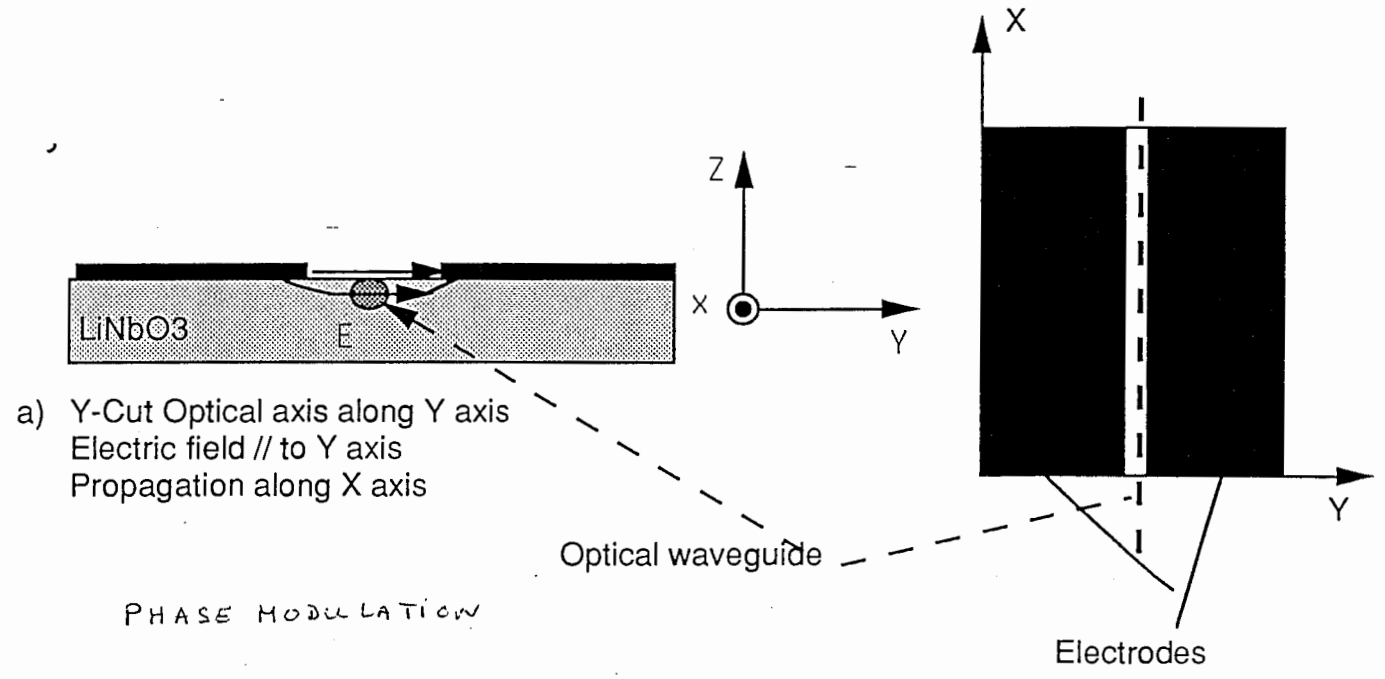

a) Y-Cut Optical axis along Y axis
Electric field // to Y axis
Propagation along X axis

PHASE MODULATION

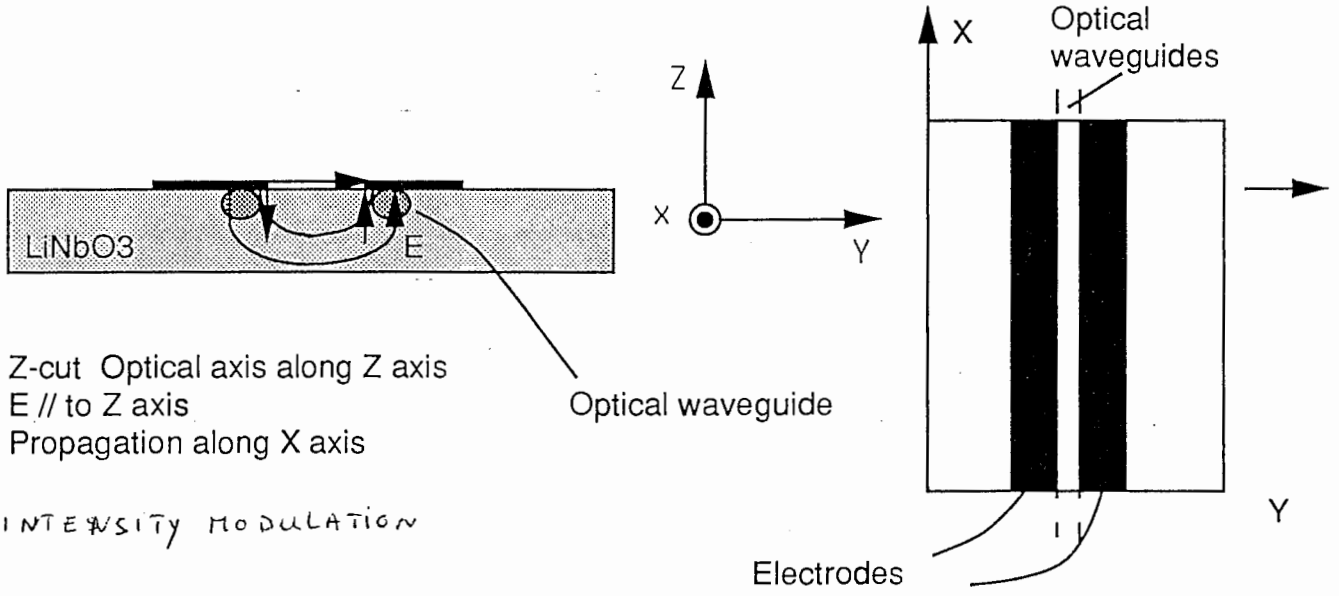

b) Z-cut Optical axis along Z axis
E // to Z axis
Propagation along X axis

INTENSITY MODULATION

Figure 3-3 Z-cut and Y-cut LiNbO3

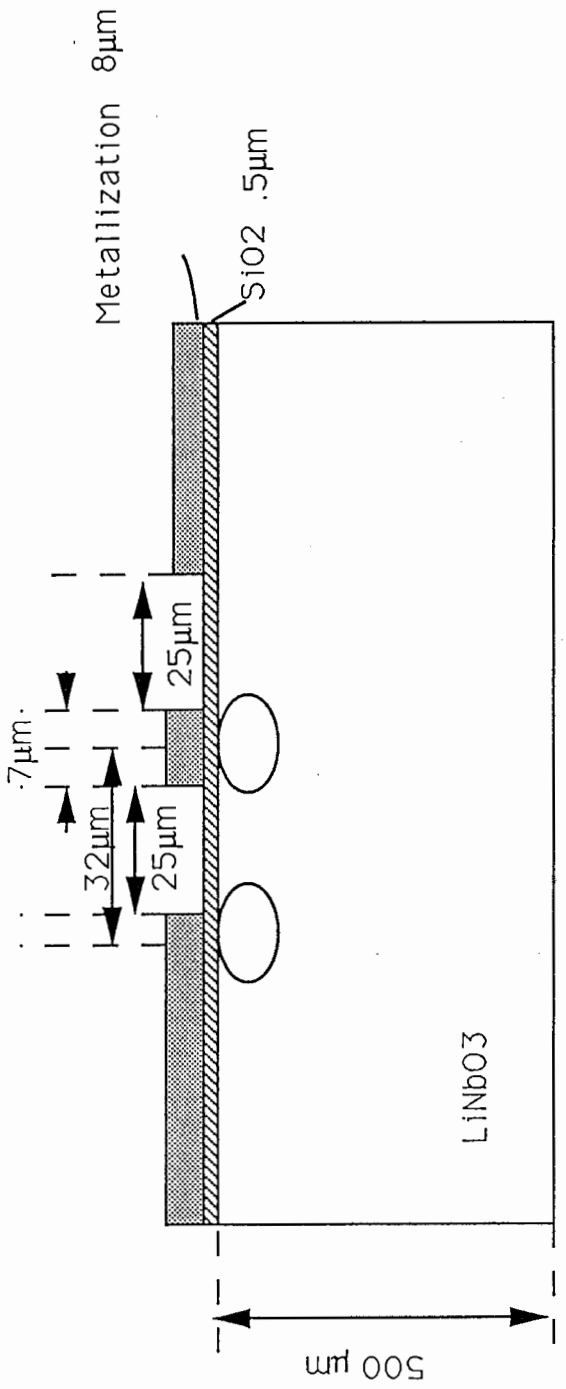

Figure 3-4 Substrate dimensions

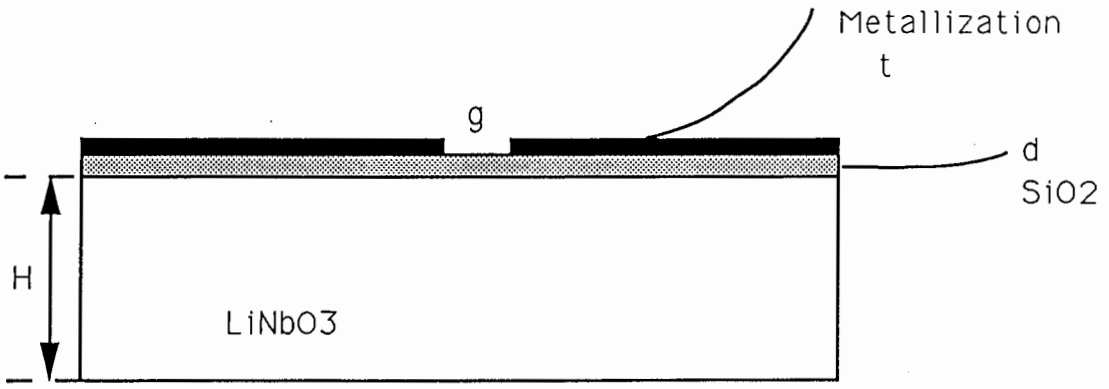

Slot Line

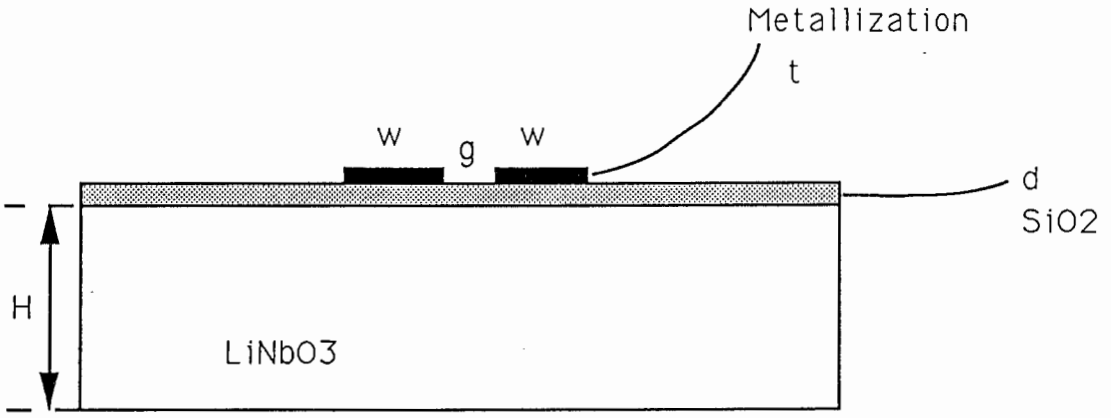

Coplanar Strips

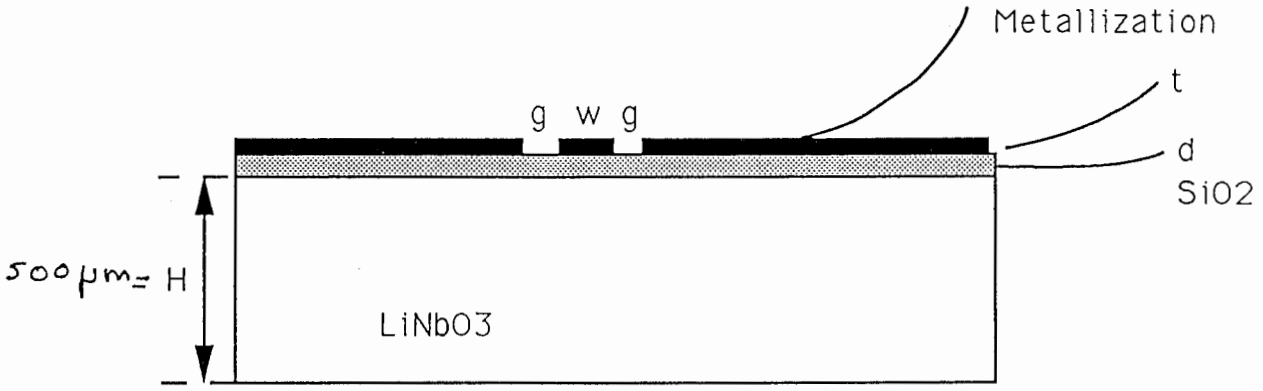

Coplanar Waveguide

Figure 3-5-a Transmission lines geometry $t = 8\mu m$, $d = 0.5\mu m$

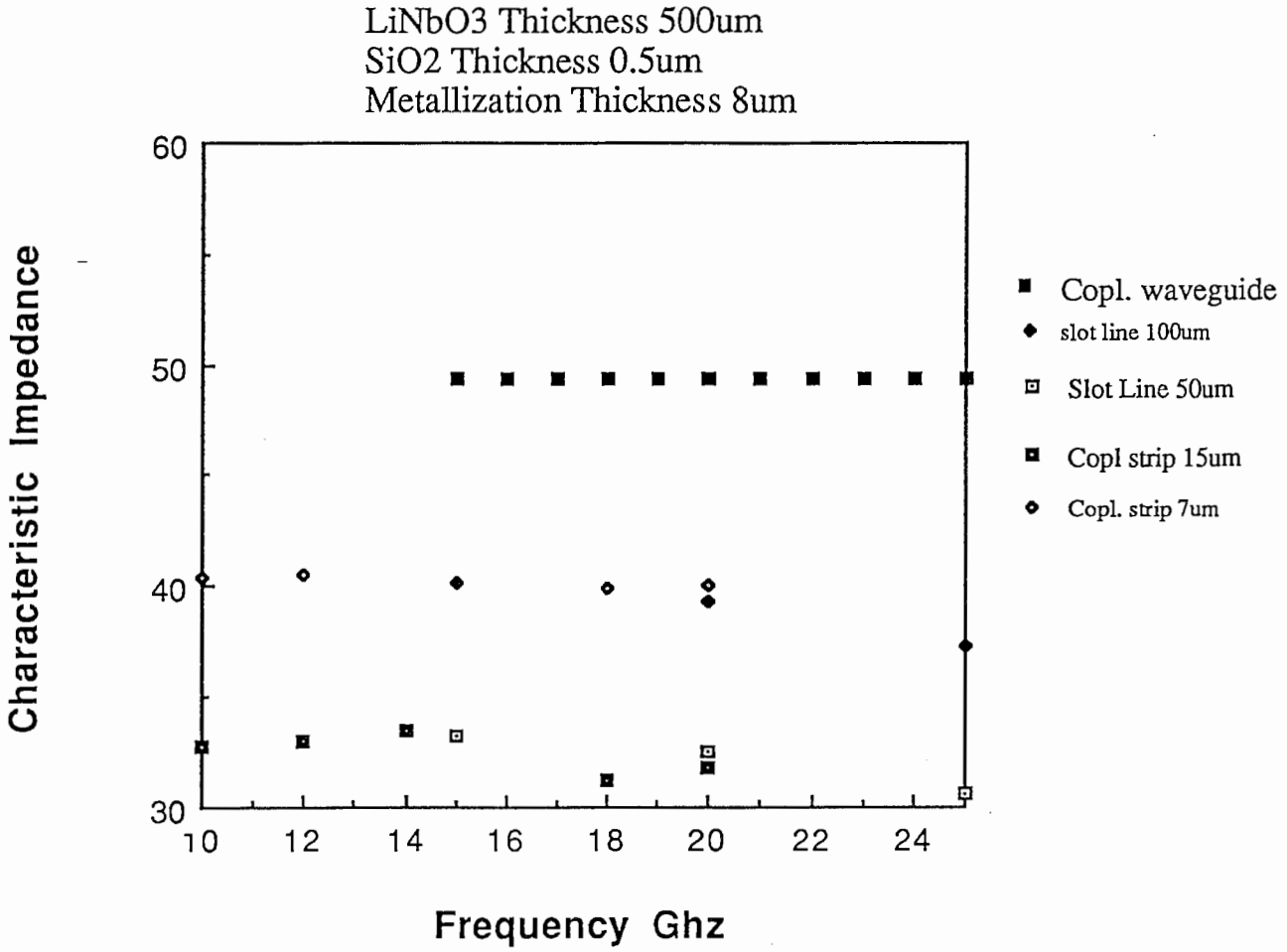

Figure 3-5-c Characteristic impedance

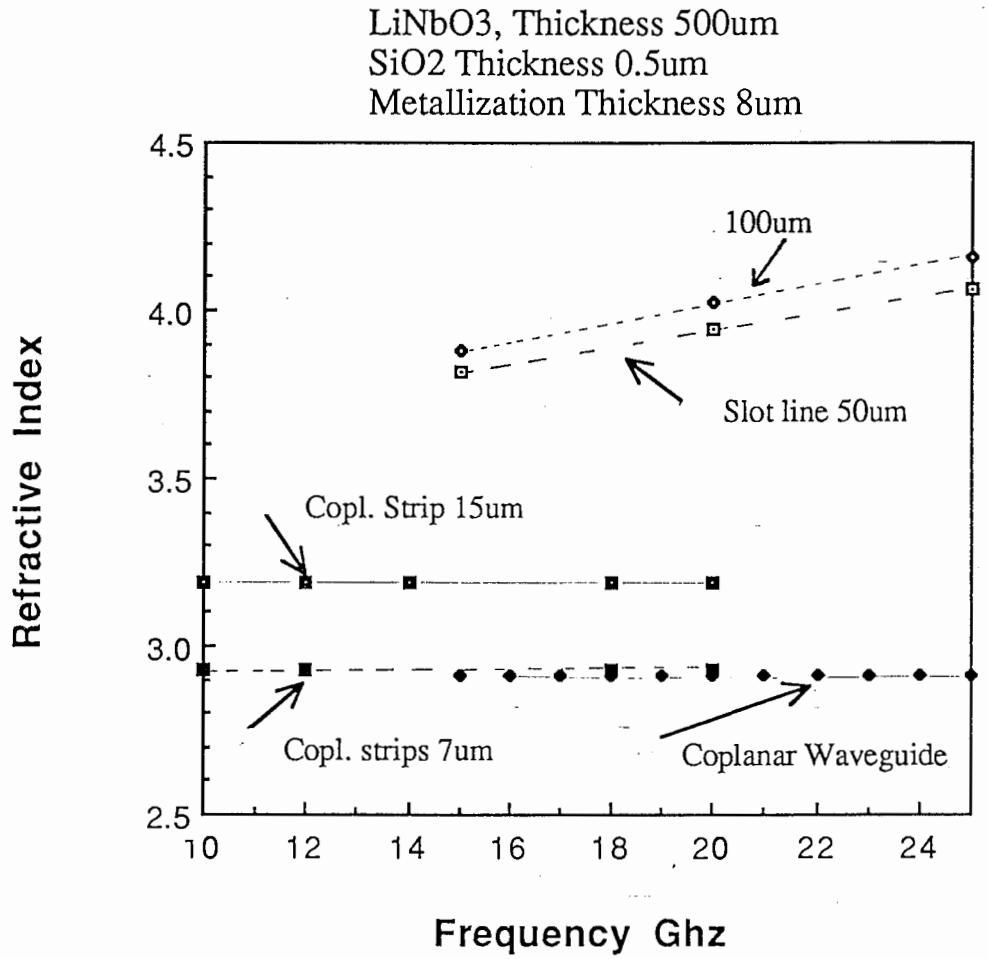

Figure 3-5-b refractive index

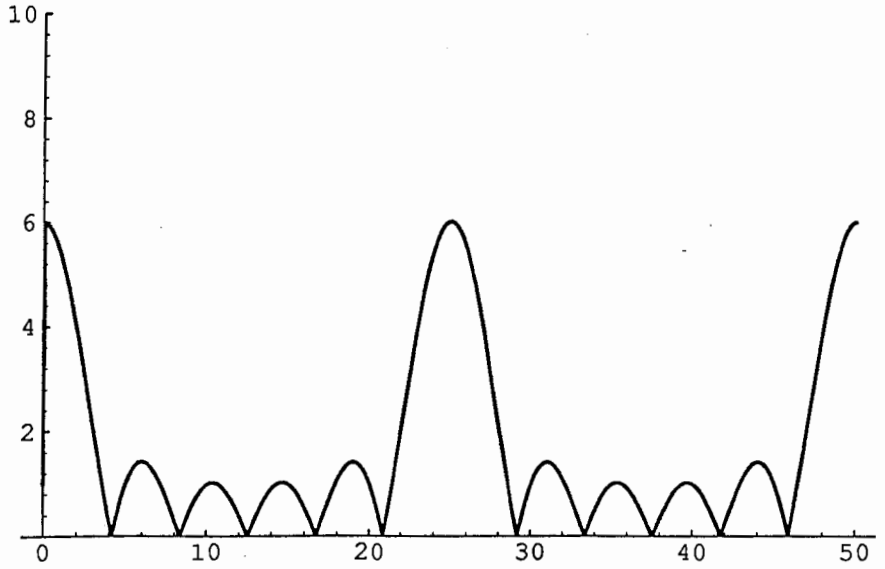

Out[21]=

-Graphics-

Figure 3-6-a Phase-locking term versus frequency

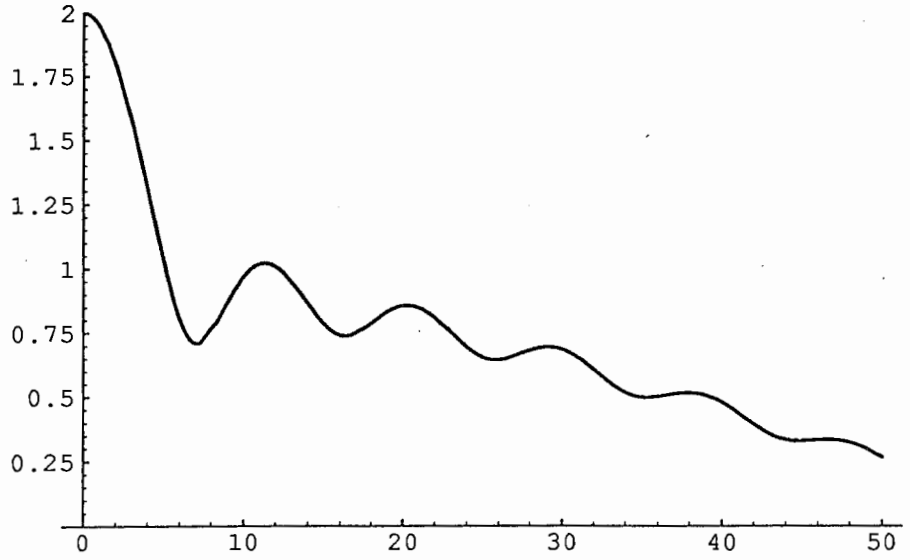

Figure 3-6-b Frequency response of the amplitude term

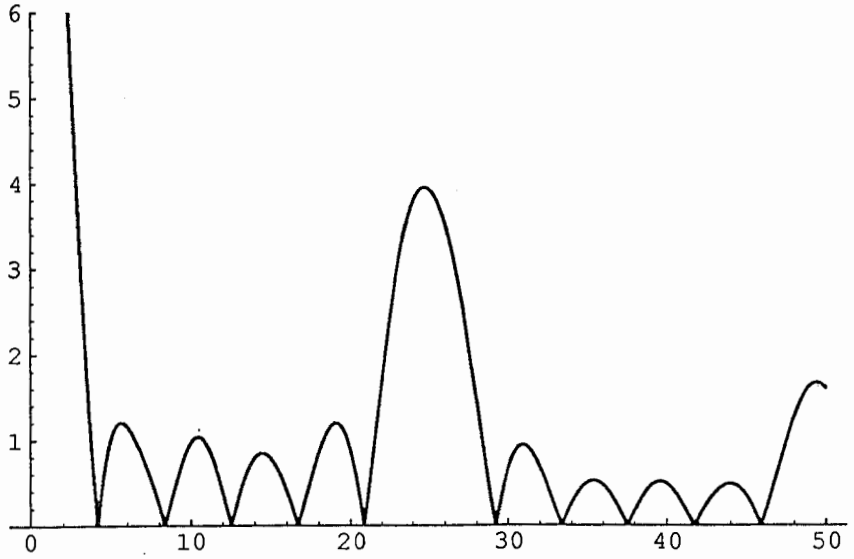

Figure 3-6-c Frequency response of $\Delta\phi$

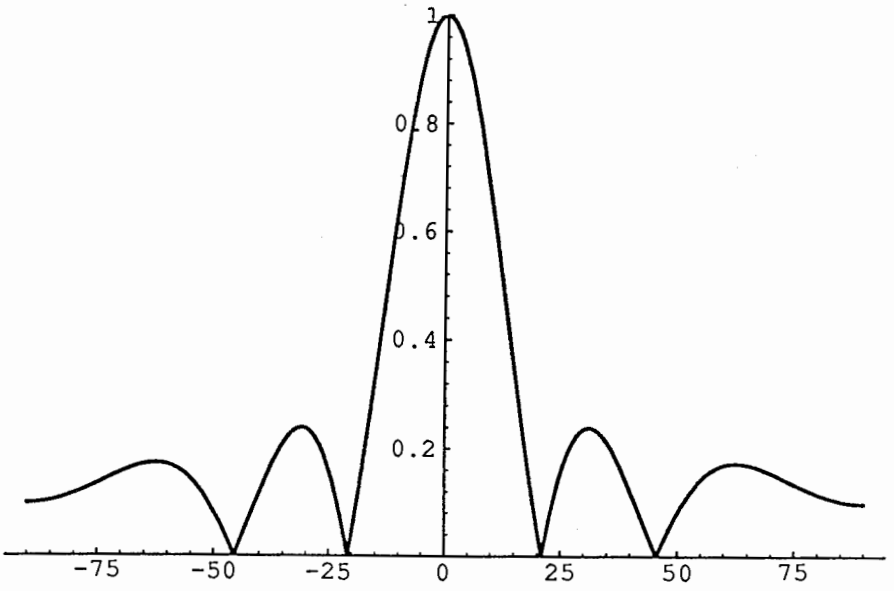

Figure 3-7-a Radiation Pattern. 6 elements, spacing 0.466λo

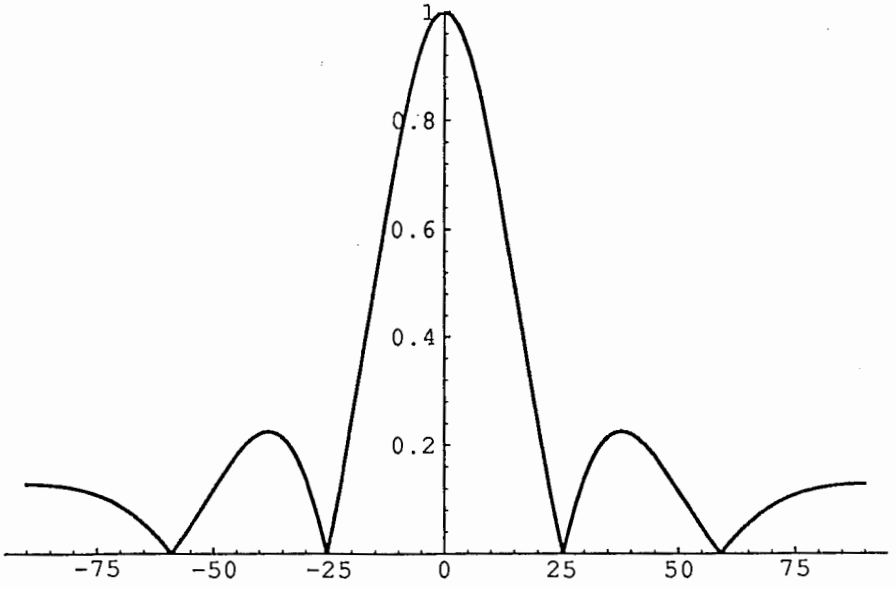

Figure 3-7-b Radiation pattern, 11 elements, spacing 0.233λo

PHASE REVERSAL

LINSLOT3 AND LINSLOT4 .

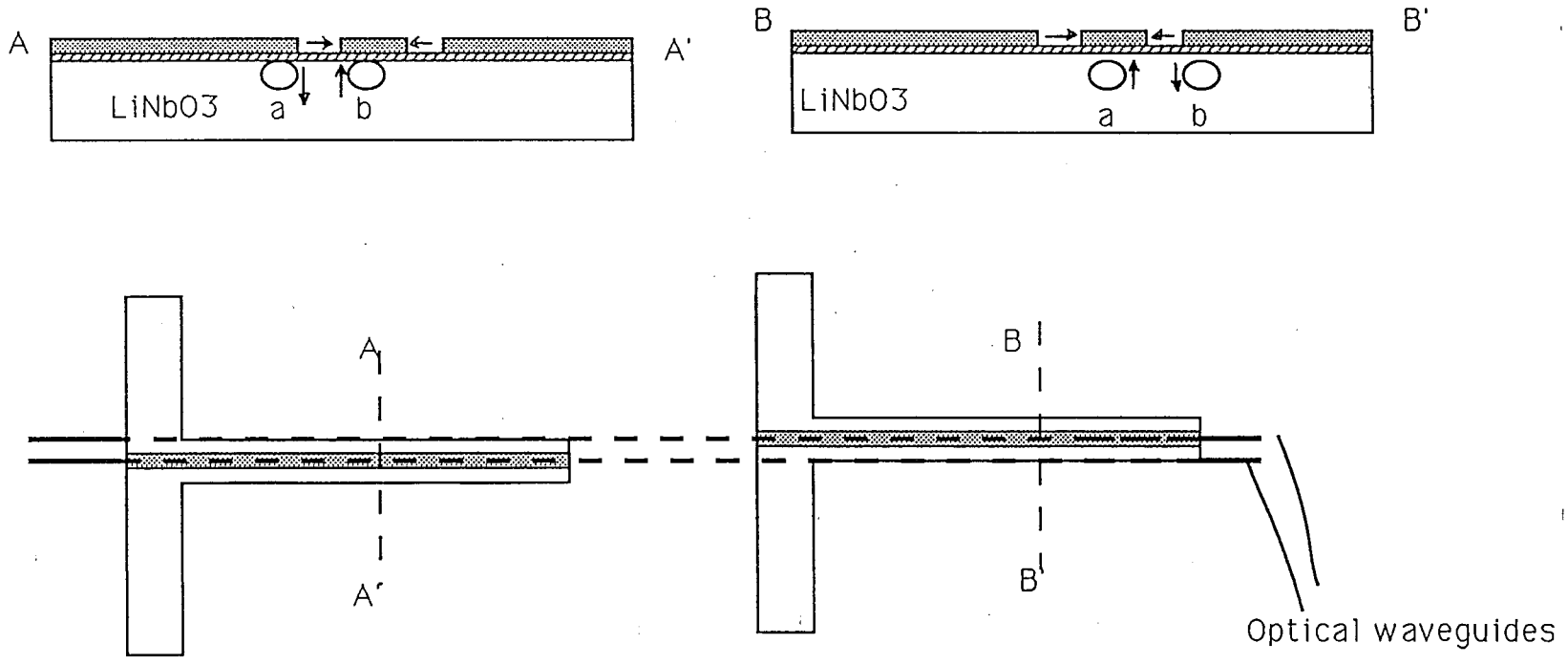

Figure 3.8. PHASE REVERSAL

Eesof -- Touchstone -- Thu Dec 05 02:32:48 1991 -- LINSLOT1

□ S11 LINSLOT7

+ S11 LINSLOT7 (WAFER 2)

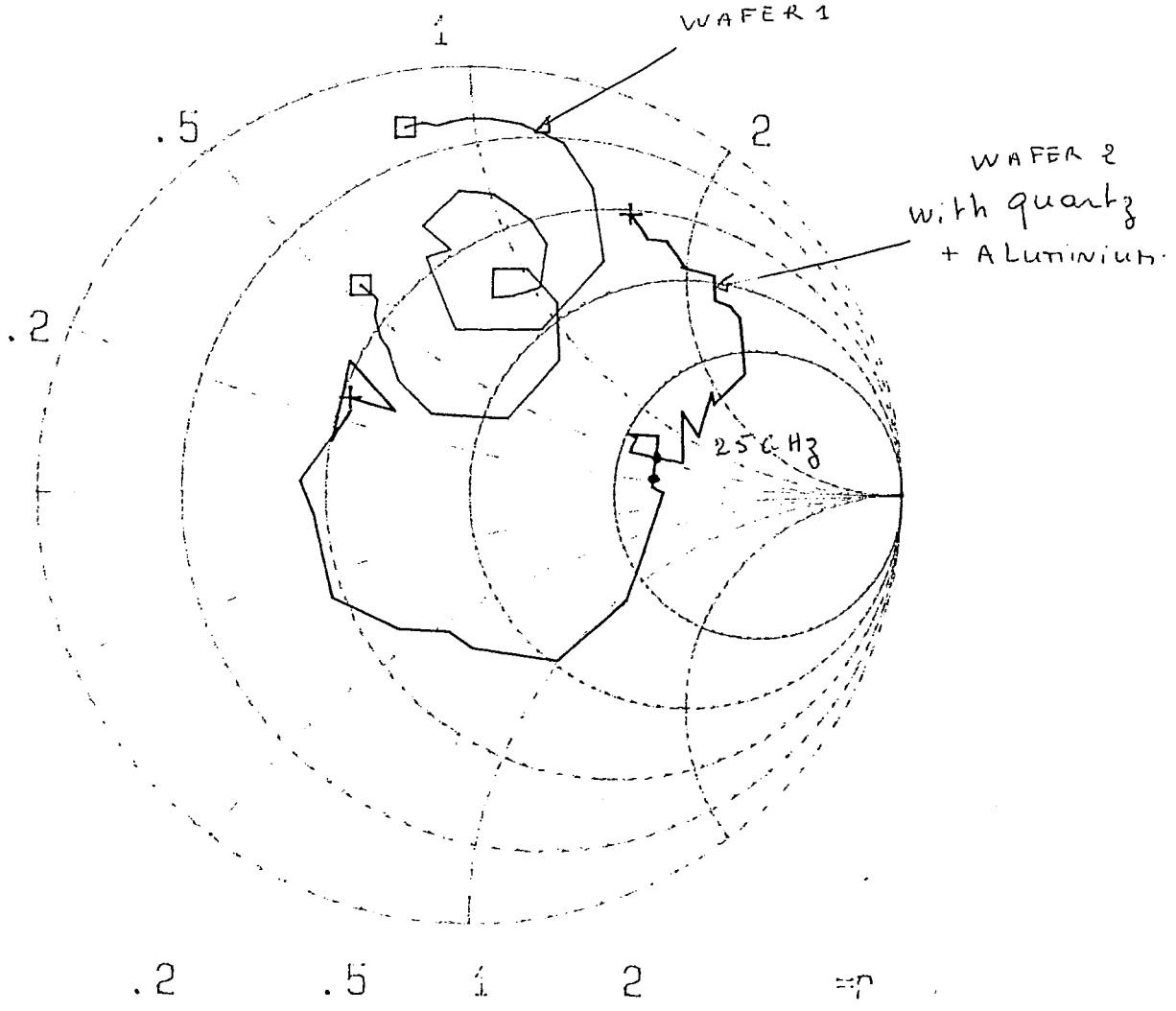

f1: 23.0000
f2: 26.5000

Figure 3-9-a

EEsof - Touchstone - Sat Nov 30 05:56:56 1991 - LINSLOT1

Resonant Frequency

□ S11 L = 1300 μm 20.7 GHz
LINSLOT4

+ S11 L = 1400 μm 20.15 GHz
LINSLOT5

◇ S11 L = 1500 μm 19.8 GHz
LINSLOT6

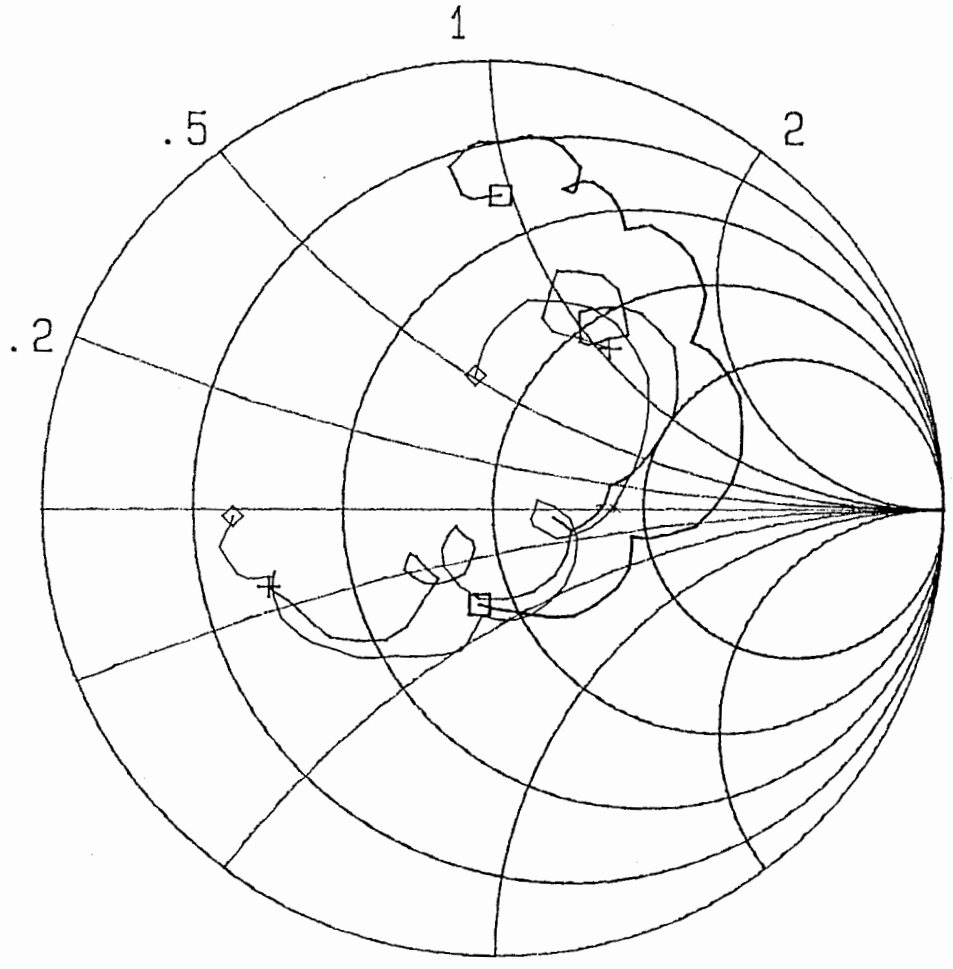

f1: 19.5000
f2: 21.0000

Figure 3-9-b

2LINSLOT7

WAfer 2

1.0 Units
200.0 mUnits/
135.53 Ω 11.602 Ω

ARKER 3
25.05 GHz

1) 23.7 63.67 124.2
2) 24.3 147.8 54.8
3) 25.05 134.61 11.367
4) 25.35 62.35 -57.5

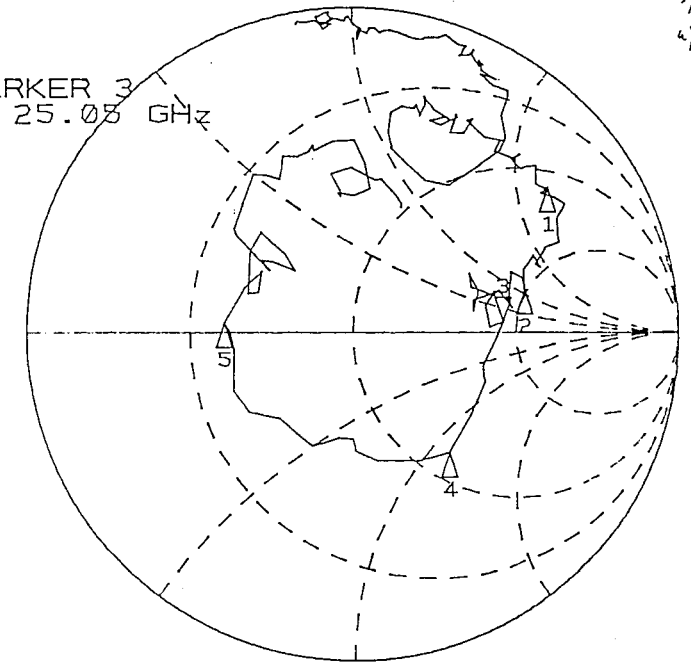

START 18.000000000 GHz
STOP 28.000000000 GHz

LINSLOT7

WAFER 1

1.0 Units
200.0 mUnits/
69.34 Ω 56.039 Ω

ARKER 5
26.25 GHz

1) 24.6 10.47 100 Ω
2) 25.3 72.56 154.27
3) 25.5 131.03 84.99
4) 25.7 92.15 77
5) 26.25 70 56.2

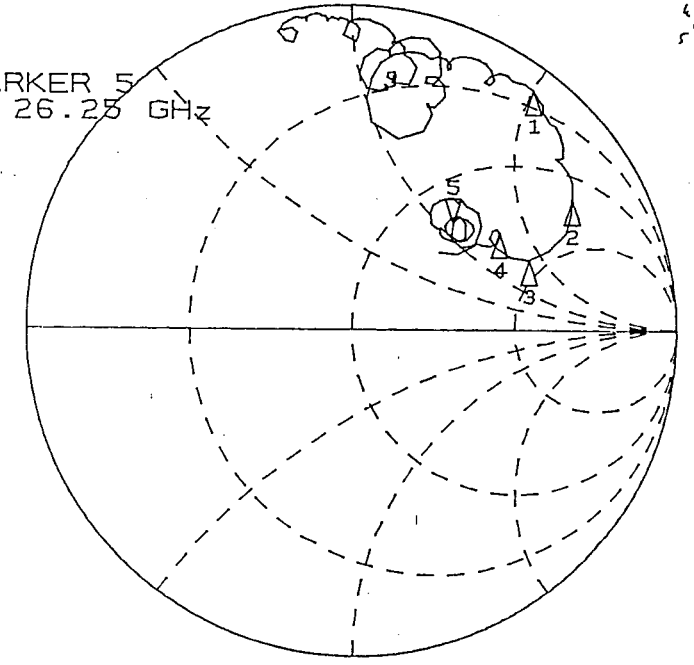

START 18.000000000 GHz
STOP 28.000000000 GHz

Figure 3-9-c

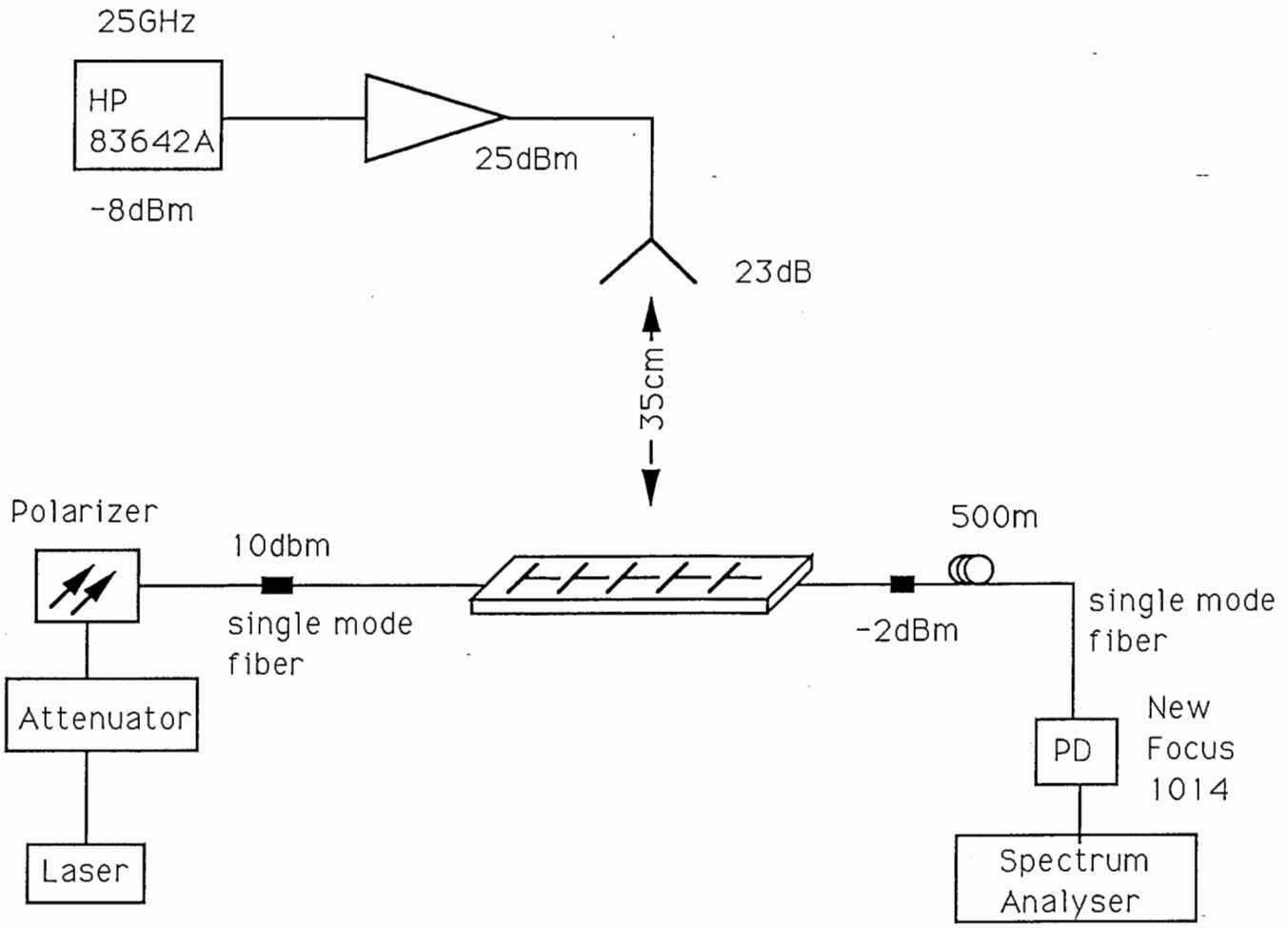

Figure 3-10 Quasi-optic modulator measurements. Experimental set-up

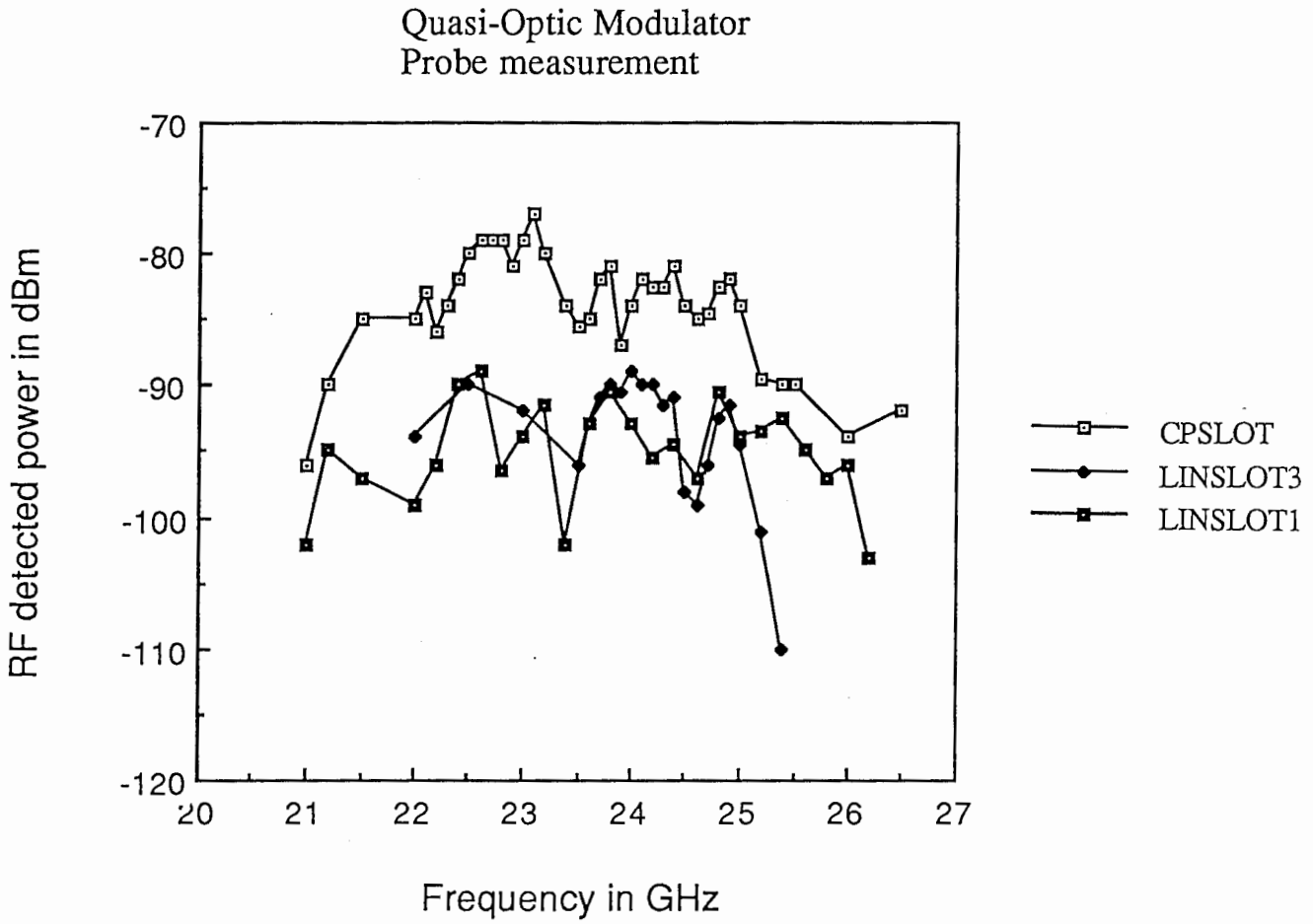
Quasi-Optic Modulator
Probe measurement
RF detected power in dBm
-70
-80
-90
-100
-110
-120
20
21
22
23
24
25
26
27
Frequency in GHz
CPSLOT
LINSLOT3
LINSLOT1

Figure 3-11

4 SLOT ANTENNAS ON ALUMINA

We have designed and measured 5 different types of slot antennas (figure 4-1) at 20Ghz on alumina 254μm and 630μm.

- Design 1 : 0.5λg linear slot , inductive coupling with coplanar waveguide
- Design 2 0.5λg linear slot, capacitive coupling
- Design 3 λg linear slot, inductive coupling
- Design 4 Square slot, total length is λg , inductive coupling
- Design 5 Modified square slot,

The analysis method is based on a transmission line model developed by University of Rennes France[13]. Radiation losses are computed and introduced as extra loss in the transmission line attenuation factor. The slot antenna is modeled as two lossy transmission lines short circuited and in parallel. This is illustrated figure 4-2.

4-1 Linear slot antenna (figure 4-2)

4-1-1 Slot design

University of Rennes provided the following basic parameters :

- Zc: Slot line characteristic impedance
- εr: Effective dielectric constant at 20GHz
- α: total loss due to radiation and dielectric.

The slot is 0.5 wavelength in dielectric. Taking into account the end effect, the actual physical dimension can be approximated by:

$$L=0.5\ \lambda g - h/2$$

where h is the substrate thickness, L is the slot length

w is the slot width

Parameters given below are for slot antenna without ground plane

h=254μm

w mm	Zc ohms	εeff	α NP/m	L mm
200μm	102	3.36	11.66	3.94
100μm	81.3	3.72	8.858	3.76

h=630μm

w mm	Zc ohms	εeff	α NP/m	L mm
200μm	86.4	4.51	8.554	3.22
400μm	11	4.308	11.27	3.27

4-1-2 Input impedance versus feed position

Antenna dimensions and substrate parameters are given figure 4-2.
The input impedance for a center fed antenna is very high, around 2000 ohms. (figure 4-3-a) This is major problem if we want to characterized the antenna. But, as shown on figure 4-3-b the impedance is extremely sensitive to the feed position. The impedance varies with the feed position as a raised sinus:

$$Zin = Z_{center}\ Sin^2(\pi\ dx\ /(L+h/2))$$

Zcenter is the input impedance for a center fed antenna
dx is the feed posotion referenced to the slot edge (see figure 4-2)

Input impedance for various feed position are tabulated below, around the resonant frequency.

x (mm) / xd / Freq	3.60 0.350	3.65 0.300	3.70 0.250	3.75 0.200	1.97 1.97
19.6GHz	149.6 +j76	110 +j59	70.3 +j43.8	49.7 +j30.7	1700 +j1000
19.8GHz	136 -j50	100.7 -j34	70.37 -j21.15	45.25 -j11	2100 -j583

Impedance function of the feed position

The slot antenna can be matched to 50 Ω when the feed is moved very close to the slot edge, but the value of the impedance is extremely sensitive, 100µm variation is enough to increase the input impedance from 50Ω to 110 Ω, this accuracy is difficult to achieve with a standard technology.
In the case of 630µm alumina thickness it is even impossible to achieve 50 ohms impedance.

So given those conditions we did not even try to match the antenna to 50 ohms, but just moved the feed point toward the slot edge in order to get a return loss that would allow us to do some radiation measurements.

4-2 excitation

All the different type of slot antennas are excited by a tapered coplanar waveguide. Dimensions were calculated with Touchstone. Connections between the slot and the central conductor of the coplanar line are made by wire bonding. A direct connection of the central connector would have been far better, but at that time of the design we did not consider that type of connection.

4-3 Measurements

4-3-1 Antenna dimensions

Total alumina board dimensions are 2cm by 2cm

Linear slots

thickness	L mm 254µm	L mm 630µm	xd mm 254µm	xd mm 630µm	w mm 254µm	w mm 630µm
Slot 1	3.662	3.22	0.193	0.190	0.100	0.200
Slot 2	3.762	3.22	0.300	0.300	0.100	0.200
Slot 3	6.788	6.540	3.394	3.27	0.200	0.400

Square slots

Total perimeter L of the square slots is equal to one wavelength in dielectric. In the table is given average side length. For slot 5, xw is width of the window, yw is height of the window.

thickness	254µm L/4 mm	630µm L/4 mm	254µm w mm	630µm w mm
Slot 4	2.045	1.750	0.200	0.400
Slot 5 Window	2.045 xw=1.277 yw=0.500	1.750 xw=1.220 yw=0.500	0.200	0.400

Coplanar feed line

All the antennas are excited by the same feed line. Dimensions are given in figure 4-4.

4-3-2 Impedance and radiation measurements.

The connection to a coplanar waveguide is very difficult to achieve, a good ground contact is necessary. We used connectors from Cascade (see appendix 1) which were available in the lab. Transmission coefficient and return loss of a straight coplanar line are given figure 4 -5 , for alumina 254µm. Return loss is around -10 dB except at 20GHz (we are lucky) where it is about -25dB

for-1.6dB transmission loss. This is due first to the connection, and also probably to transverse resonances in the substrate (width is more than one wavelength in free space). Usually it is necessary to reduce the ground plane width to cut off these modes; But here we are limited by the antenna dimensions. A narrow ground plane would modified the antenna characteristics.

- All the antennas are assembled on a plastic test fixture.
- All the results are for antennas without ground plane.

- *Calibration for impedance measurements*:
It was too difficult with the type of connector we used, to do a good calibration in the plane of the slot, so the measurement plane is at the input of the coplanar line .

- *Radiation characteristics* were measured in the antenna group small anechoic chamber. The receiver is the HP network analyser.
Precise measurements of single printed antennas is always very difficult because of their very low directivity. So gain characteristics we are giving here are just an indication that the antenna is working or not, and allow us to compare the different types of slots. Gain figures are given after matching corrections. Slot antennas have bidirectionnal radiations characteristics, so we expect to measure gain at least 3dB lower than for patch antenna or less in case of linear slot which have a very wide radiation pattern.
Radiation patterns were only measured in the H plane (more directive) . All antenna people know how depressing it is to look at an E plane pattern, so let stay happy !!

a) Linear slot antenna on 254µm Alumina

We have made a complete set of measurements of the linear slot antenna on 254µm thickness alumina, and we have compare with theory. In figure 4-5 shows measured and theoretical curve calculated using the method described above. The antenna is well matched. The connection between the coplanar waveguide and the slot is modeled by an inductor for the wire bonding and by a capacitor to the ground for the coplanar line end effect. The tapered coplanar waveguide is modeled as a line with different sections. So for the following theoretical parameters: L=3.95mm, xd=.200mm, l=.2nH and c=.050pF we find a very encouraging agreement between theory and experiment.

Gain and cross polarization measurement in function of frequency are given figure 4-6.

Maximum gain occurs at 19.5Ghz. Cross polarization is about -15dB at 19.5Ghz. Radiation patterns (figure 4- 7) show typical characteristics.

b) Comparison between different types of slot antennas.

We could not get good measurement conditions in the case of antennas on 630μm alumina thickness. We think that is due to connection problems or/and to transverse modes in the substrate.

a) One wavelength slots

Figures 4-8 a,b,c and 4-9 a,b,c we can compare the one wavelength long slots (slot 3) on 254μm and 630μm alumina thickness.

As expected, gain is slightly higher than for 1/2 wavelength slot.

The slot printed on 630mm is better matched, has a wider gain bandwidth and better cross polarization characteristics.

b) 1/2 wavelength slot on 630μm thickness figure 4-10

Although the input impedance is matched to 50Ω, we measured 0dB or negative gain.

c) Square slot antennas. Figure 4-11 and figure 4-12

Measurements for 630μm thickness were too difficult , and results not very satisfying.

We will only compare square slots for 254μm thickness.

Square slots are more directive in the E plane than linear 1/2λg slot, so the gain is higher (figure 4-11). Figure 4-12 shows that when a window is open in the center conductor of the slot, the resonant frequency is shifted from 19.5GHz to 20GHz and the gain is smaller. Some power must be lost in the substrate or diffracted.

4-3 Conclusion

The results are encouraging. Theory seems to fit well with experiment in the case of the 1/2λg slot. Measurements on 630μm thick alumina where difficult to achieve. More measurements with better connectors and more accurate calibration are needed for better characterization and comparison of the different types of slots.

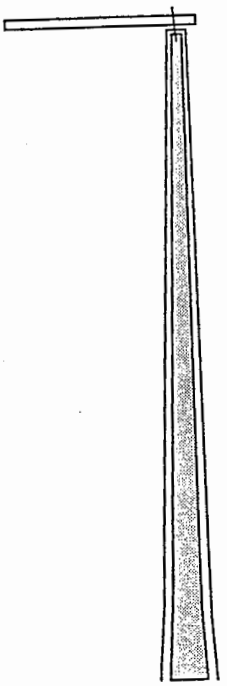

Type 1

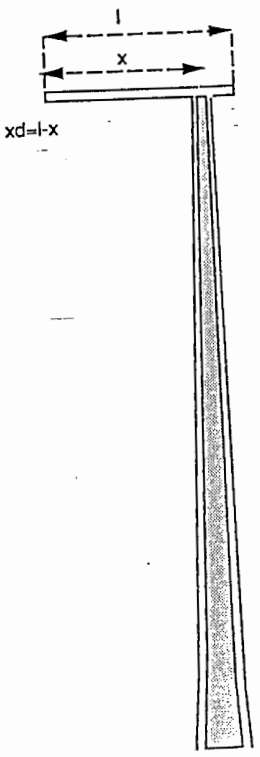

Type 2

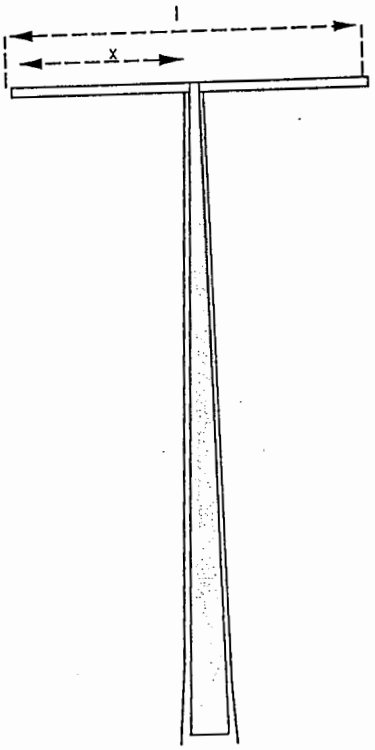

Type 3

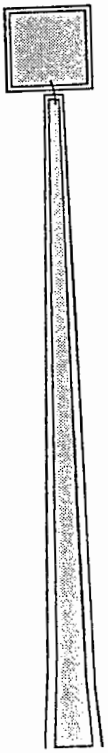

Type 4

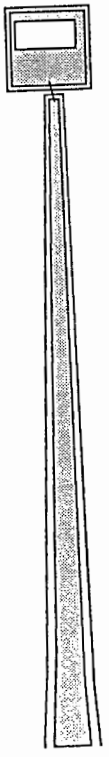

Type 5

Figure 4-1

Slot impedance in function of feed position
Reference Plane is located at A-A', Theory

l=3.95mm
1) x=3.60mm, xd=0.350mm
2) x=3.65mm, xd=0.300mm
3) x=3.70mm, xd=0.250mm
4) x=3.75mm, xd=0.200mm

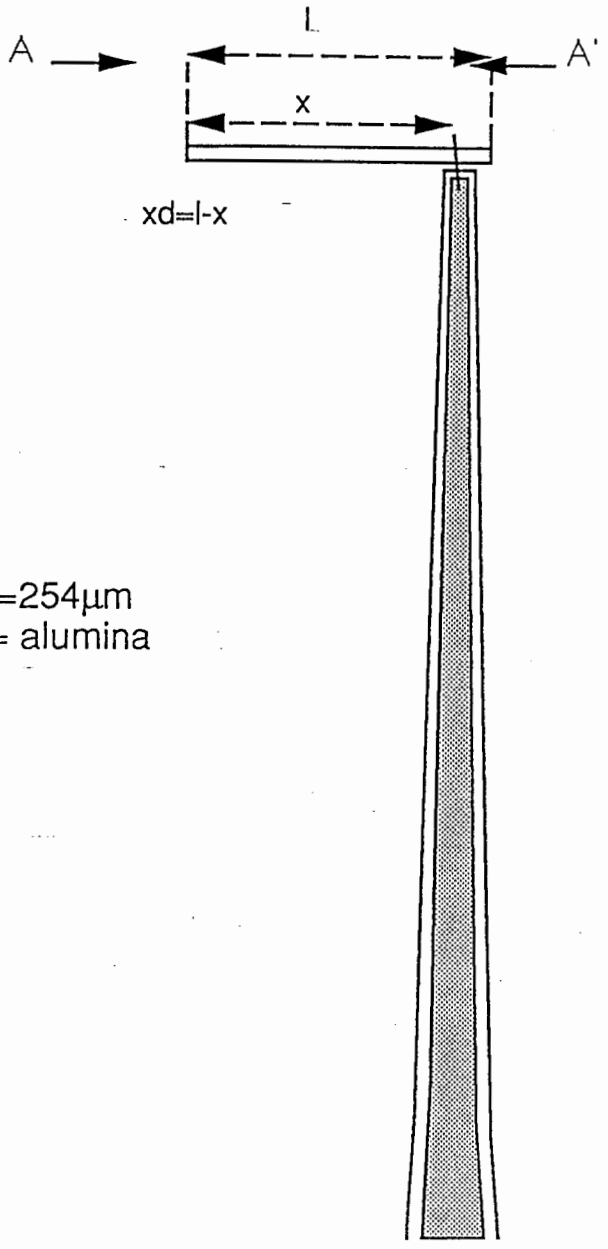

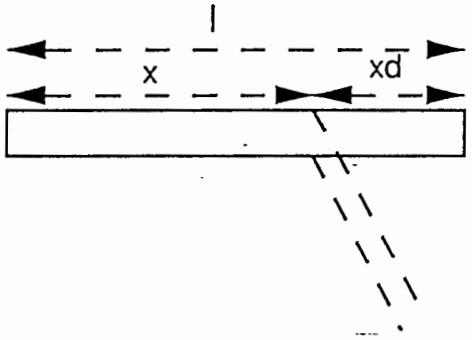

w=100µm
Thickness=254µm
Substrate= alumina

The slot is modelized as two short circuited transmission lines.

Zc=81.3ohms
er=3.716
loss 0.076dB/mm

Type 1

Figure 4-2

EEsof - Touchstone -

SLOT254

□ S11
DIPOL1

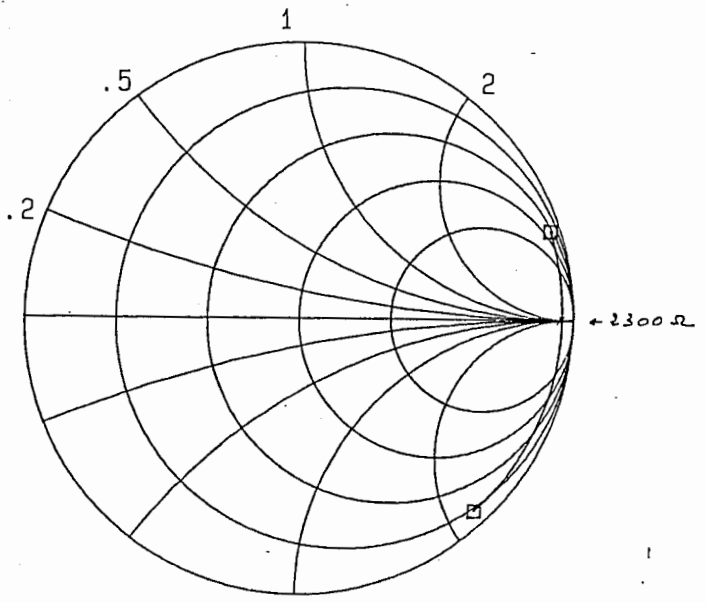

f1: 18.0000 GHz
f2: 24.0000 GHz
STEP 0.2

FIGURE 4-3a

SLOT254

l=3.95mm
1) x=3.60mm, xd=0.350mm
2) x=3.65mm, xd=0.300mm
3) x=3.70mm, xd=0.250mm
4) x=3.75mm, xd=0.200mm

1) □ S11
DIPOL1

2) + S11
DIPOL2

3) ◇ S11
DIPOL3

4) × S11
DIPOL4

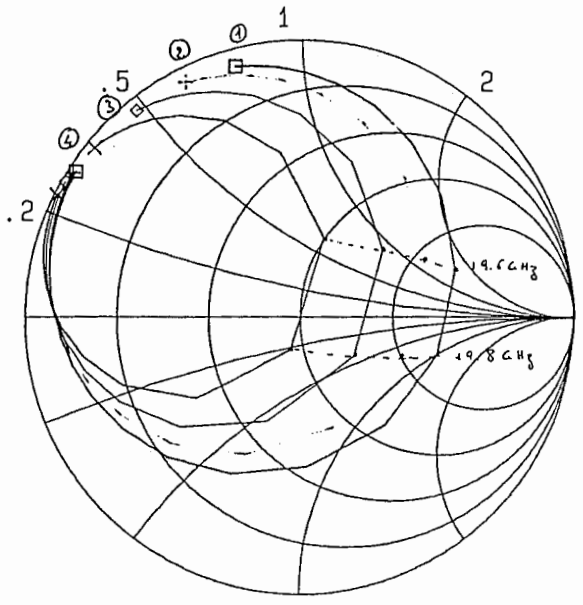

f1: 18.0000
f2: 24.0000
STEP 0.2

Figure 4-3-b

DETAIL E

254 µm.

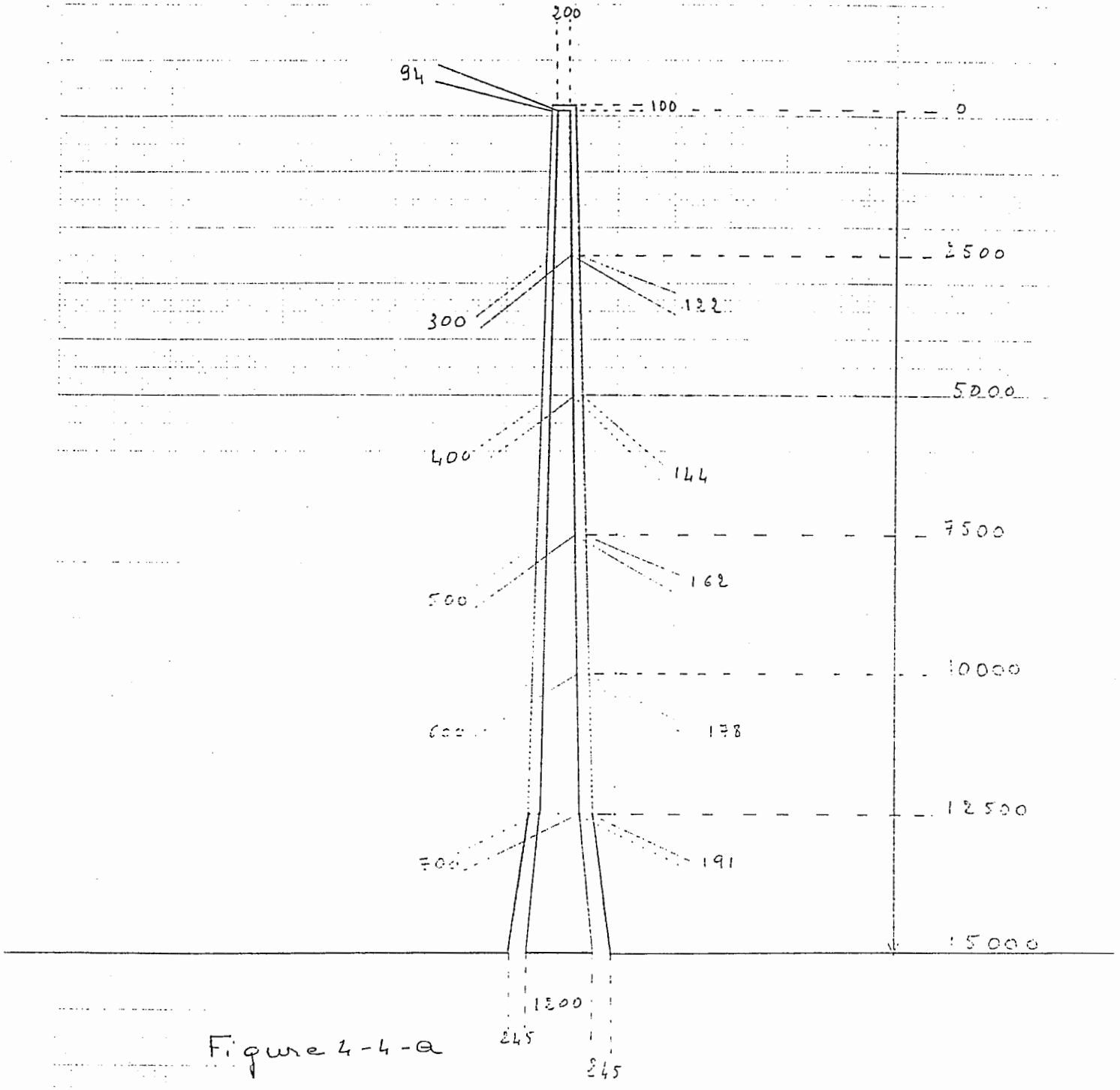

Figure 4-4-a

LOCAL - 630

Dimensions in Microns

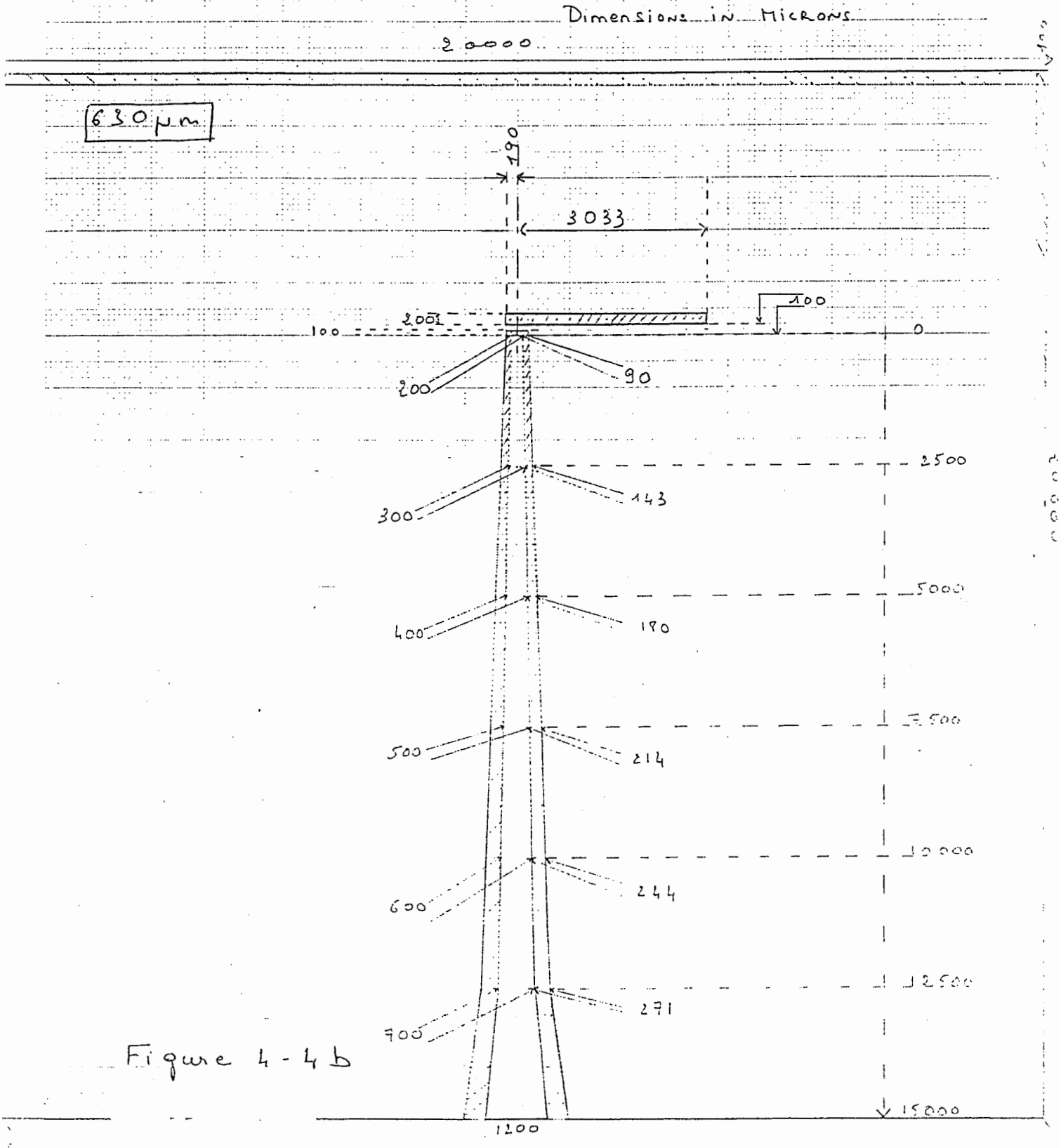

Figure 4-4b

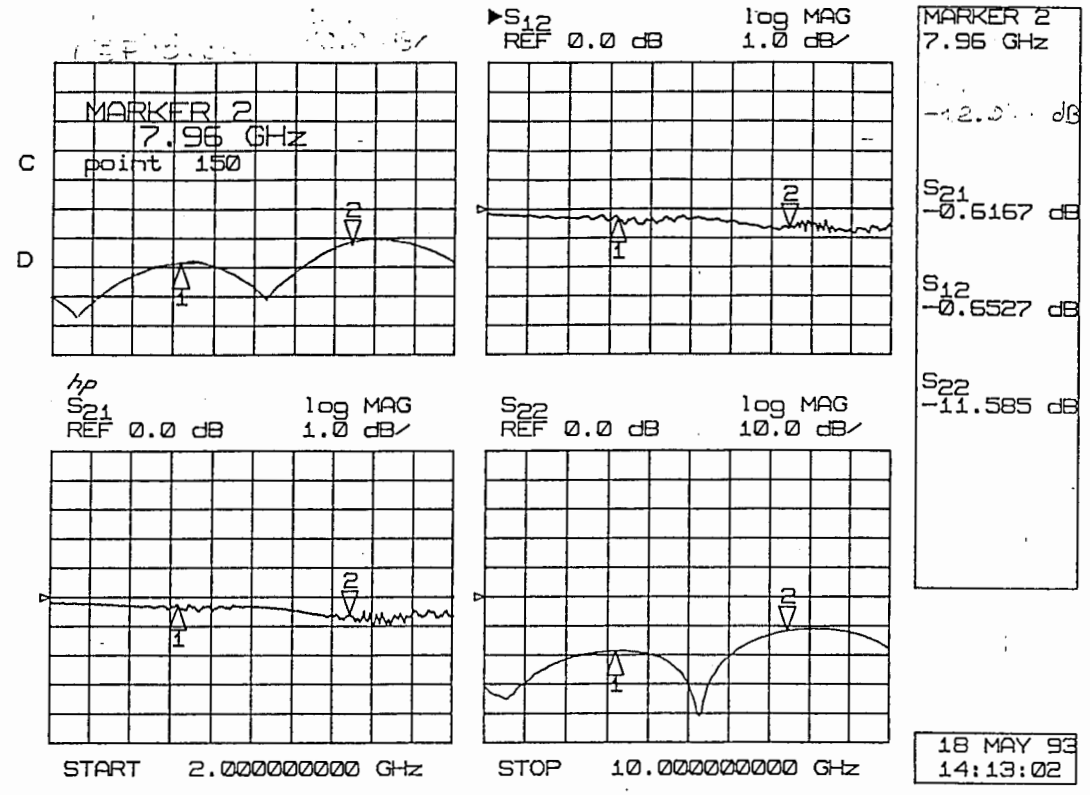
MARKER 2
7.96 GHz
point 150
C
D
S12
REF 0.0 dB
log MAG
1.0 dB/
MARKER 2
7.96 GHz
S21
-0.6167 dB
S12
-0.6527 dB
S22
-11.585 dB
hp
S21
REF 0.0 dB
log MAG
1.0 dB/
S22
REF 0.0 dB
log MAG
10.0 dB/
START 2.000000000 GHz
STOP 10.000000000 GHz
18 MAY 93
14:13:02

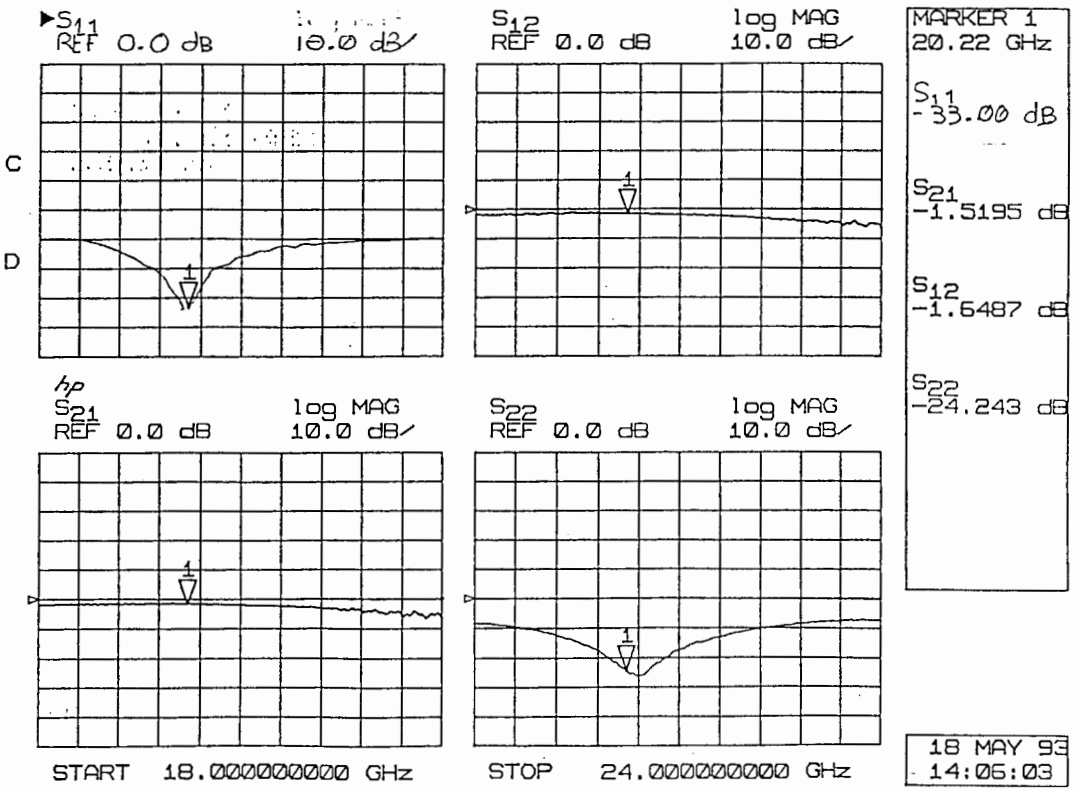
S11
REF 0.0 dB
10.0 dB/
C
D
S12
REF 0.0 dB
log MAG
10.0 dB/
MARKER 1
20.22 GHz
S11
-33.00 dB
S21
-1.5195 dB
S12
-1.6487 dB
S22
-24.243 dB
hp
S21
REF 0.0 dB
log MAG
10.0 dB/
S22
REF 0.0 dB
log MAG
10.0 dB/
START 18.000000000 GHz
STOP 24.000000000 GHz
18 MAY 93
14:06:03

Figure 4-5

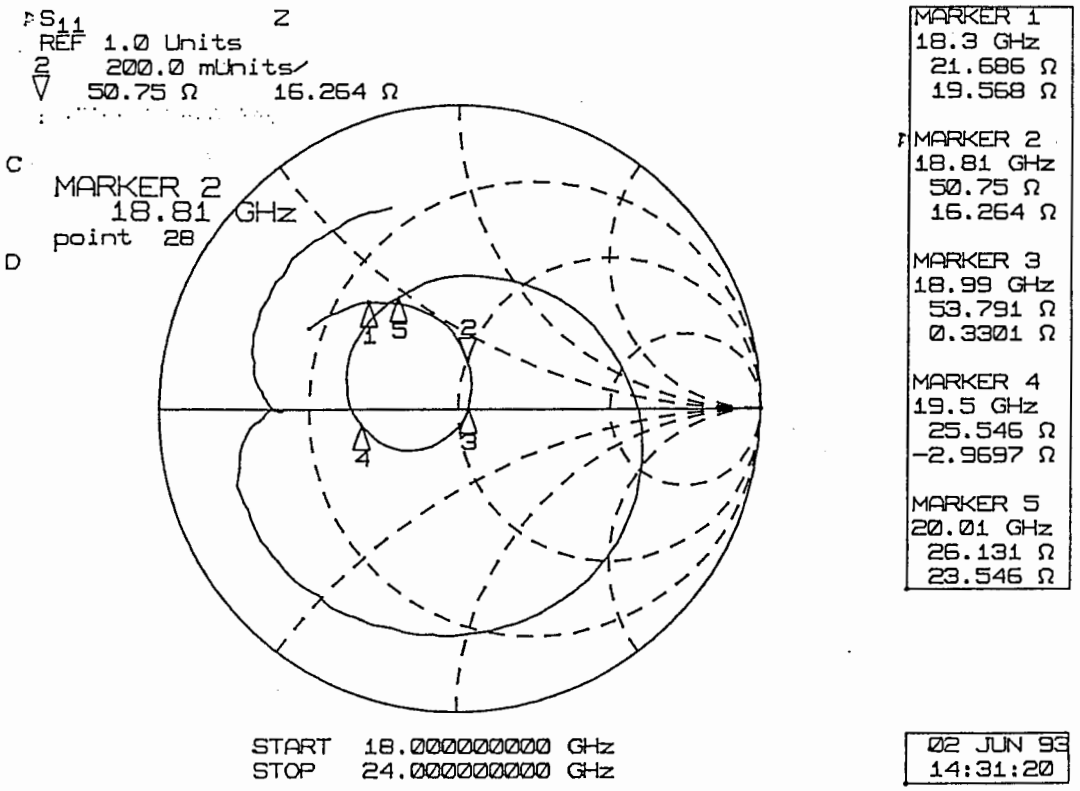

Figure 4-5-a Experiment

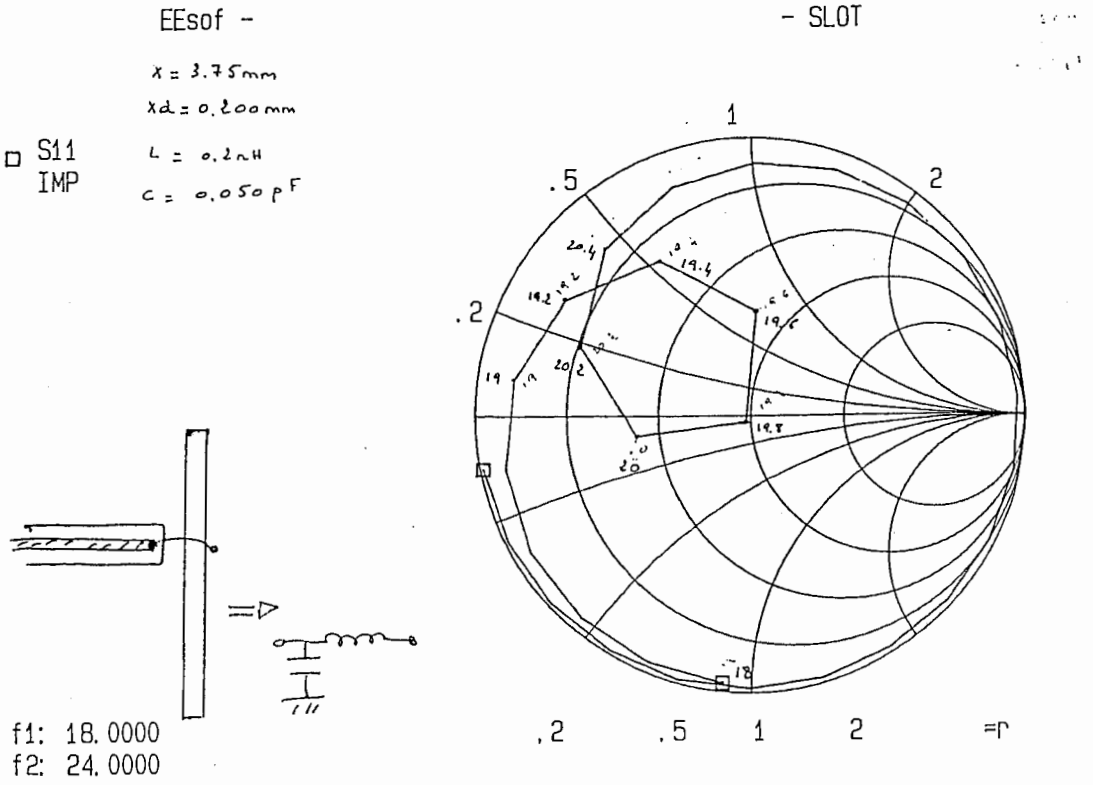

Figure 4-5-b Calculations.

Gain Slot 1
Thickness 254um

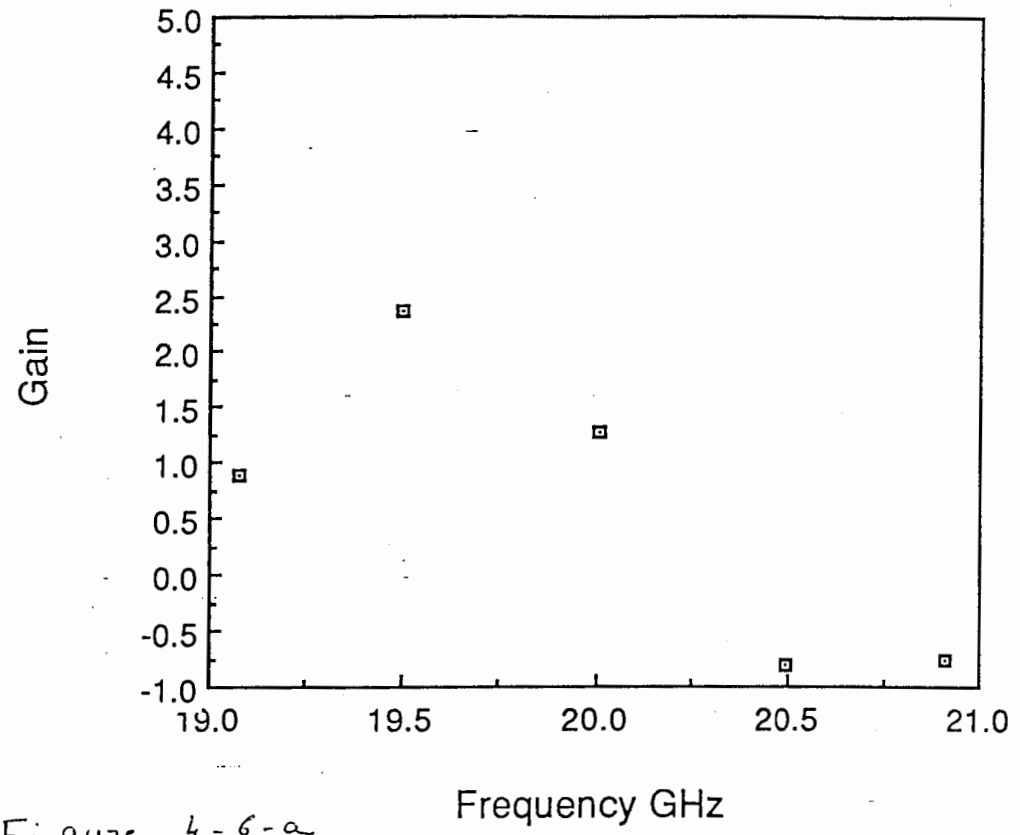

Figure 4-6-a

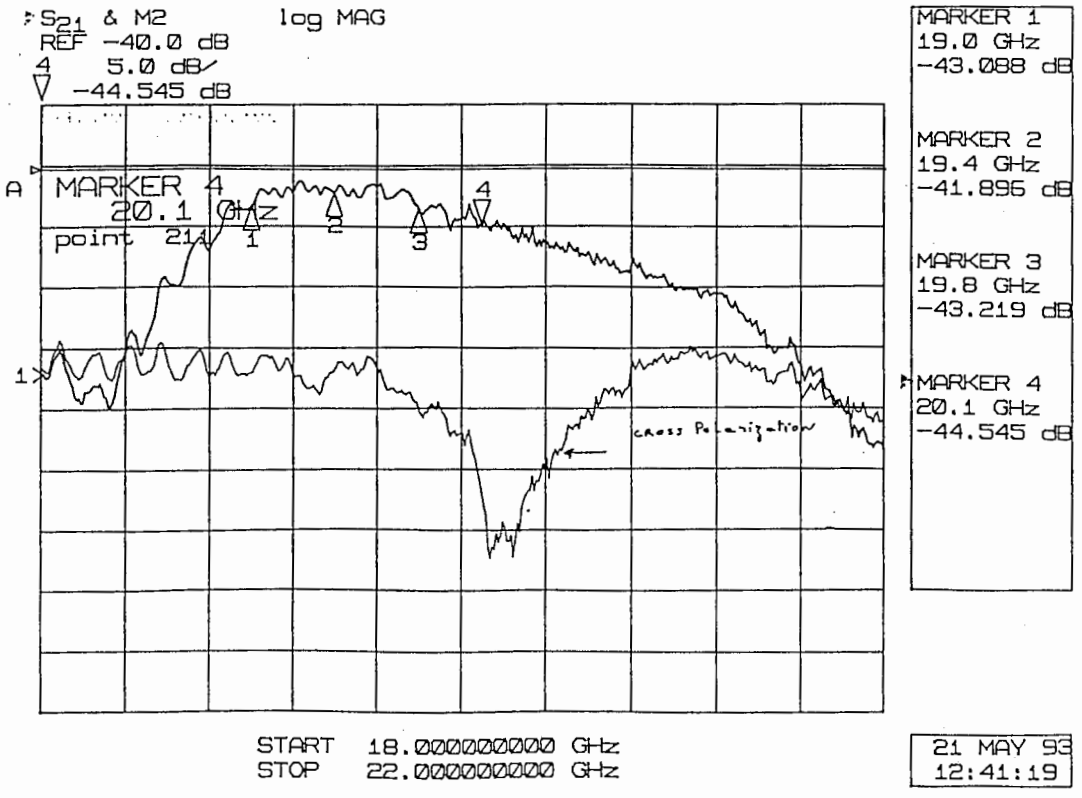

Figure 4-6-b

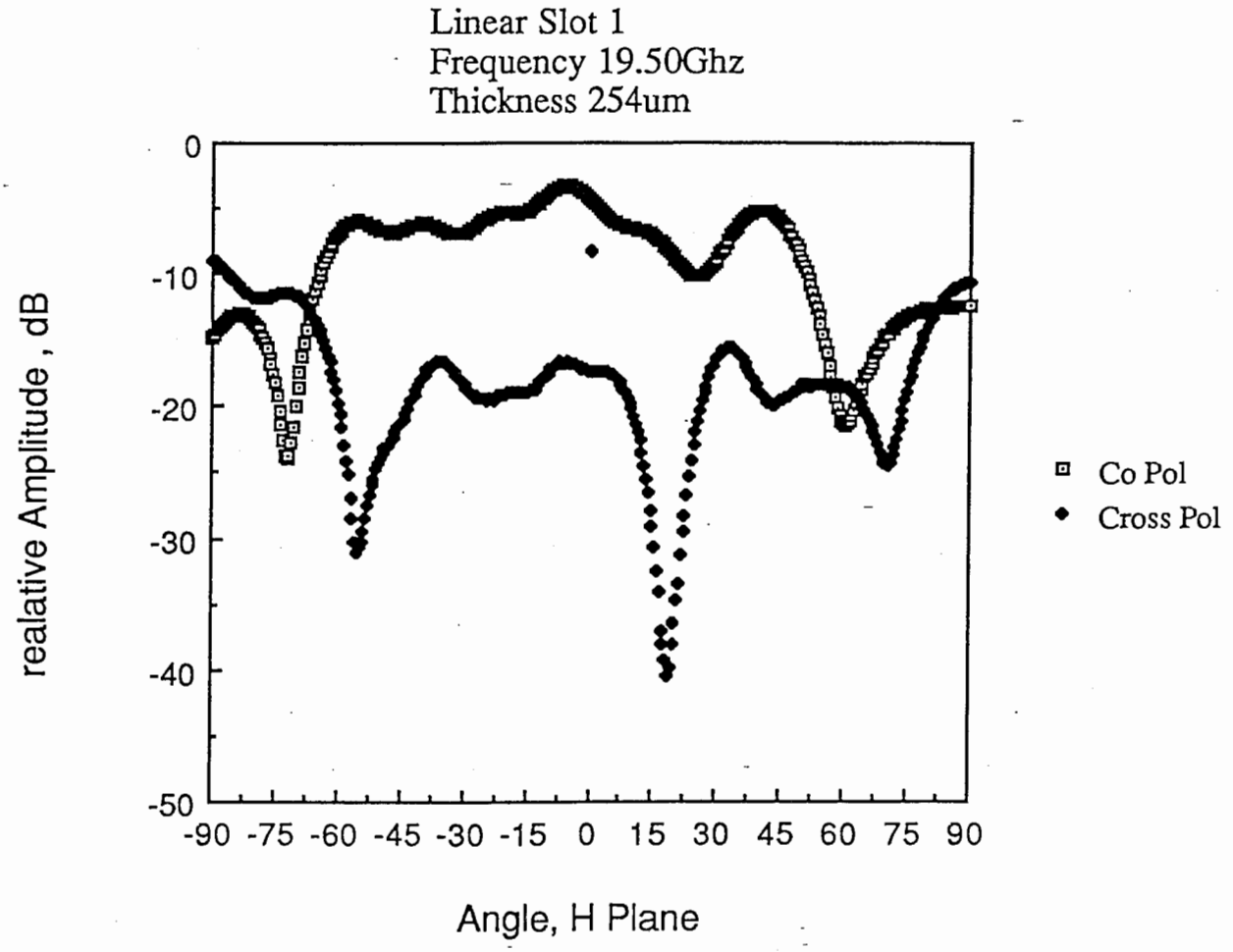
Linear Slot 1
Frequency 19.50Ghz
Thickness 254um
realative Amplitude , dB
0
-10
-20
-30
-40
-50
-90 -75 -60 -45 -30 -15 0 15 30 45 60 75 90
Angle, H Plane
Co Pol
Cross Pol

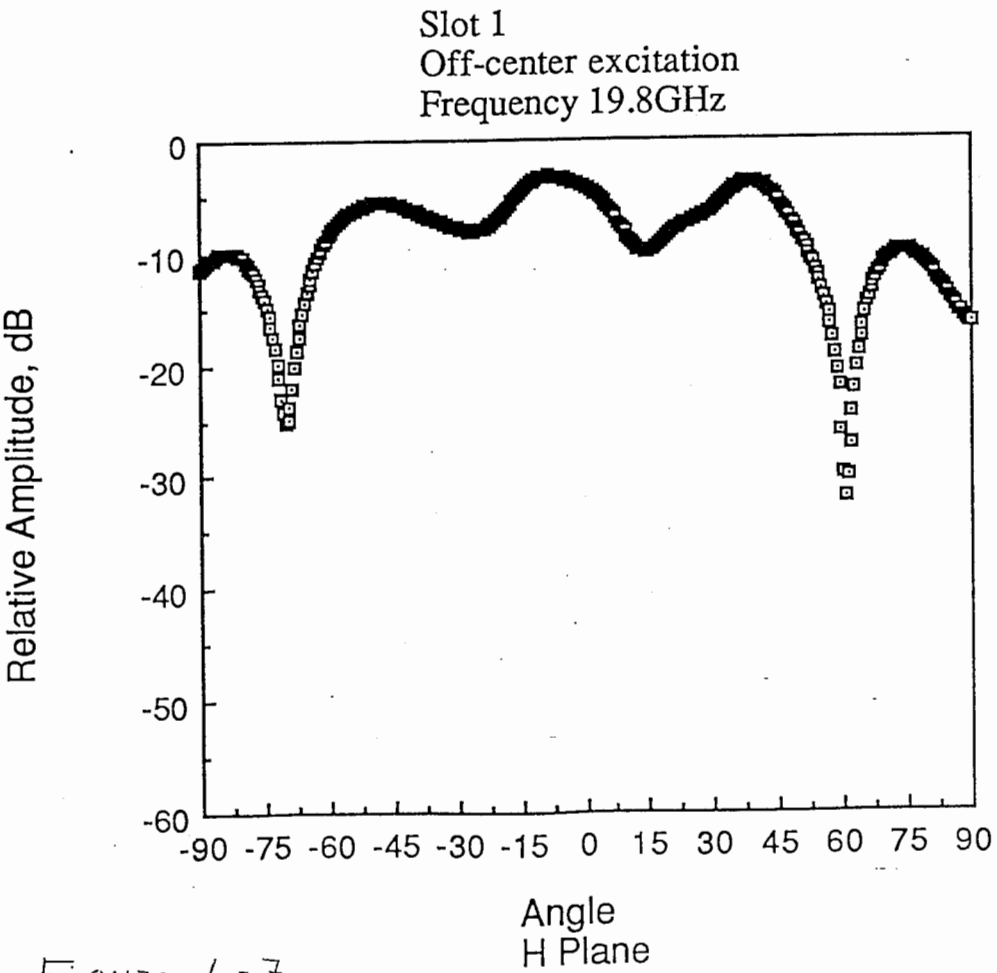
Slot 1
Off-center excitation
Frequency 19.8GHz
Relative Amplitude, dB
0
-10
-20
-30
-40
-50
-60
-90 -75 -60 -45 -30 -15 0 15 30 45 60 75 90
Angle
H Plane

Figure 4-7

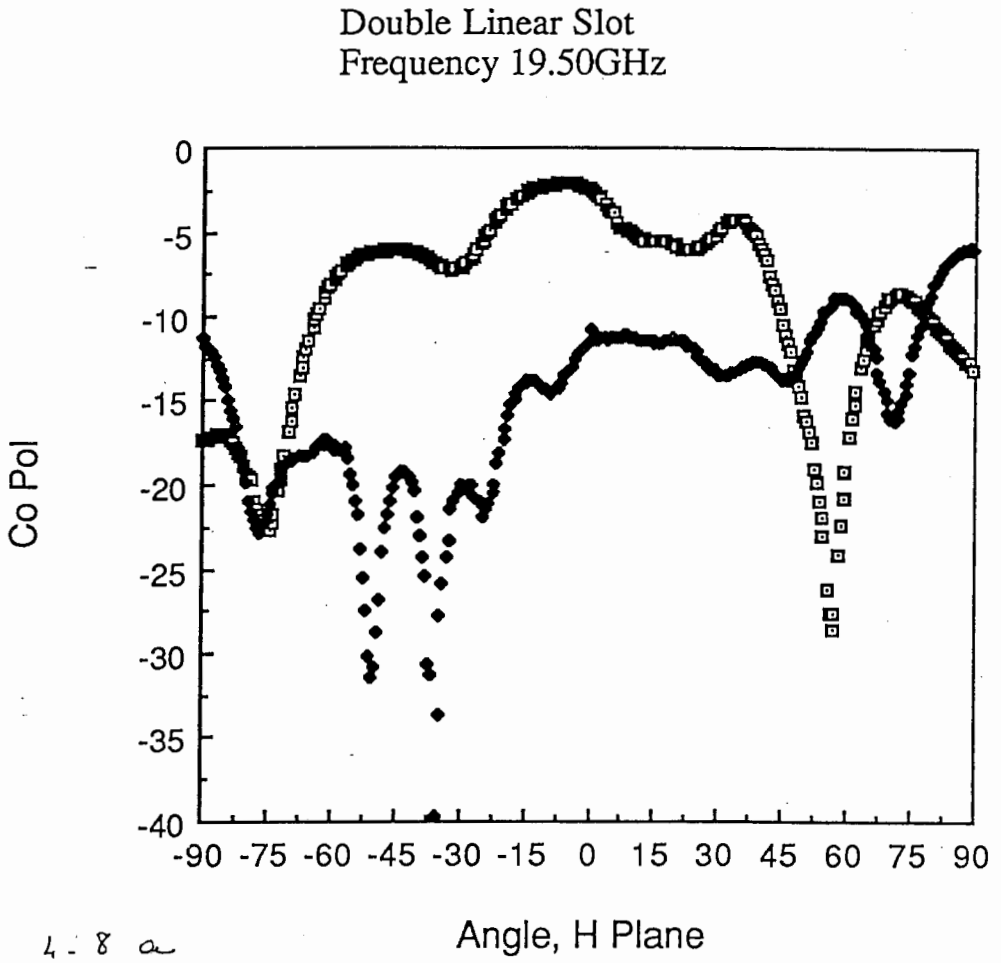

Figure 4-8 a

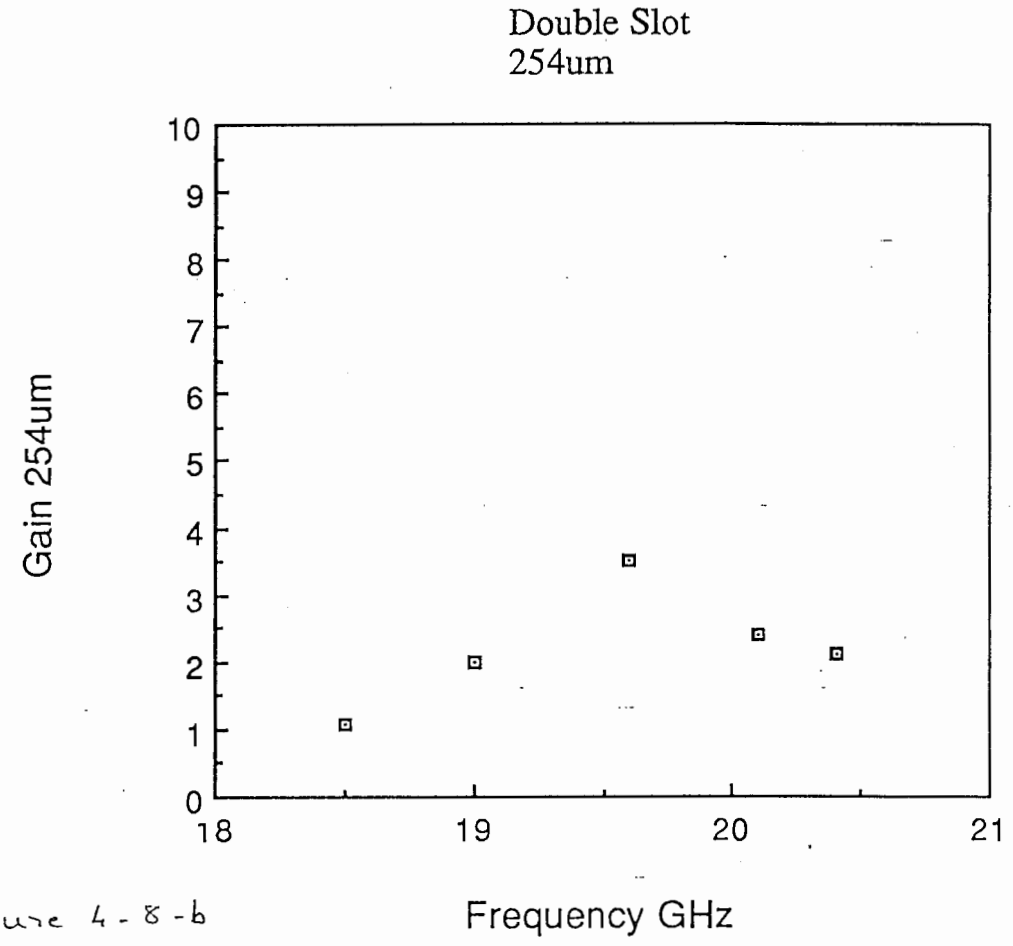

Figure 4-8-b

h = 254 μm

h = 254 μm

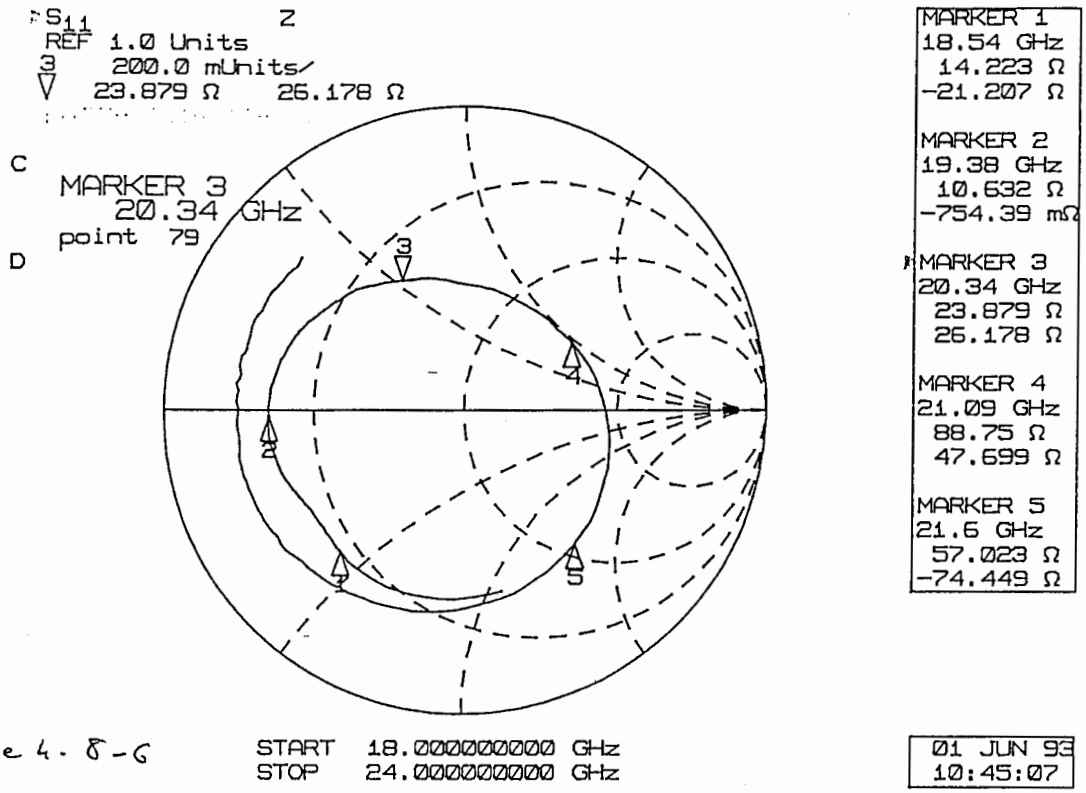

Figure 4.8-6

h = 630μm

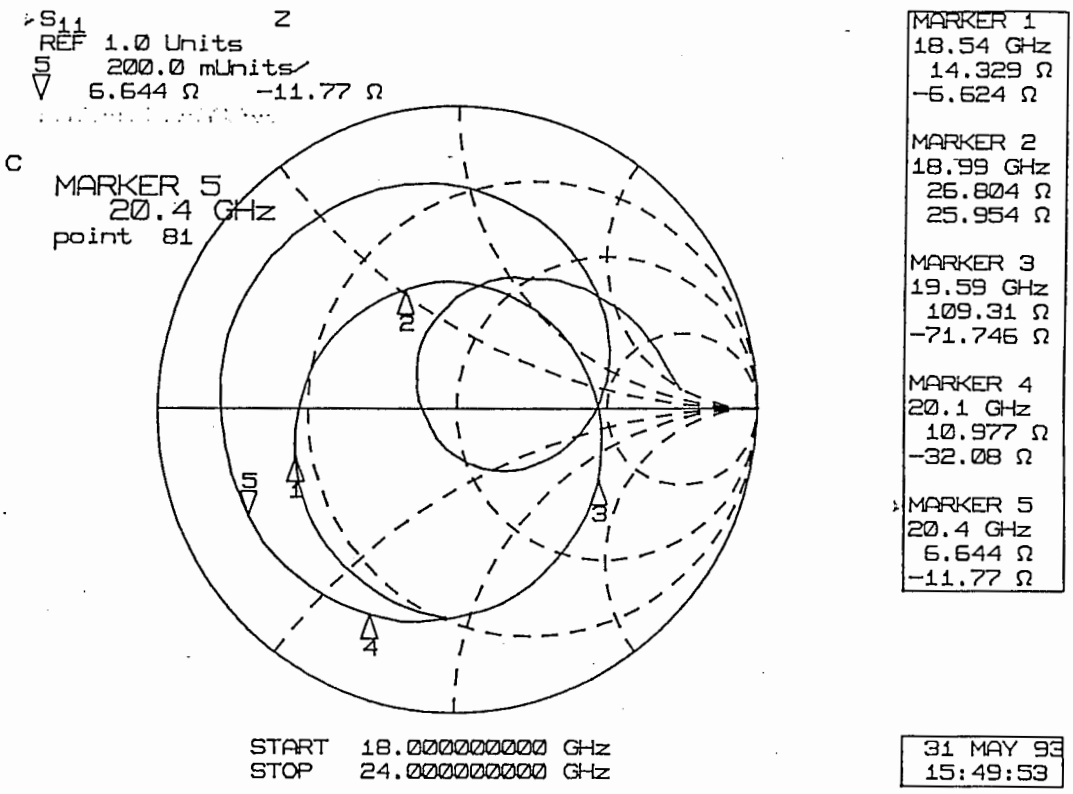

Figure 4.9.a

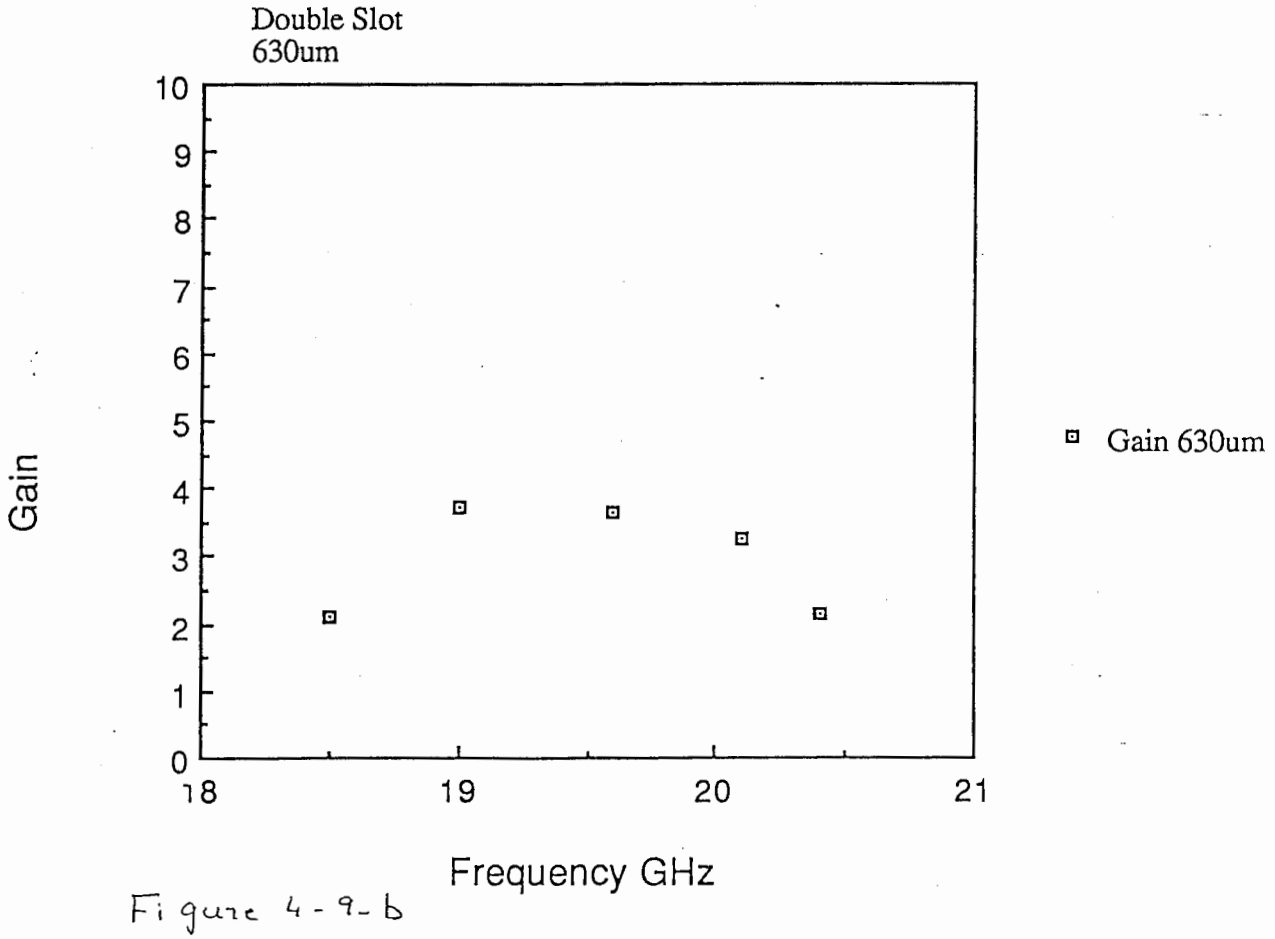

Figure 4-9-b

Double linear slot
Frequency 19.5GHz
Thickness 630um

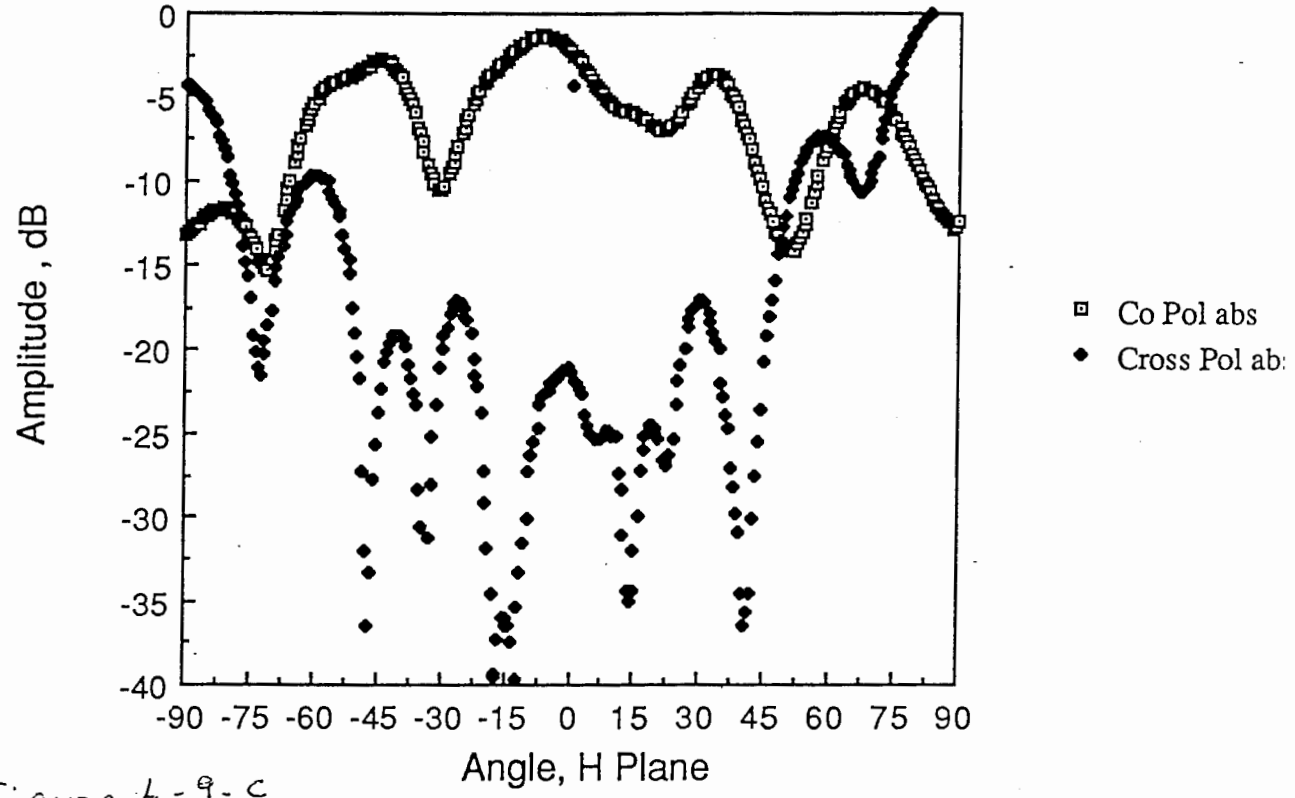

Figure 4-9-c

Double Linear Slot
Frequency 19.1GHz Thickness 630um

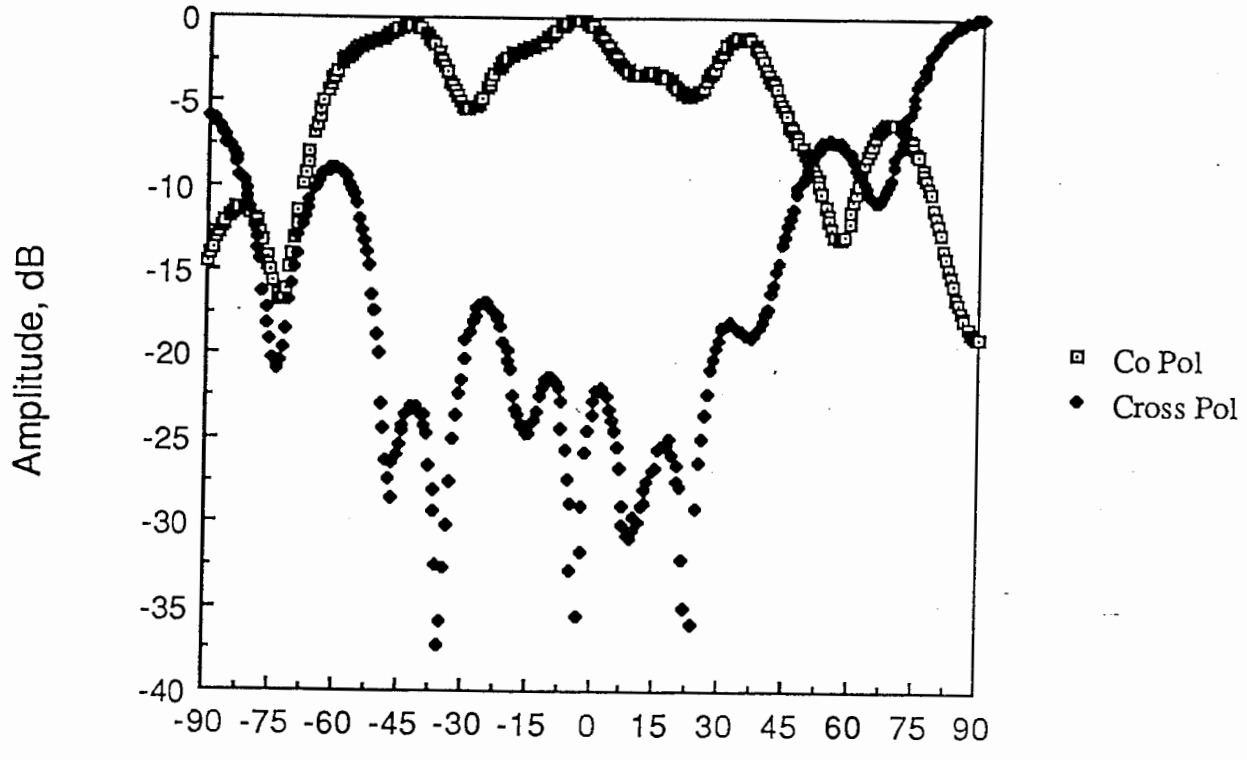

Figure 4-9-d.

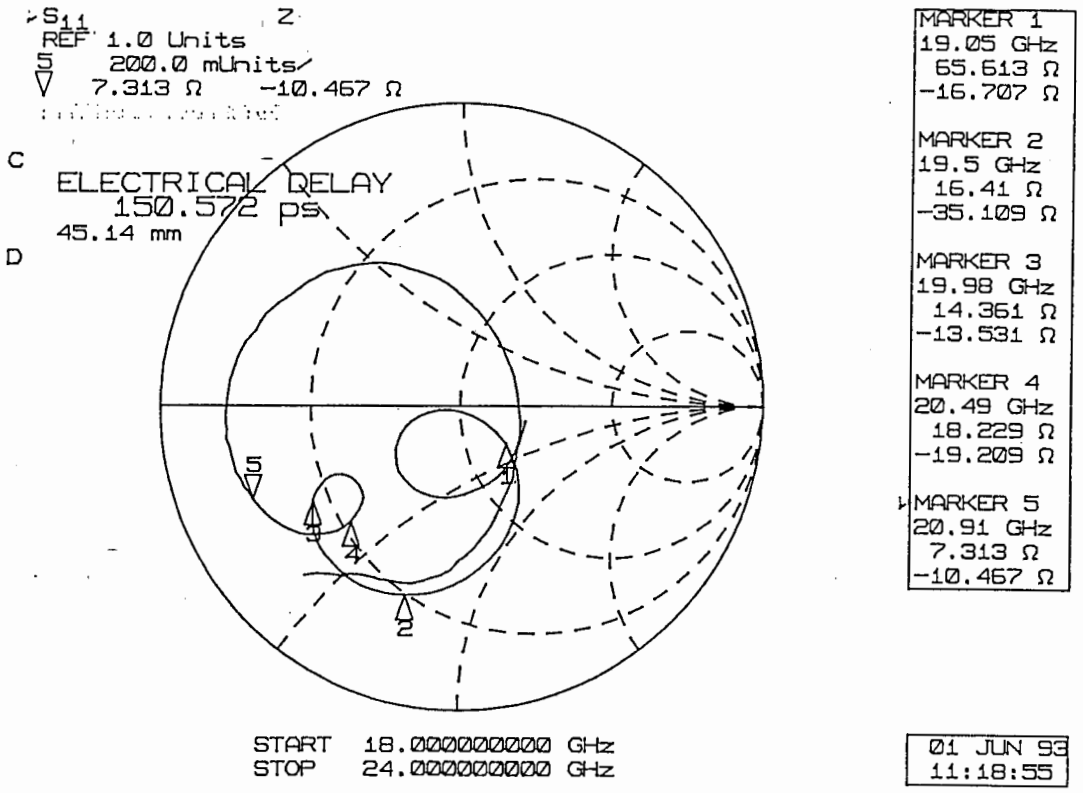
S11
REF 1.0 Units
200.0 mUnits/
7.313 Ω -10.467 Ω
ELECTRICAL DELAY
150.572 ps
45.14 mm
MARKER 1
19.05 GHz
65.613 Ω
-16.707 Ω
MARKER 2
19.5 GHz
16.41 Ω
-35.109 Ω
MARKER 3
19.98 GHz
14.361 Ω
-13.531 Ω
MARKER 4
20.49 GHz
18.229 Ω
-19.209 Ω
MARKER 5
20.91 GHz
7.313 Ω
-10.467 Ω
START 18.0000000000 GHz
STOP 24.0000000000 GHz
01 JUN 93
11:18:55

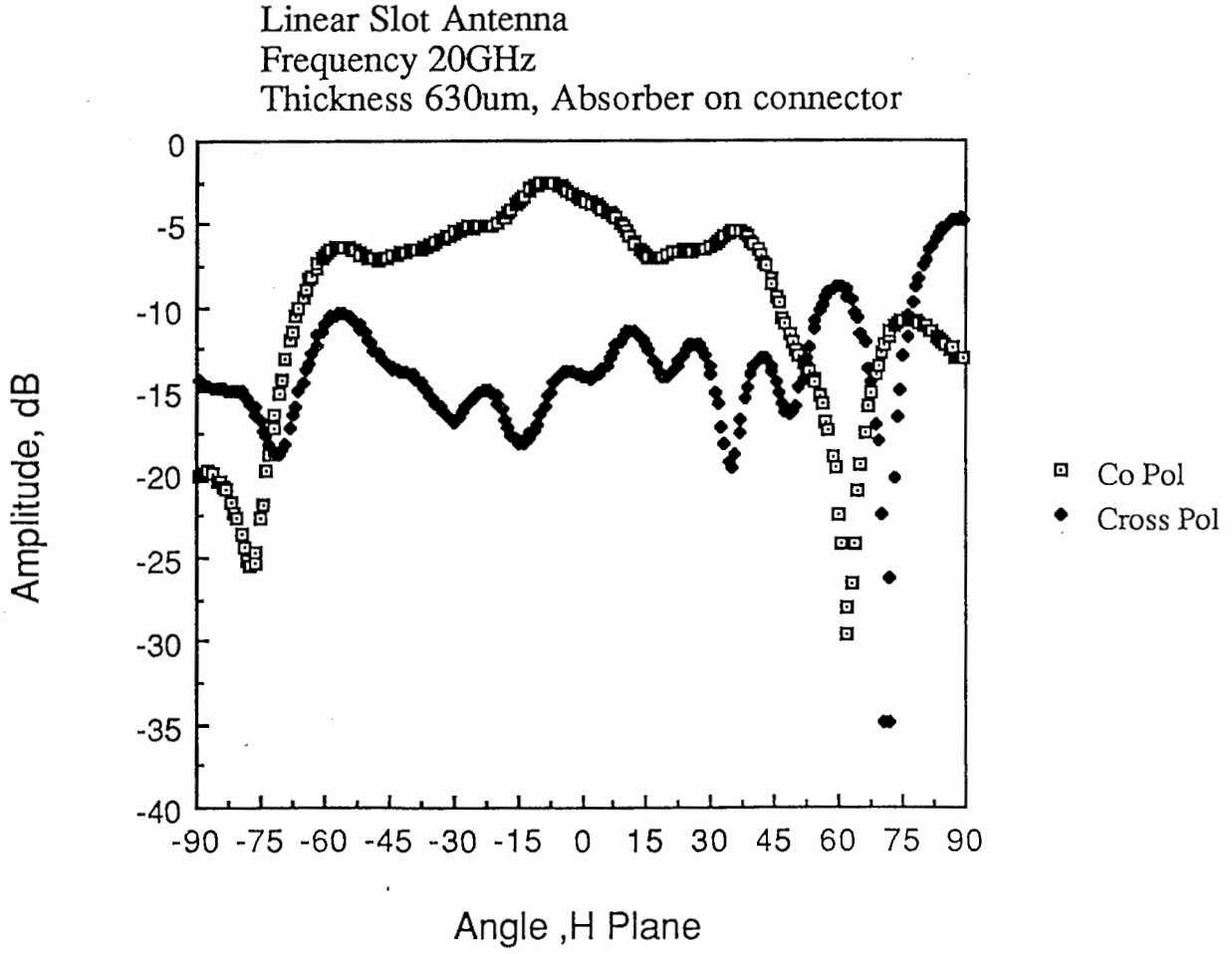
Linear Slot Antenna
Frequency 20GHz
Thickness 630um, Absorber on connector
Amplitude, dB
0
-5
-10
-15
-20
-25
-30
-35
-40
-90 -75 -60 -45 -30 -15 0 15 30 45 60 75 90
Angle ,H Plane
Co Pol
Cross Pol

Figure 4-10

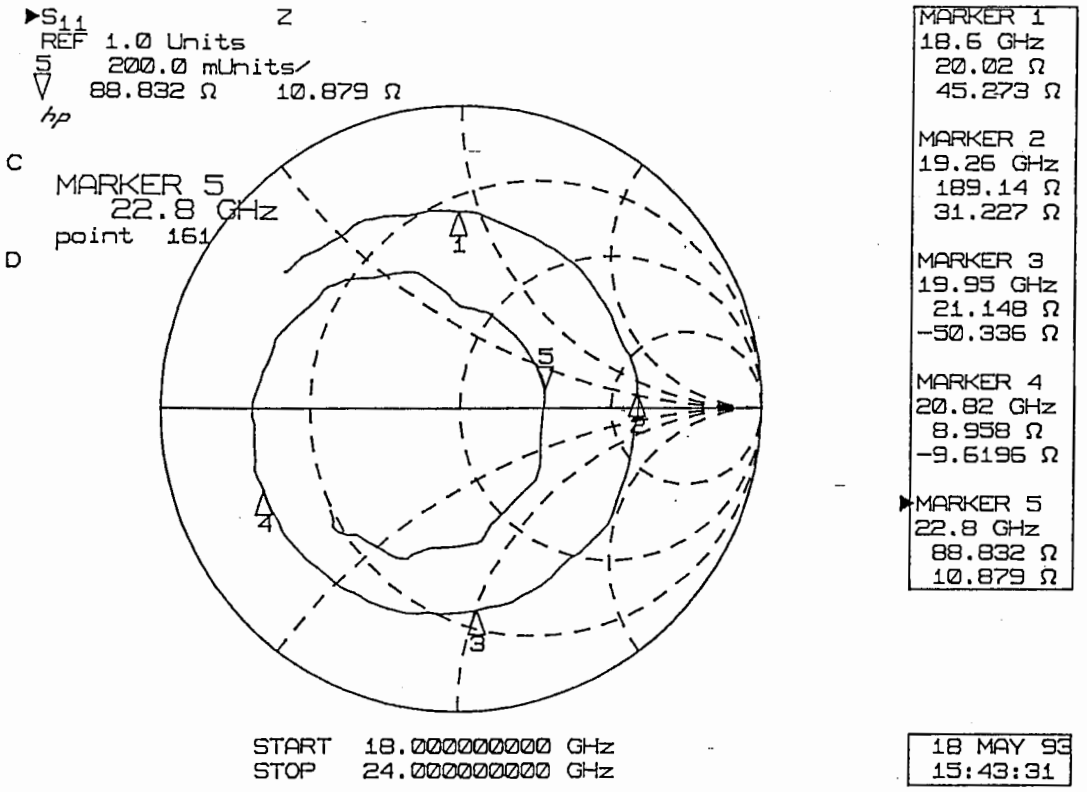

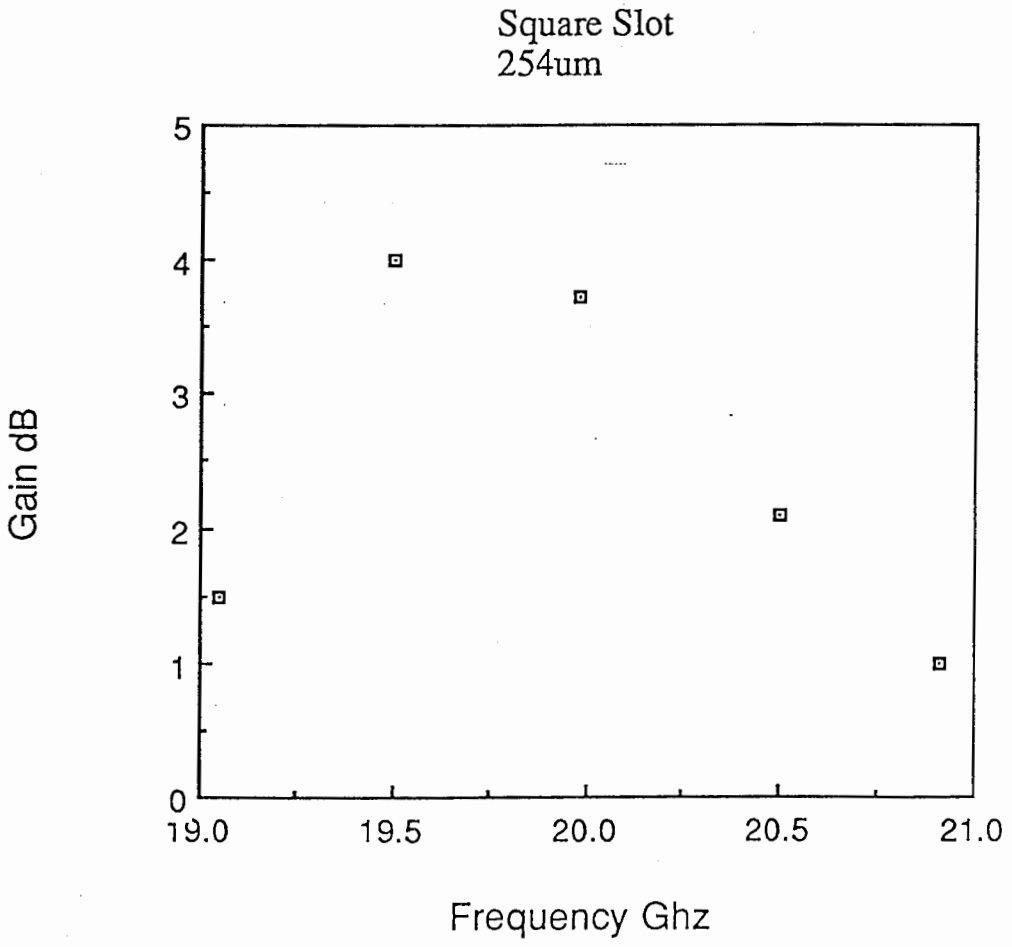

Figure 4-11-a Square slot

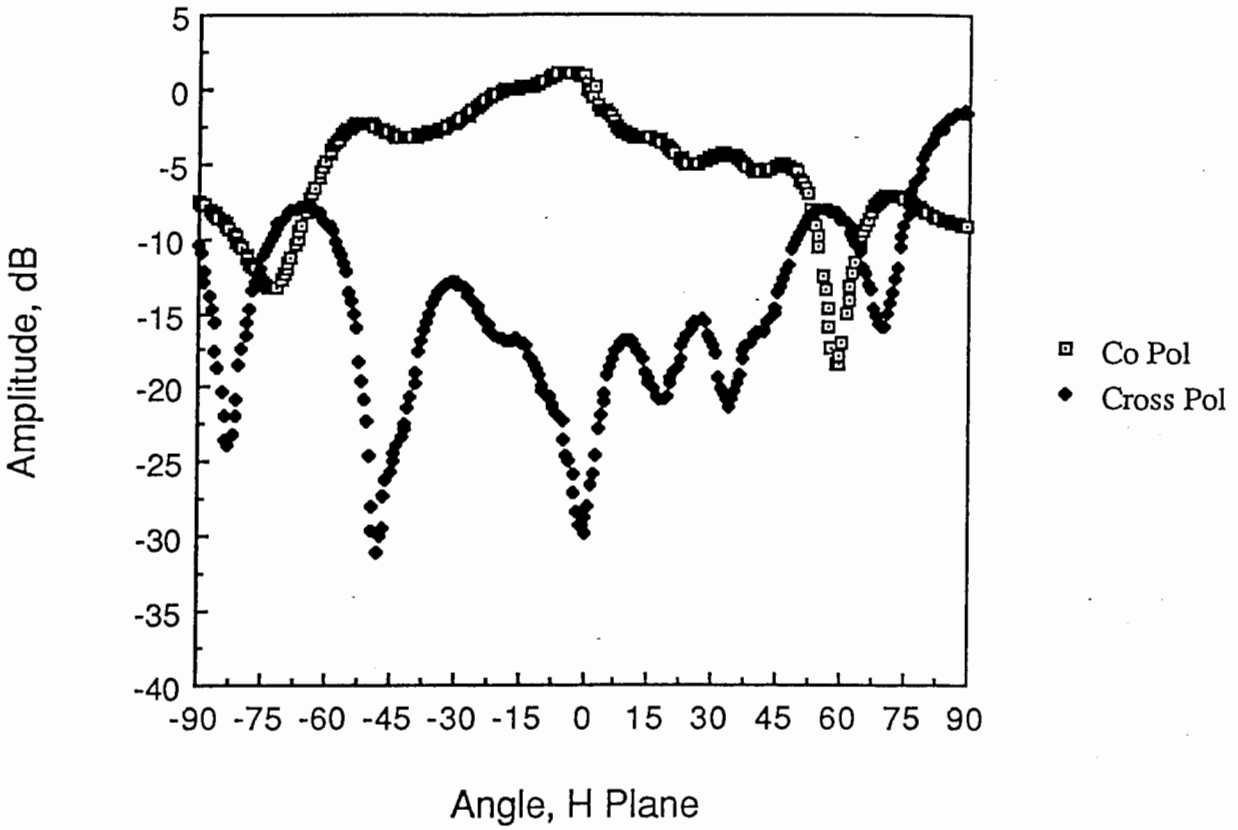

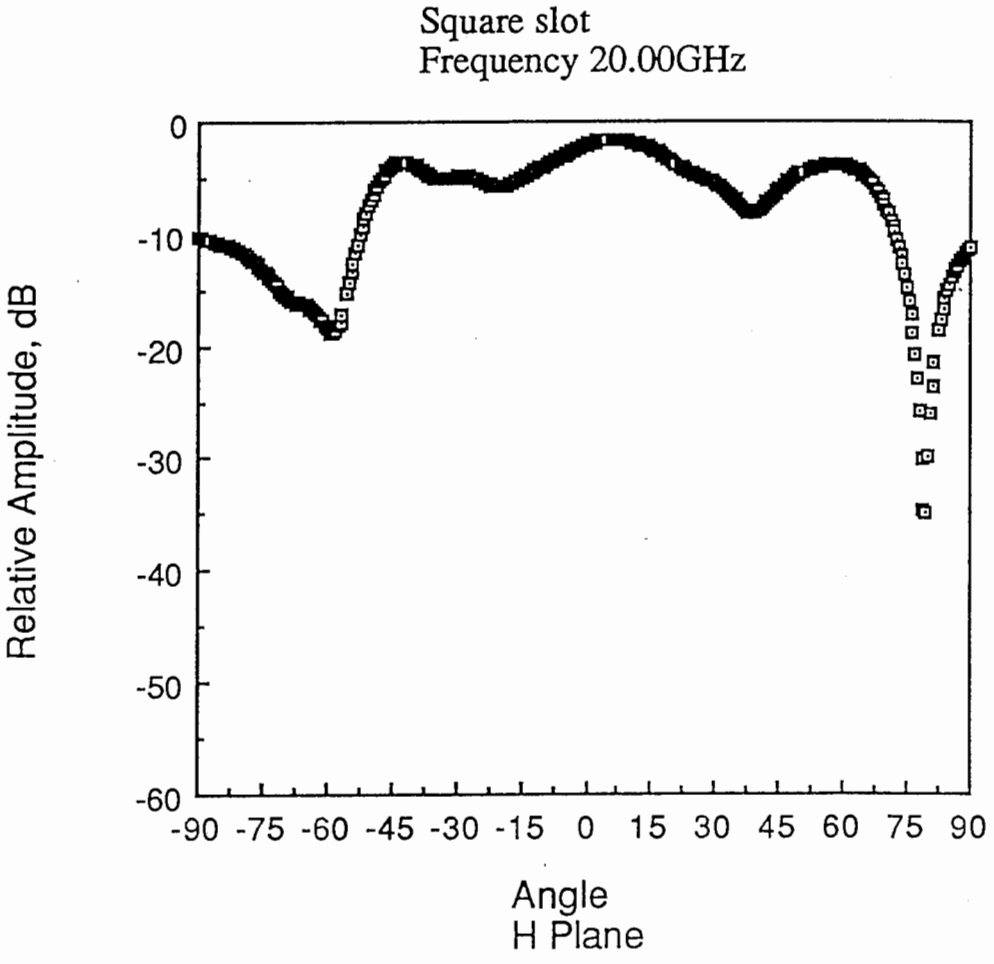

Figure 4-11-b. square slot

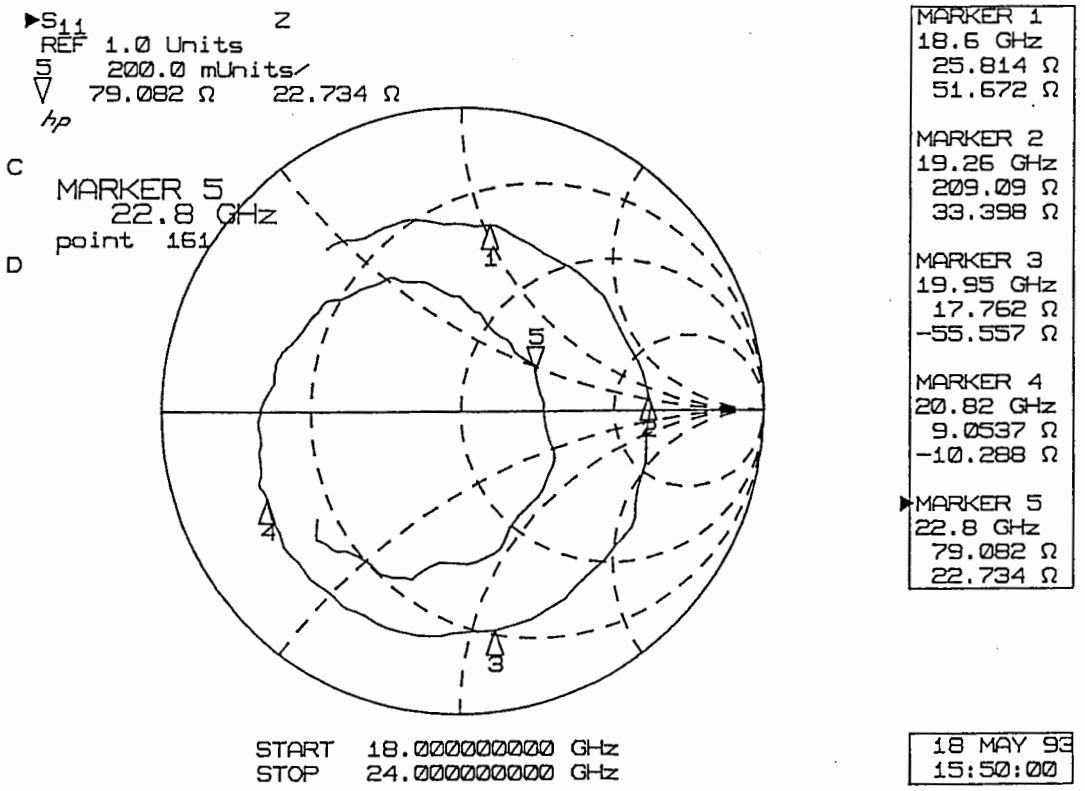

Square Slot 4
Thickness 254um

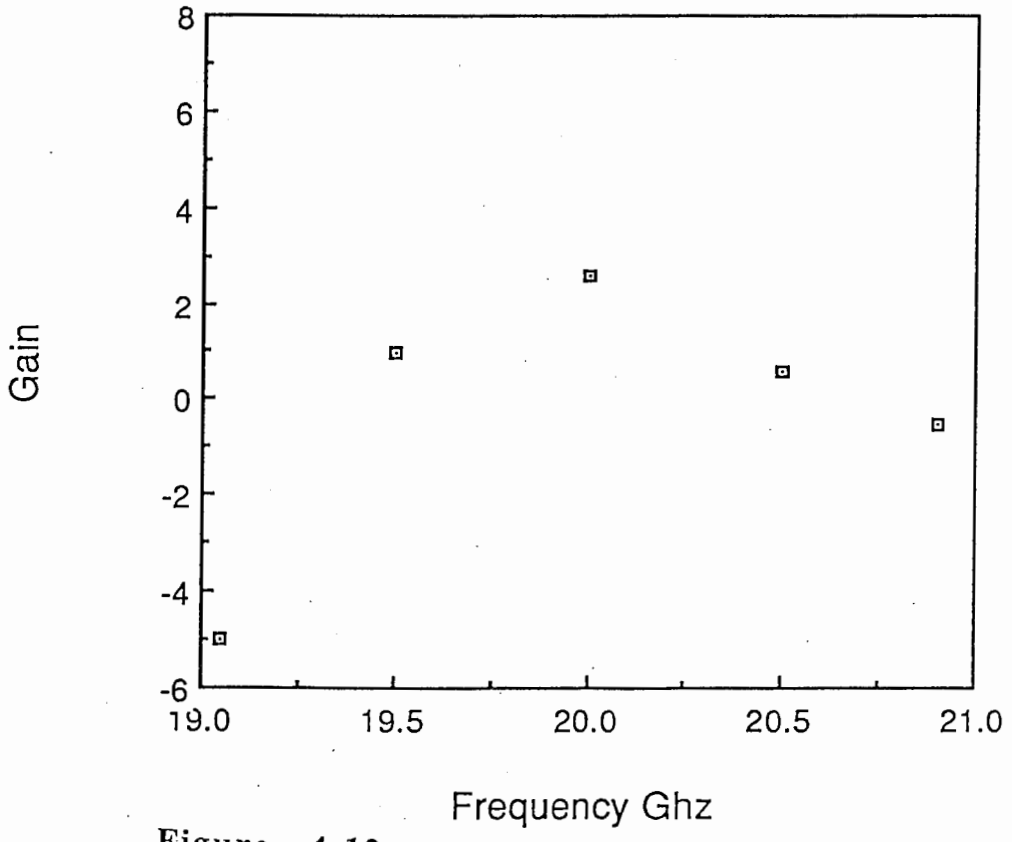

Figure 4-12

Square slot with window.

5 CONCLUSION

During this past 6 months we have initiated a research on a quasi-optic modulator.
We have demonstrated that it is possible to modulate an optical signal by a free space radiated signal.
Before being able to conclude on the applicability of such modulator to a microwave/optic system, a lot of work remains to be done, an phenomena do be understood.

First, all the modulator should be measured in good conditions, with a polarization maintaining fiber and chip polarizer, without reflector plane and in a "clean " environment . Then it should be possible to make a fair comparison between the different designs. In these conditions the dynamic range, of such modulator should be measured, and the link loss calculated and compared with the link loss obtained with usual intensity modulator driven by the same RF power. We have shown that because the electrodes are very short, the sensitivity should be higher, and there is almost no problem of velocity matching.

A specific software should be developed to allow an accurate design of the antennas.

The substrate thickness should be reduced in order to eliminate the modes propagating into the substrate.

A better design, the development of wide bandwidth antennas, a good analysis of the measurements should lead to an improvement of a second design and better characteristics of the modulator.

[[1] Waveguide Electrooptic Modulator
R Alferness
IEEE MTT August 1982

[2] Velocity-Matching Techniques for Integrated Optic Travelling wave switch/Modulator
R Alferness, S K Korotky, E A Martcatili
IEEE Journal of Quantum Electronics Vol QE-20 N°3 March 1984

[3] Velocity- Matched Electro-Optic Modulator
W B Bridges and F T Sheehy J Schaffner
Spie Vol 1371 High frequency Analog Fiber Optic System 1990
pp 68-77

[4] A small wideband Antenna printed on the same LiNbO3 Substrate as Integrated Optical Modulator
N Kuwabara, R Kobayashi, T Ideguchi, T Yoshino
proceeding ISAP'92 SAPPORO, pp817-820

[5] Broadband electromagnetic environment monitoring using semiconductor electroabsorption modulators
S A Pappert, S Lin.....
Spie Vol 1476 Optical Technology for microwave Applications V
1991 pp 282-293

[6] Theory of Integrated optic travelling wave modulator with phase reversal electrodes
D Erasme , M G Wilson
Spie Vol 651 integrated optical Circuit Engineering III 1986
pp 154-161

[7] Polifko D .ATR Technical report

[8] 40 GHz Ti:LiNbO3 Optical Modulator with a driving voltage of 3.6v
K Noguchi, O Mitomi, M Yanagibashi
OEC'92 Makuhari Messe PD-2

[9] 60GHz and 94 GHz Antenna coupled LiNbO3 Electro-optic Modulators.
F Sheehy, W Bridges, J H Shaffner
IEEE Photonics Technology letters March 1993 pp 307-310

[10] Analisys of a millimeter wave integrated electrooptic modulator with periodic electrode.

Spie Optoelectronic Signal Processing for phased-array Antennas II (1990)
J H Schaffner.

[11] Simplified Analysis of coplanar Waveguide for LiNbO3 Optical Modulator by variationnal method.
IEICE Trans Electron. February 1993
T Kitazawa, D Polifko, H Ogawa

[12] Radiation pattern of interfacial dipole antennas
N Engheta C H Paps
Radio Science, Nov-Dec 1982

[13] Transmission line model of various printed slot antenna shapes.
M Himdi, J. P. Daniel, M EL Yazidi
Proceeding of ISAP '92' Sapporo , Japan

[14] 40Ghz, low half-wave voltage Ti: LiNbO3 intensity modulator.
G. K. Gopalakrishnan, C H Bulmer and .....
Electronics Letters23 April 1992

appendix 1

MTF- SERIES MICROSTRIP TEST STATIONS

Figure 35 (detail C) shows the slider in contact with the device carrier bottom. The slider requires a clearance of 0.060" (1.52 mm). In figure 37 this clearance is noted to as "shoulder clearance."

Some devices will have protrusions that are above the carrier surface. The only restriction in measuring these devices is that the protrusion does not interfere with the optics and allows 25 mils (0.635 mm) distance from the carrier edge so the Eisenhart gap stop (fig. 35 (detail C, and D) will make proper contact. A typical microscope will require 50 mils (1.27 mm) clearance for viewing launcher pin alignment.

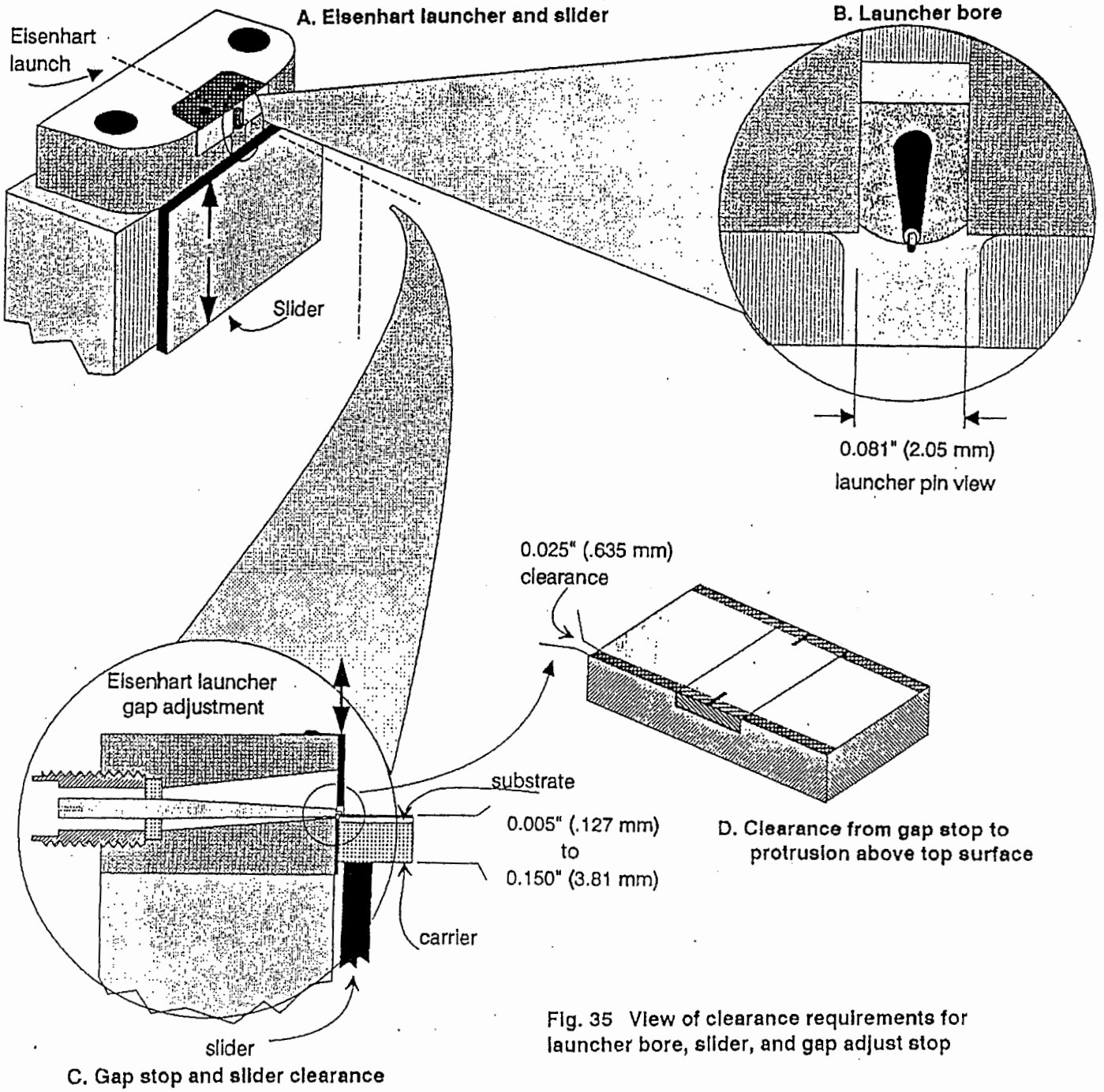

Fig. 35 View of clearance requirements for launcher bore, slider, and gap adjust stop

Appendix 2-a

Modulator lay-out

Minimum separation between antennas is 1mm

FOR PROBE MEASUREMENTS OF ANTENNAS

No interaction with optical waveguides, just for microwave measurements. Position of waveguides is ignored. Total wafer length can be used.

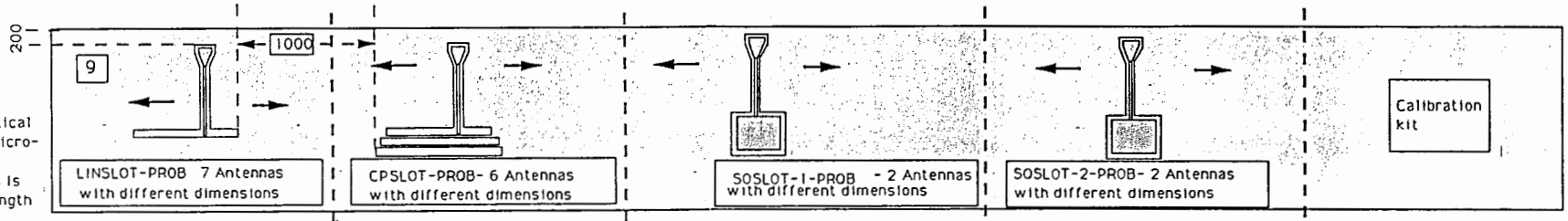

1) Ls=1190µm, Le= 50µm
2) Ls=1190µm, Le=100µm
3)Ls=1190µm, Le=150µm
4)Ls=1300µm,Le=100µm
5)Ls=1400µm, Le=100µm
6)Ls=1500µm, Le=100µm
7)Ls=1190µm,Le=595µm

1)LS1=1140µm,LS2=1190µm, LS3=1240µm, e=7µm
2)LS1=1140µm,LS2=1190µm LS3=1240µm,e=15µm
3)LS1=1140µm,LS2=1190µm LS3=1240µm,e=50µm
4)LS1=1090µm,LS2=1190µm LS3=1290µm,e=7µm
5)LS1=1090µm,LS2=1190µm LS3=1290µm,e=15µm
6)LS1=1090µm,LS2=1190µm LS3=1290µm,e=50µm

Le=100µm

1)
La=wa=1026µm,
lb=wb=826µm

2)La=wa=1100µm
, lb=wb=900µm

1)
La=wa=1026µm,
lb=wb=826µm

2)La=wa=1100µm
, lb=wb=900µm

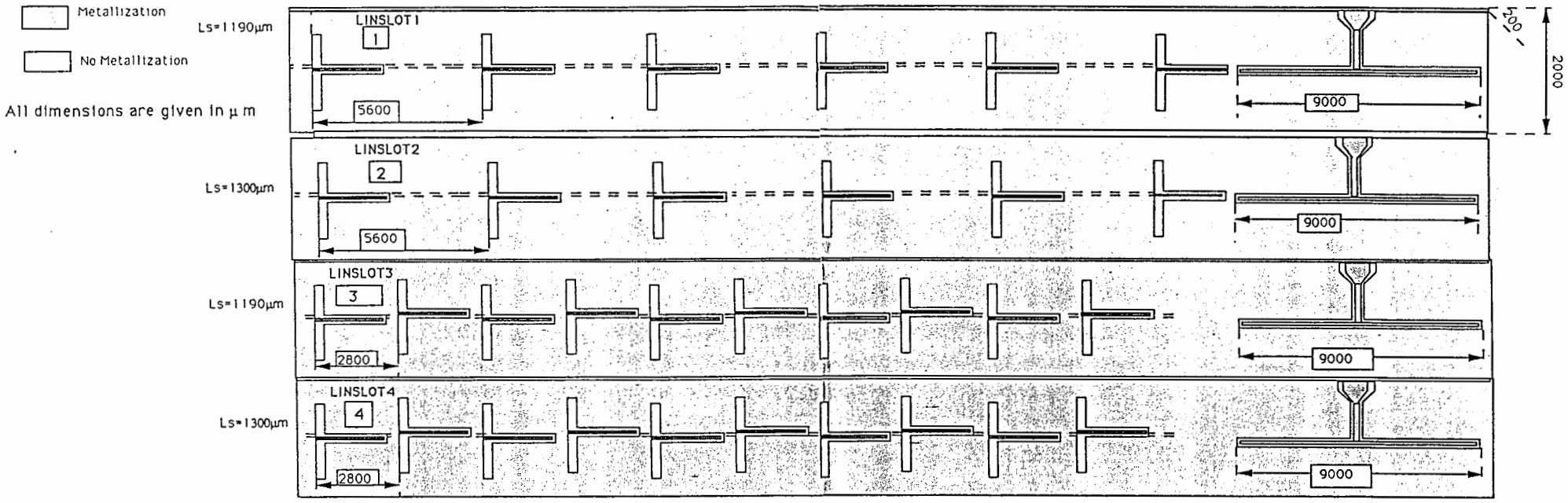
Metallization
No Metallization
All dimensions are given in μm
Ls=1190μm
LINSLOT1
1
5600
9000
400
2000
Ls=1300μm
LINSLOT2
2
5600
9000
Ls=1190μm
LINSLOT3
3
2800
9000
Ls=1300μm
LINSLOT4
4
2800
9000

La=wa=1026
Lb=wb=826

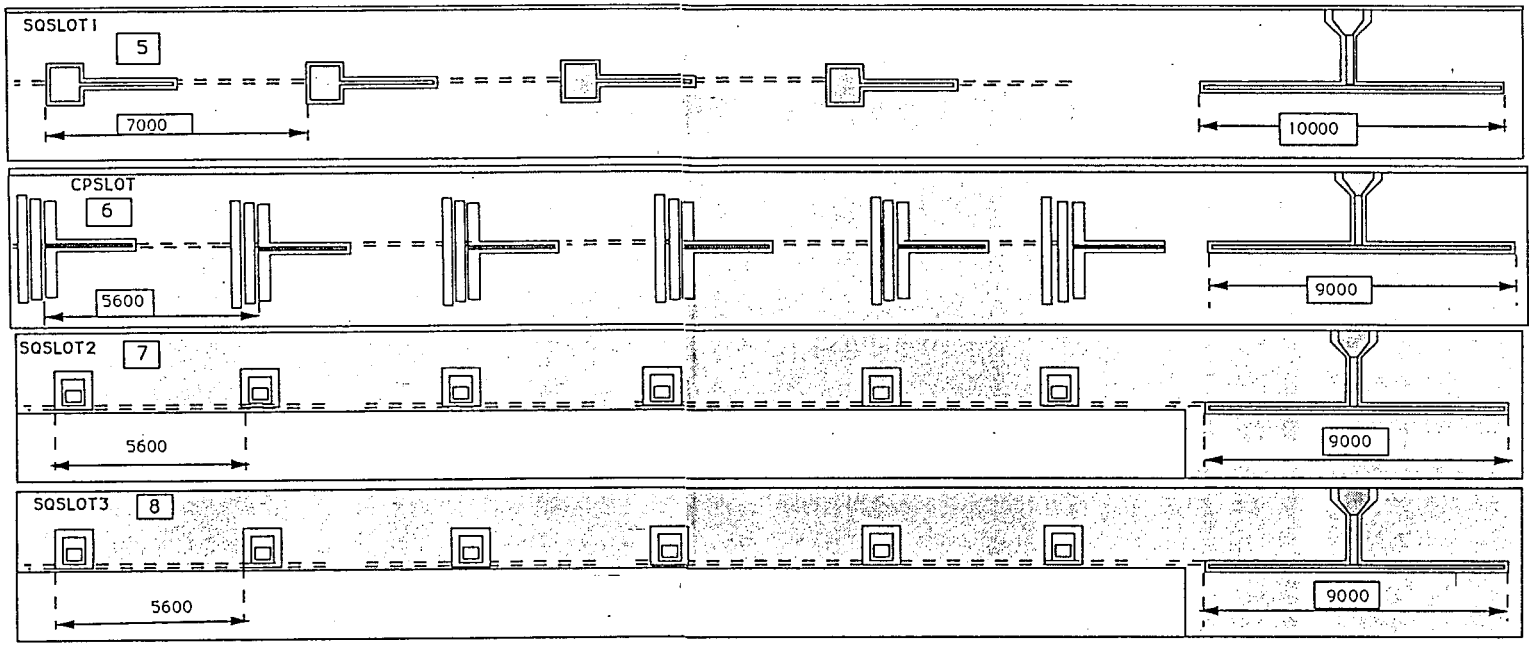

Ls1=1140
Ls2=1190
Ls3=1240

Appendix 2-b

Modulator design

LINSLOT

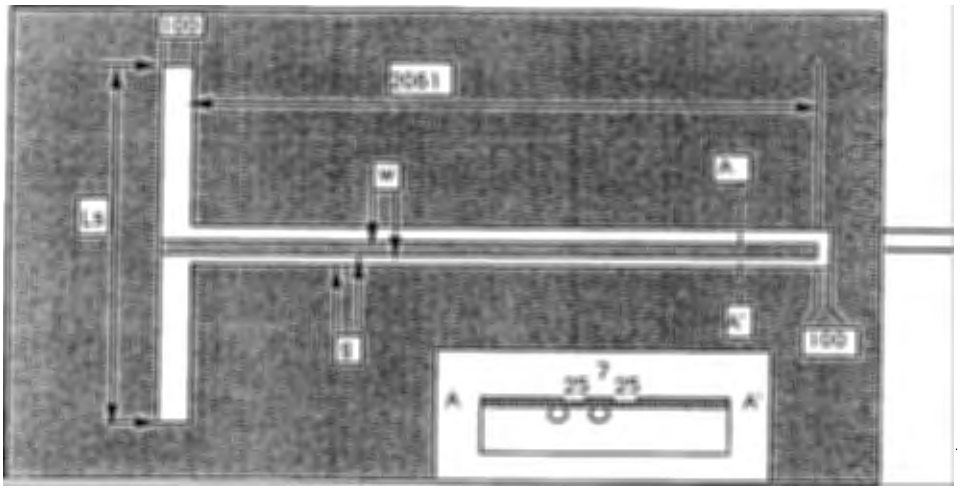

Metallization

No Metallization

SQSLOT1

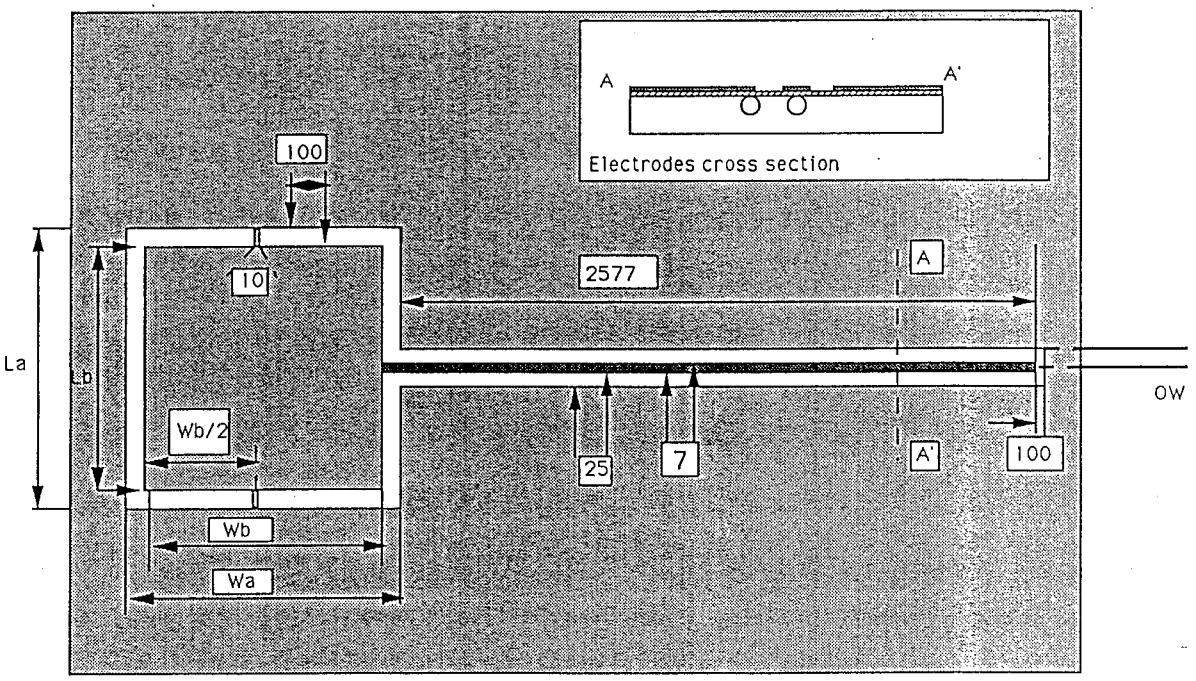

CPSLOT

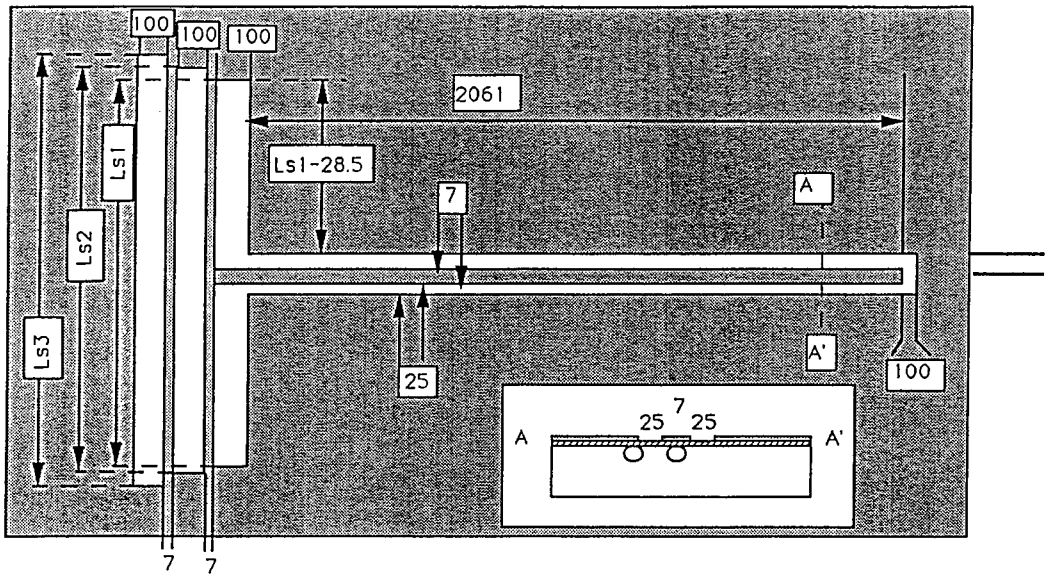

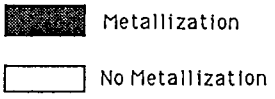

SQSLOT3

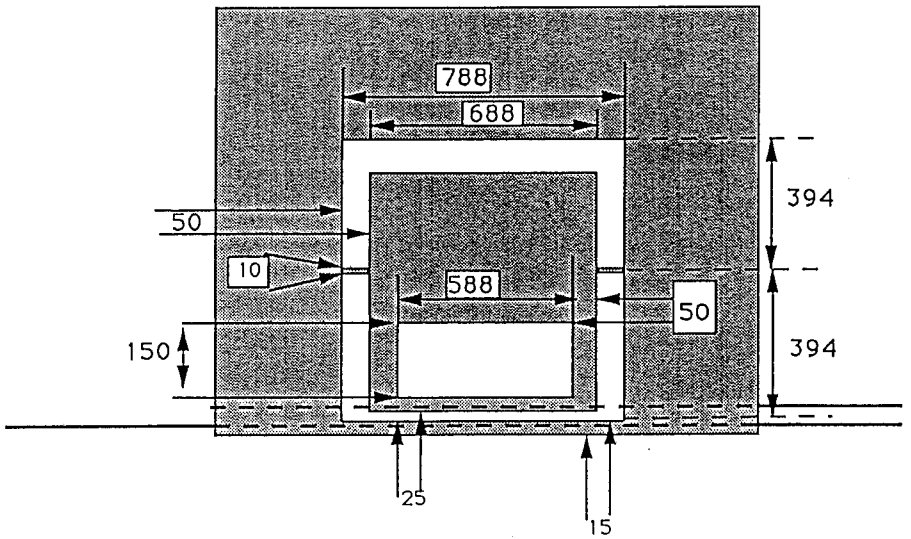

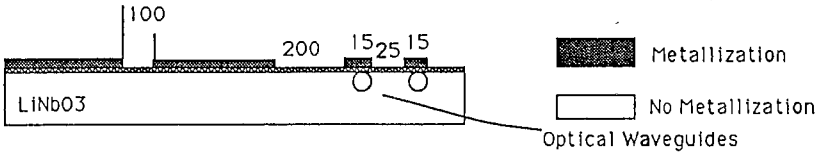

SQSLOT2

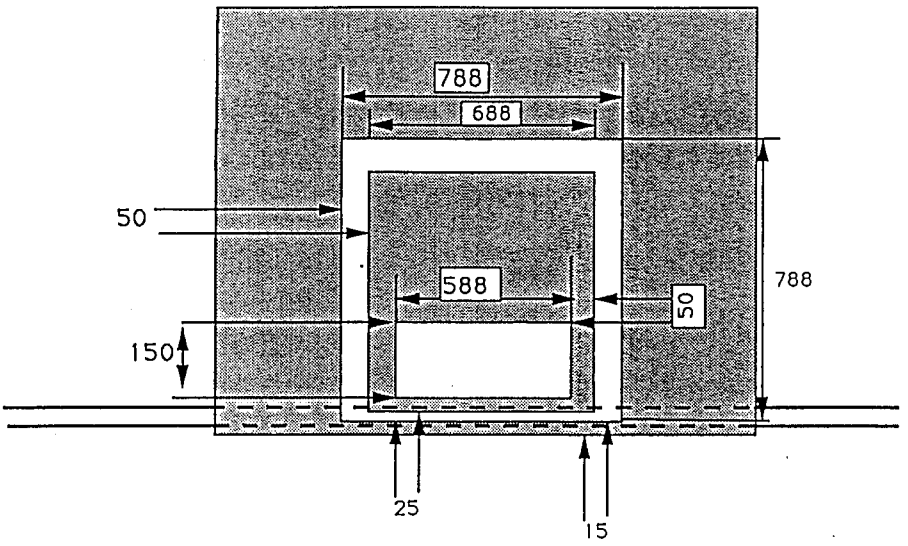
788
688
50
588
50
788
150
25
15

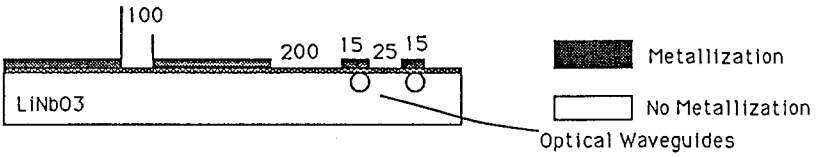
100
200
15
25
15
LiNbO3
Metallization
No Metallization
Optical Waveguides

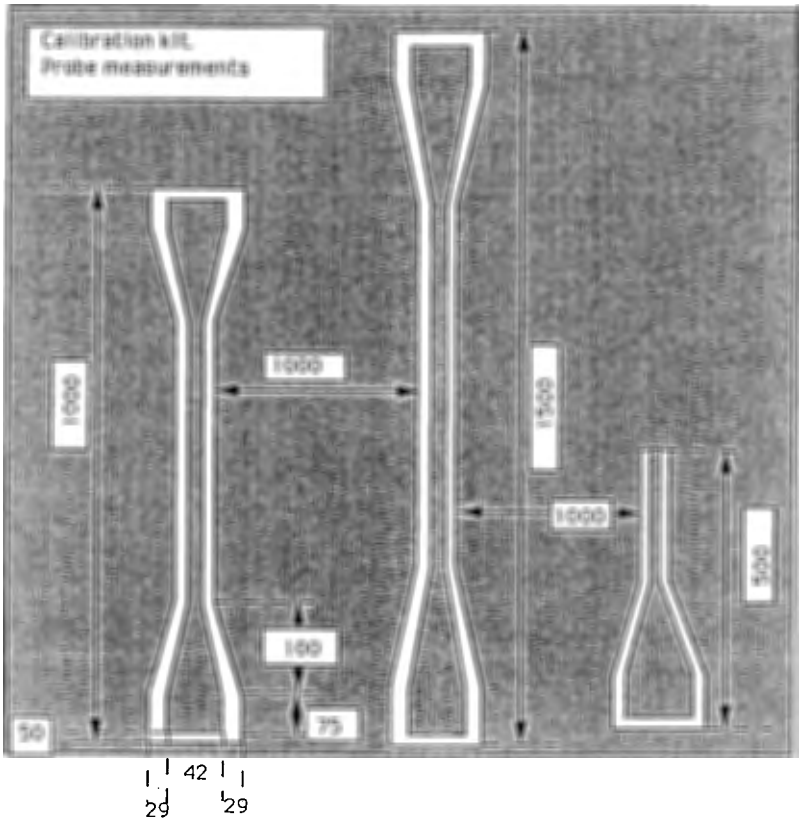
Calibration kit
Probe measurements
1000
1000
1000
1000
500
150
50
75
42
29
29

Appendix 2-c

Antennas design for probe measurement

Metallization

No Metallization

SQSLOT-1-PROB

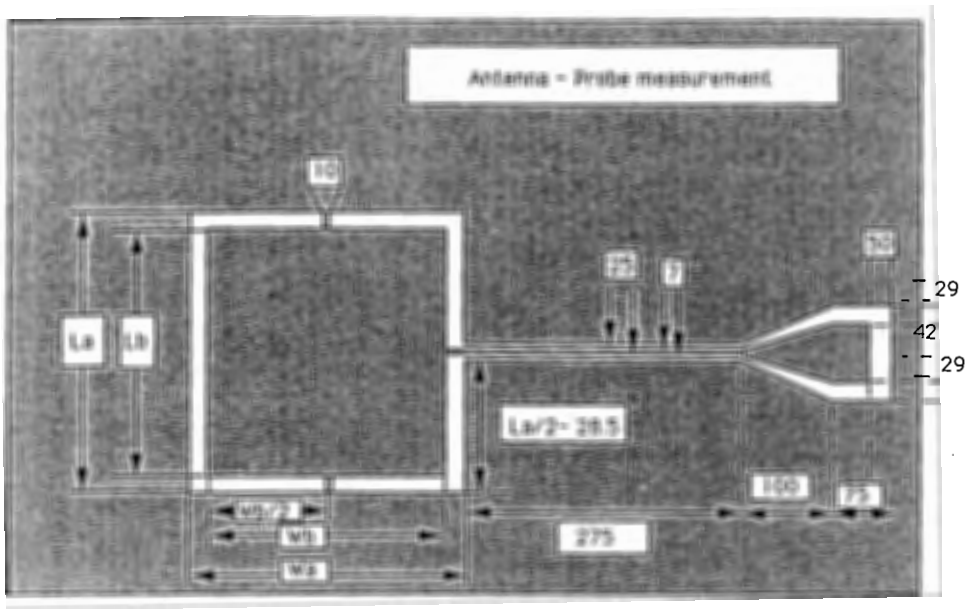

CPSLOT-PROB

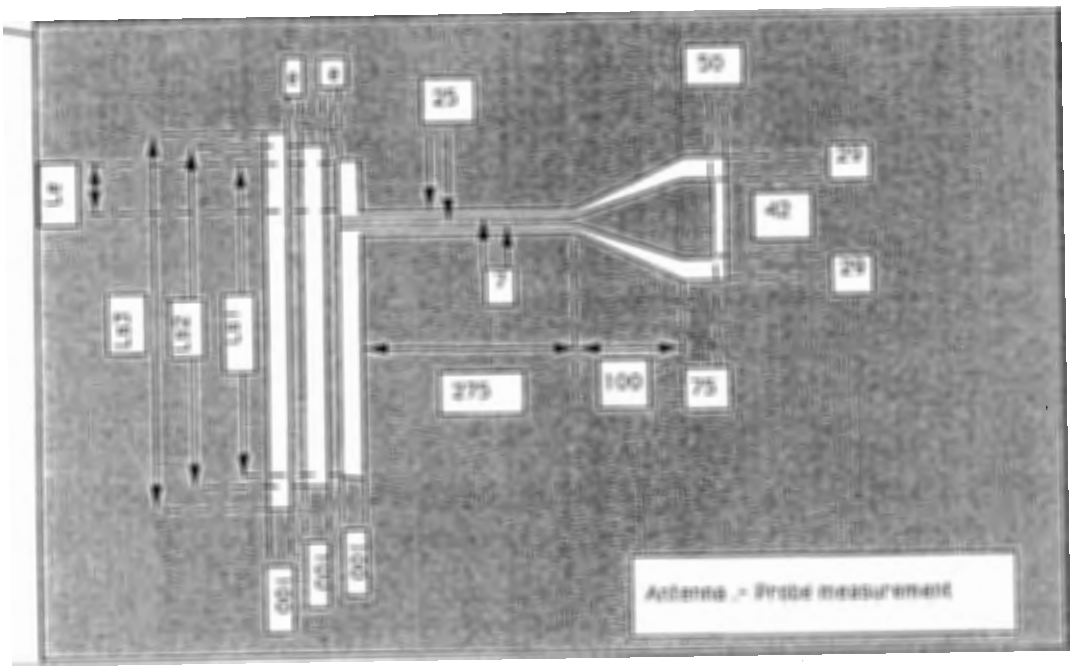

Metallization

No Metallization

SQSLOT-2-PROB

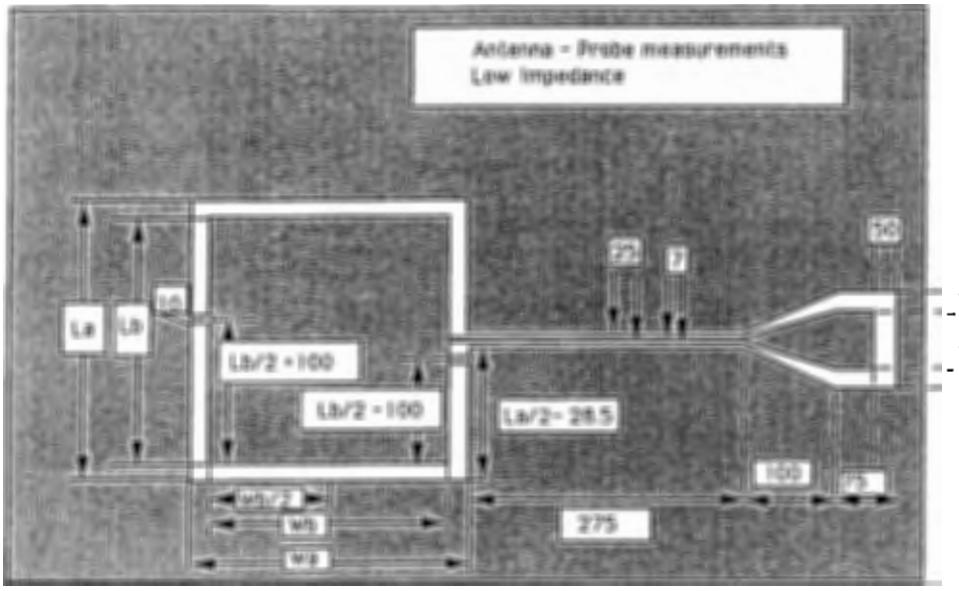

LINSLOT-PROB

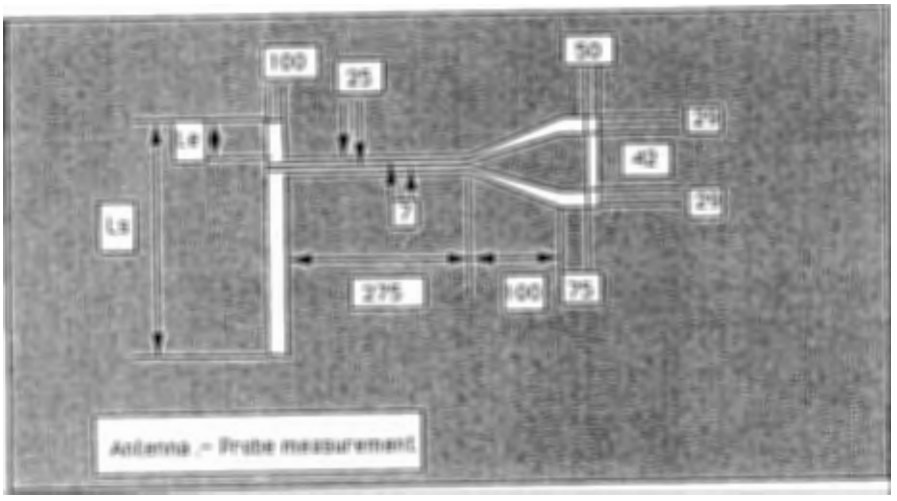

appendix 2-c

Probe measurements of antennas on LiNbO3

WAFER 2 with quartz.

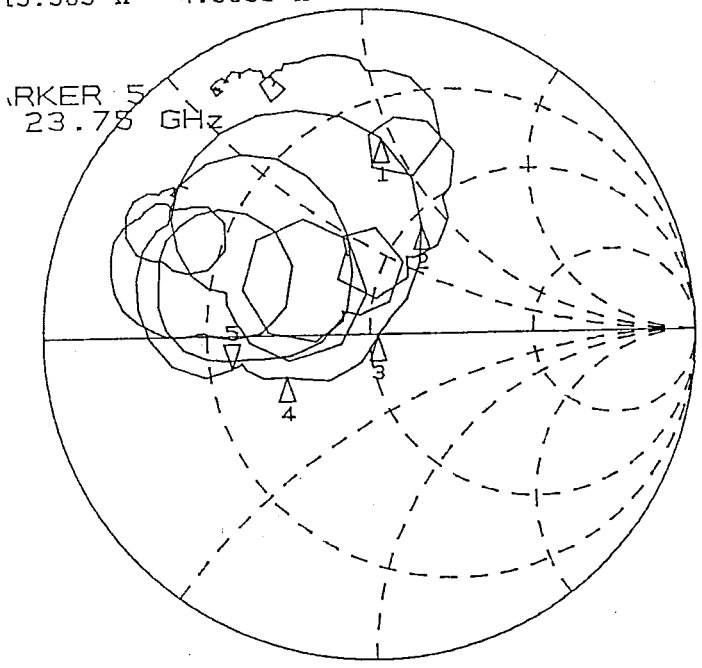

Linslot 1

1)	23.05	25	47.6 Ω
2)	23.15	51.5	41.27
3)	23.35	52.74	-0.6
4)	23.55	25.8	-7.96
5)	23.75	20	-5.017

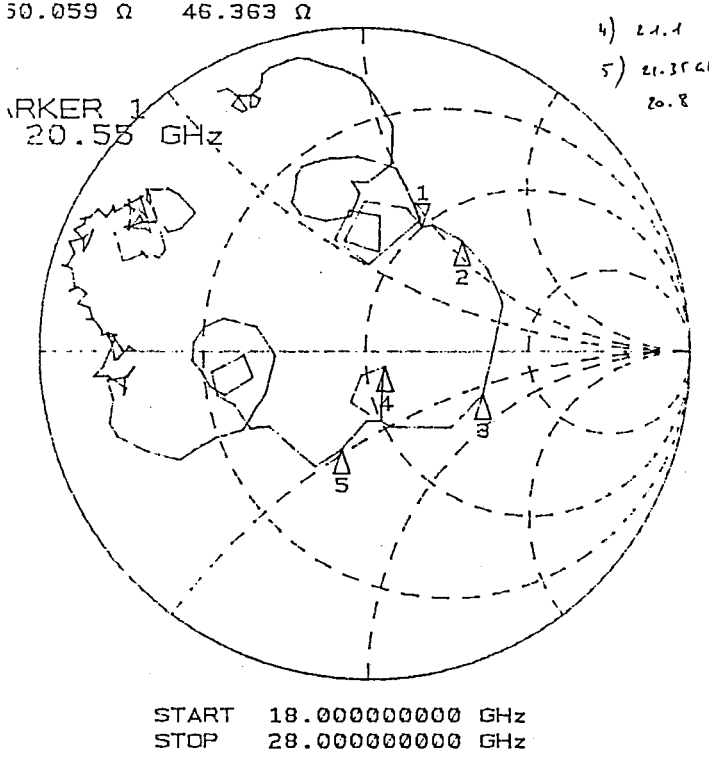

2 Linslot 1

1)	20.55	50	46.5
2)	20.65	55.54	56.15
3)	~~100.04~~ 20.85	100	-30.7
4)	21.1	56.14	-5.02
5)	21.35 GHz	36.24	-23.45
	20.8	115	2.89

WAFER 2

2 Linslot 2

1.0 Units
200.0 mUnits/
65.922 Ω -43.457 Ω

ARKER 5
21.38 GHz

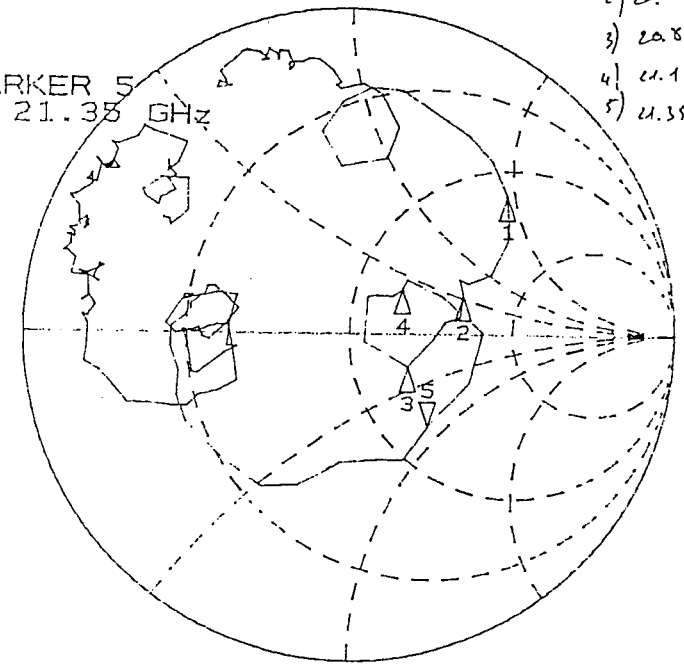

1)	20.4 GHz	66.	94.6
2)	20.65	99.184	26.97
3)	20.85	69.99	-15.129
4)	21.1	66.375	19.46
5)	21.35	65.94	-43.64

START 18.000000000 GHz
STOP 28.000000000 GHz

F 1.0 Units
200.0 mUnits/
37.436 Ω -43.404 Ω

ARKER 5
24.1 GHz

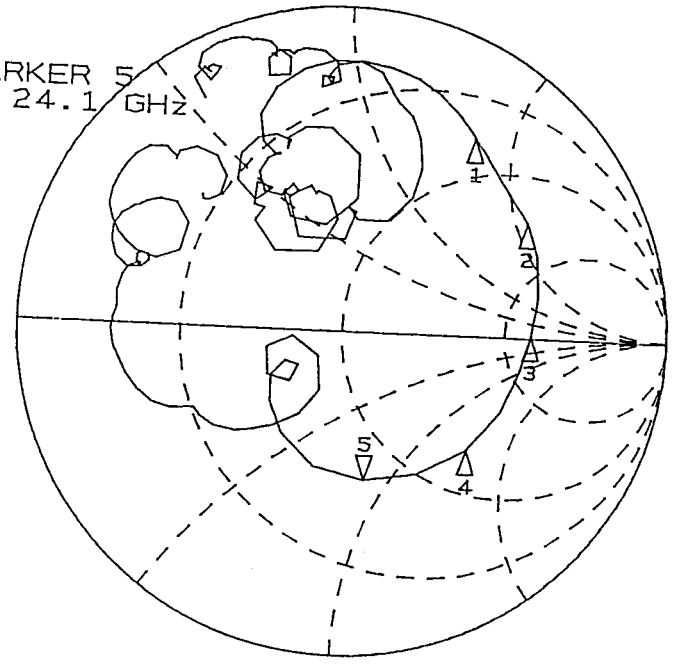

Linslot 2

1)	23.5	32.29	82.44
2)	23.7	88.7	110.6
3)	23.85	190.17	2.9
4)	24	73.89	-71.74
5)	24.1	37.36	-43.45

START 18.000000000

Wafer 2

Einstel 3

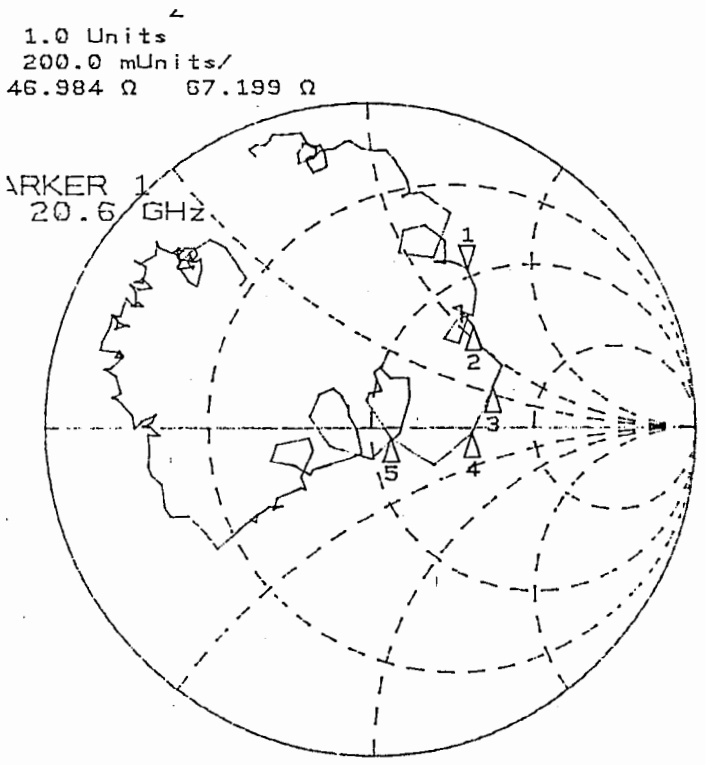

1) 20.6 47. 66.9
2) 21.15 71.27 55
3) 21.3 103.9 30.69
4) 21.35 93.89 -1.93
5) 21.45 56.21 -3.044

WAFer 8

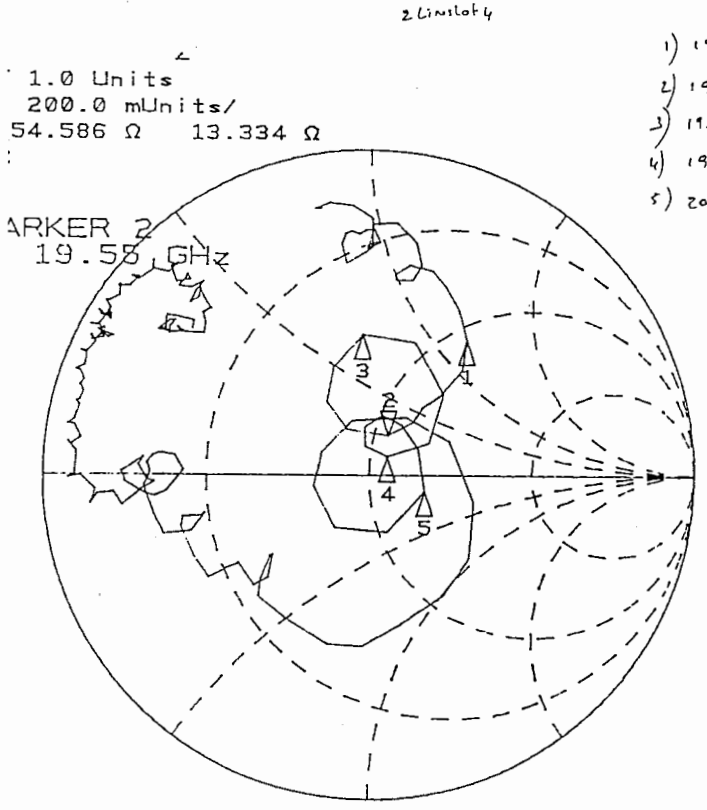

dual

1)	19.3	51.	62.52
2)	19.55	54.8	13.063
3)	19.75	33	35.11
4)	19.95	56,15	6.17
5)	20.25	70.6	-6.69

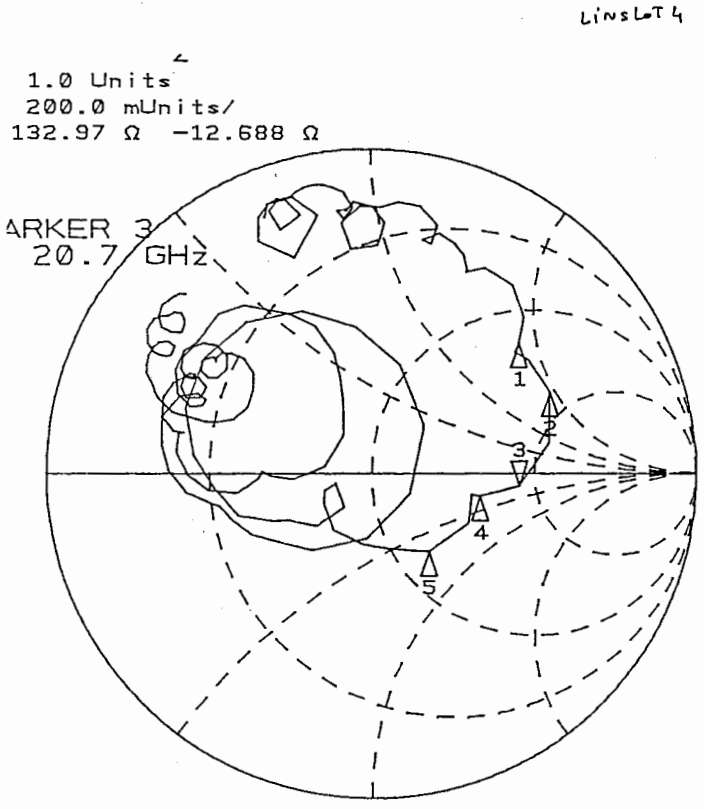

1)	20.45GHz	69 +j87
2)	20.6	120 +j 94
3)	20.7	132 -j 11
4)	20.75	99 -j 14.5
5)	20.9	61.9 -j 32.87

Linslot 5

1) 19.85 51.4, 65.8
2) 19.95 98.65, 55.28
3) 20.05 91.55 14.113
4) 20.2 70.3 - 7.6
5) 20.4 43.12 -18.7

.0 Units
00.0 mUnits/
.684 Ω 55.023 Ω

RKER 2
19.95 GHz

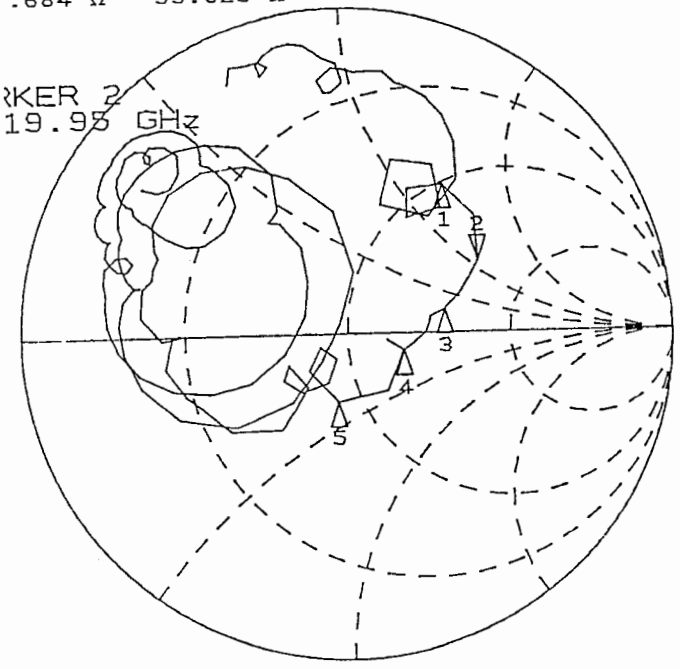

START 18.000000000 GHz

wafer 2

Linslot 1

1.0 Units
200.0 mUnits/
55.375 Ω 4.4375 Ω

ARKER 3
19.4 GHz

19.6Hz	27.54	23.75
19.2	51.19	39.15
19.4	65.86	3.7
19.7	45.91	-15.15
18.8	42.	-0.10
20	22.53	-17.3

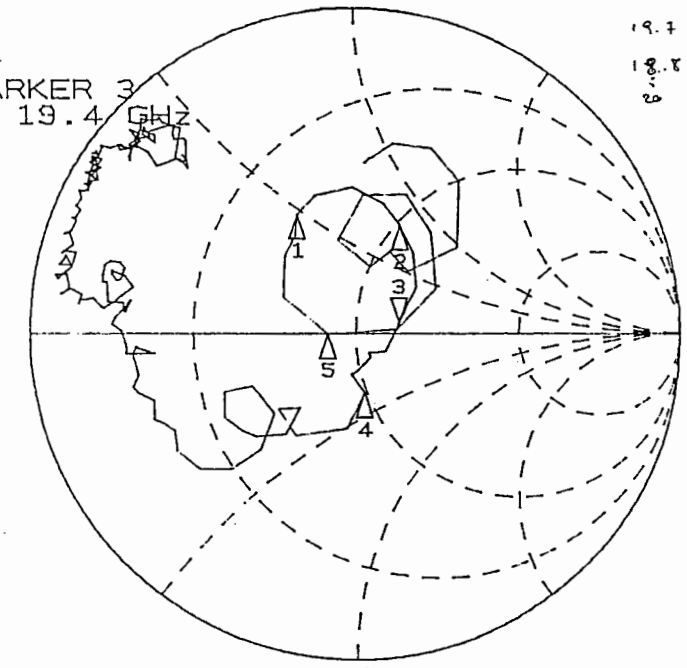

START 18.000000000 GHz
STOP 28.000000000 GHz

Wafer 2

2LINSLOTG

1.0 Units
200.0 mUnits/
4.3994 Ω 532.96 mΩ

1) 20.2 4.41 9.464
2) 19.2 24.88 -17.12
3) 19.5 12.14 -11.47
4) 20 5.57 -2.706

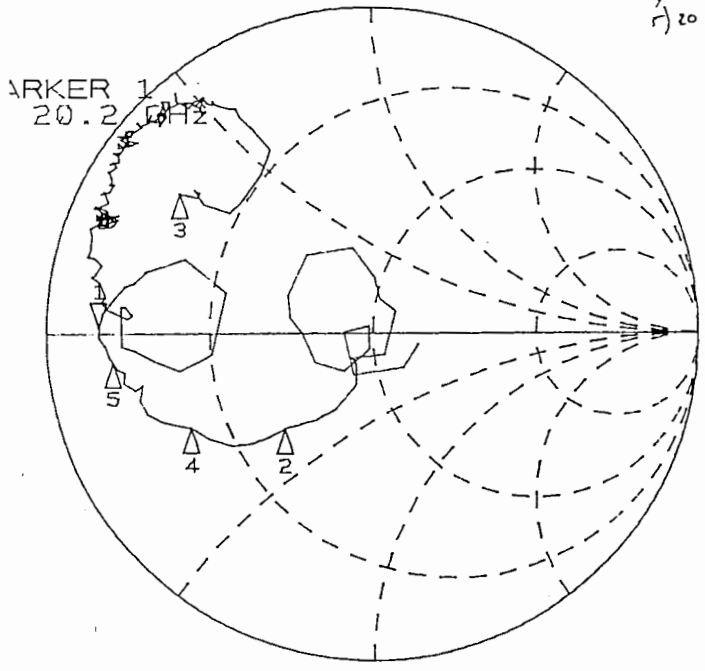

START 18.000000000 GHz
STOP 28.000000000 GHz

LINSLOT C

1.0 Units
200.0 mUnits/
1.328 Ω 11.535 Ω

1) 19.65 49.8 55.32
2) ~~19.85~~ 19.8 91.3 11.1
3) 20.05 72.6 -6.75
4) 20.2 42.81 -21.79
5) 20.4 26.54 -20.65

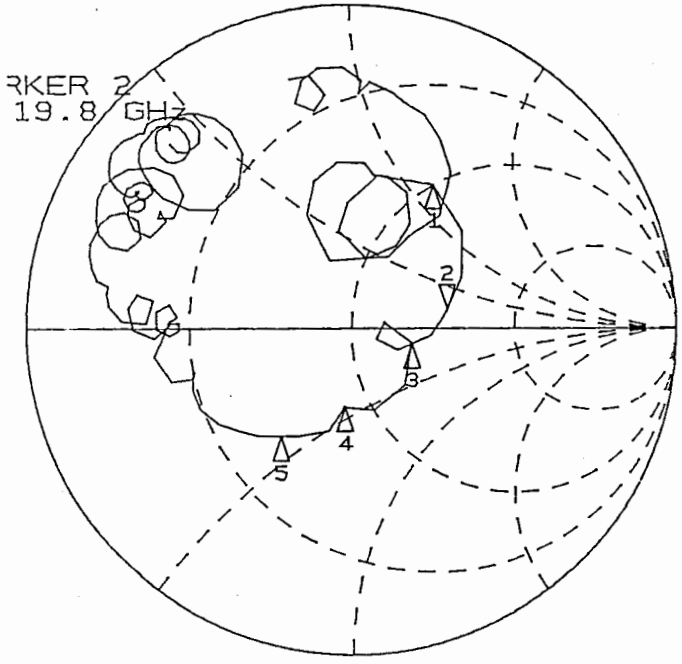

START 18.000000000 GHz
STOP 28.000000000 GHz

Wafer 2

cpsLH1

1 24.8 GHz 25.7 55.9
2 25.2 GHz 30. 41.03
3 25.53 54 50.2
4 25.75 42.2 15.17
5 25.9 31.63 18.3

1.0 Units
200.0 mUnits/
47.256 Ω 15.377 Ω

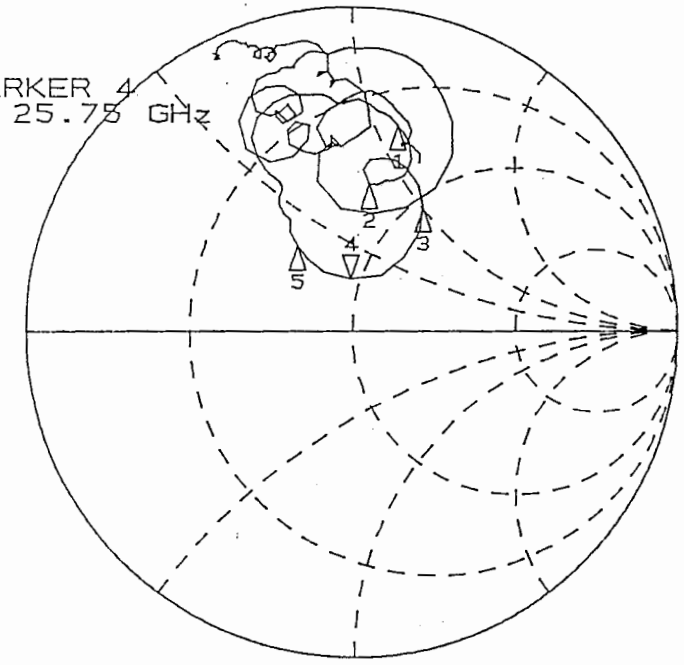

START 18.000000000 GHz
STOP 28.000000000 GHz

2 cpsLH1

0 Units
)0.0 mUnits/
295 Ω 13.738 Ω

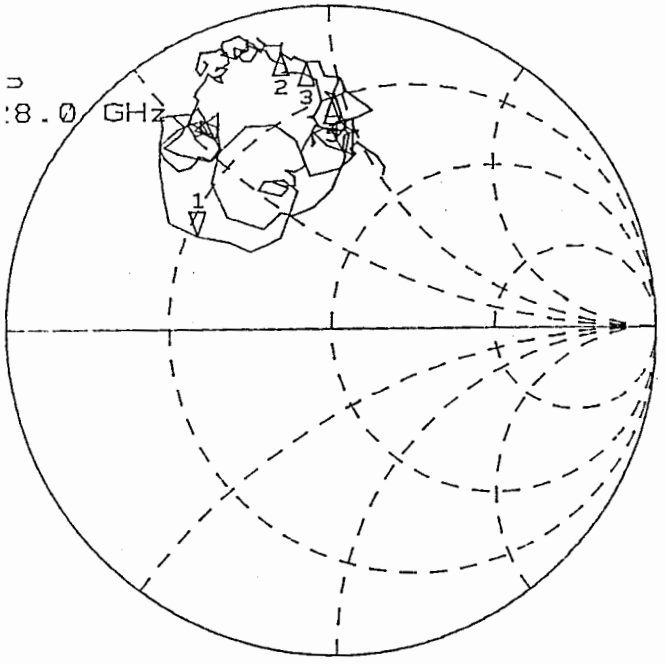

START 18.000000000 GHz
STOP 28.000000000 GHz

cpslot 2

1) 24.7GHz 28.6 64.5
2) 25.1 63.35 52.2
3) 25.3 58.02 27
4) 25.45 41.47 25.89
5) 25.8 24.85 25.96

1.0 Units
200.0 mUnits/
5.67 Ω 27.762 Ω

RKER 3
25.3 GHz

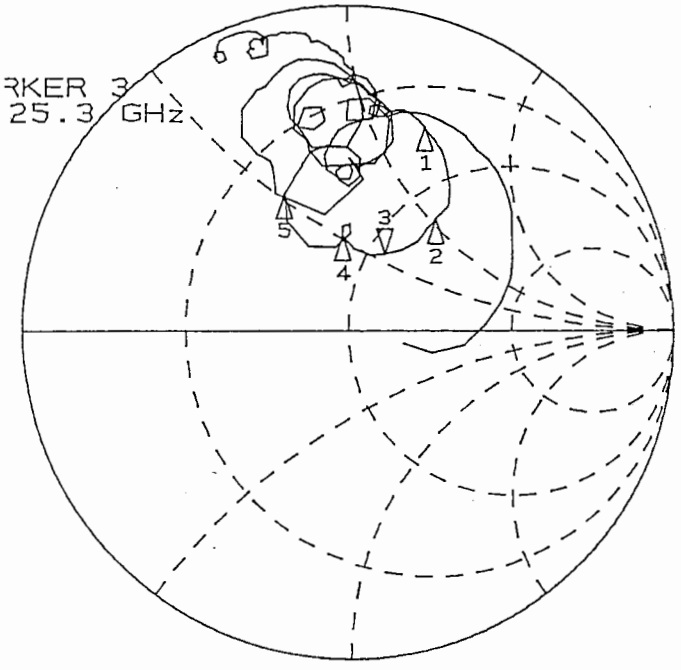

START 18.000000000 GHz
STOP 28.000000000 GHz

Wafer 2

2 cpslot 2

1) 21.5 12.2 14.16
2) 25.3 11. 41.45
3) 25.5 16.5 35.012
4) 25.8 17.59 47.8
5) 26. 21.2 35.11

0 Units
)0.0 mUnits/
.239 Ω 14.098 Ω

KER 1
:1.5 GHz

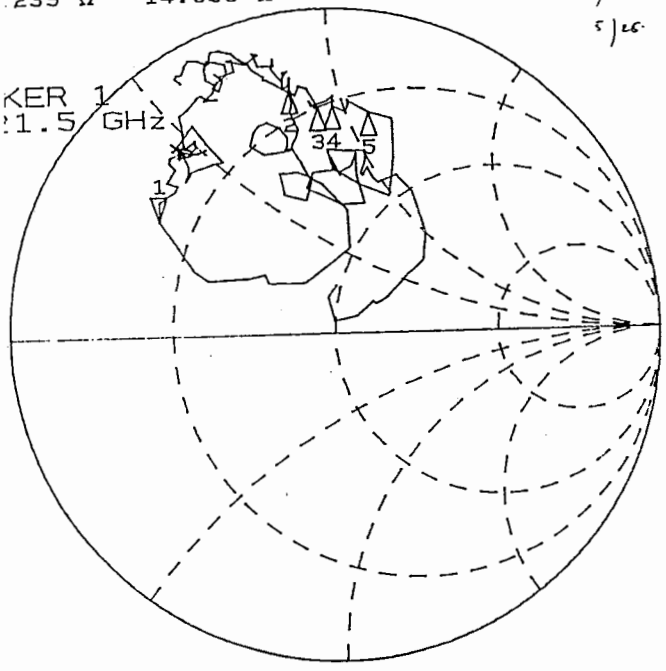

START 18.000000000 GHz
STOP 28.000000000 GHz

2 cpslot3

Wafer 2

1) 25 GHz 39 85.62
2) 25.3 82.9 53.5
3) 25.5 107. 8.57
4) 25.65 56.73 -27.34
5) 25.95 39.7 27.77

1.0 Units
200.0 mUnits/
6.623 Ω -27.365 Ω

RKER 4
25.65 GHz

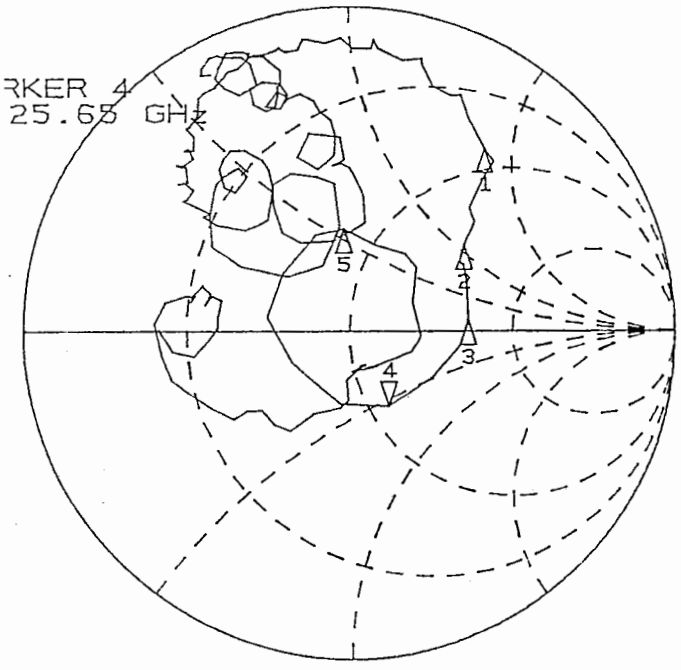

START 18.000000000 GHz
STOP 28.000000000 GHz

cpslot3

1/24.55 65.96 63.73
24.85 74.19 3.5
25.3 39.9 4.71
25.9 49.5 16
26.2 29.63 36.53

L.0 Units
:00.0 mUnits/
3.965 Ω 63.957 Ω

RKER 1
24.55 GHz

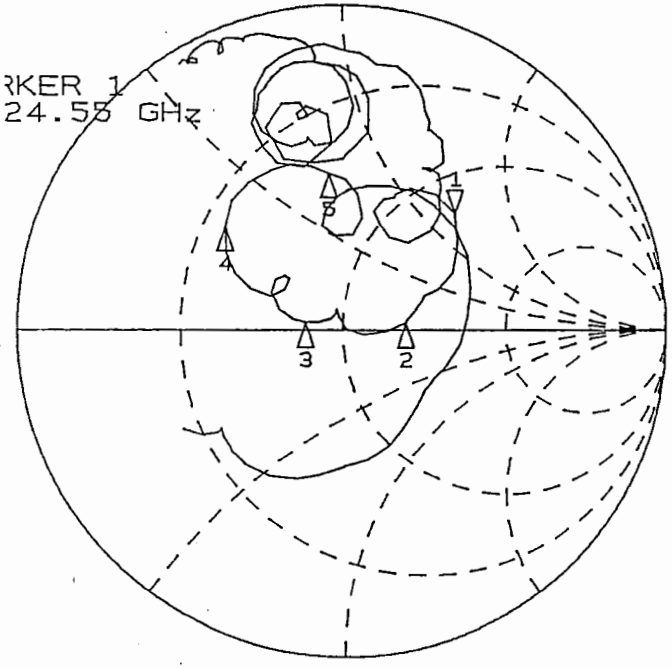

START 18.000000000 GHz
STOP 28.000000000 GHz

cpslot 4

..0 Units
:00.0 mUnits/
:.385 Ω 59.002 Ω

JP
28.0 GHz

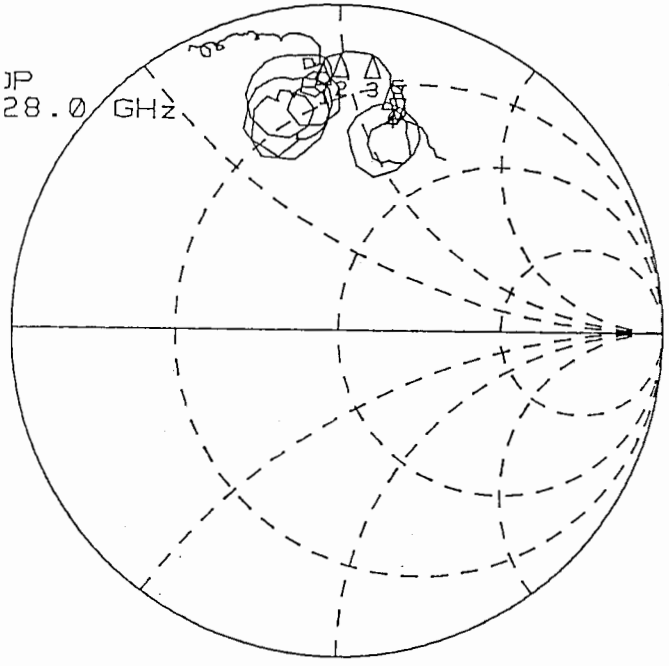

START 18.000000000 GHz
STOP 28.000000000 GHz

wafer 2

2 cpslot 4

Dut

.0 Units
00.0 mUnits/
.168 Ω 55.344 Ω

KER 2
26.65 GHz

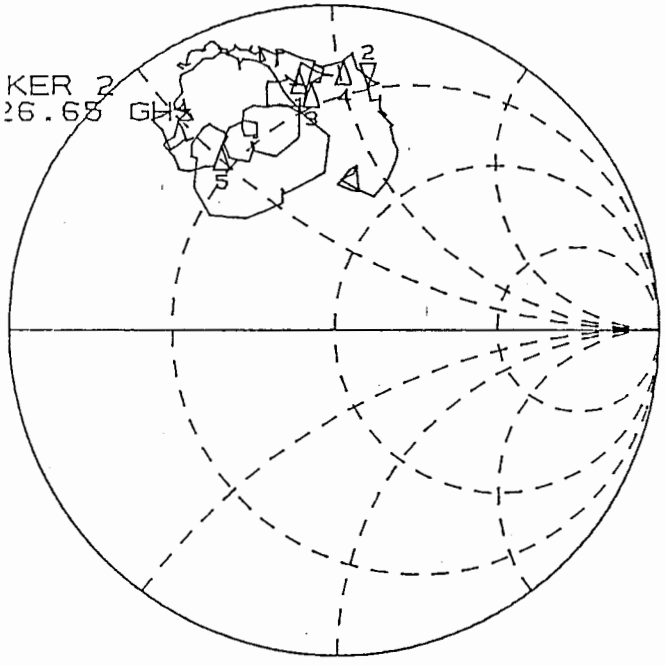

START 18.000000000 GHz
STOP 28.000000000 GHz

epslot5

1.0 Units
200.0 mUnits/
5.533 Ω 59.896 Ω

RKER 5
25.95 GHz

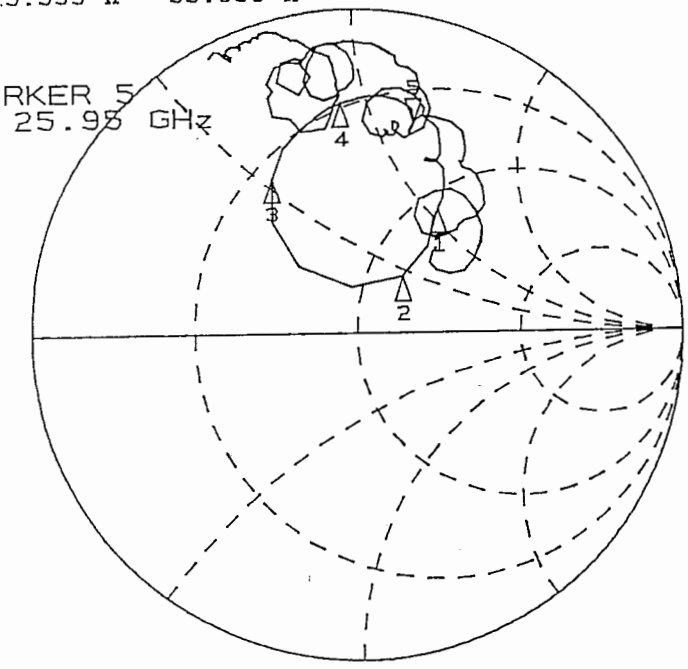

START 18.000000000 GHz
STOP 28.000000000 GHz

1 25.05 GHz 57.22, 54
2 25.2 GHz 62.40 22.27
3 25.4 19.69, 26.68
4 25.65 15.55 46.86
5 25.95 25.61 60.15

wafer 2

2cpslot5

1.0 Units
200.0 mUnits/
43.213 Ω 20.463 Ω

ARKER 4
26.4 GHz

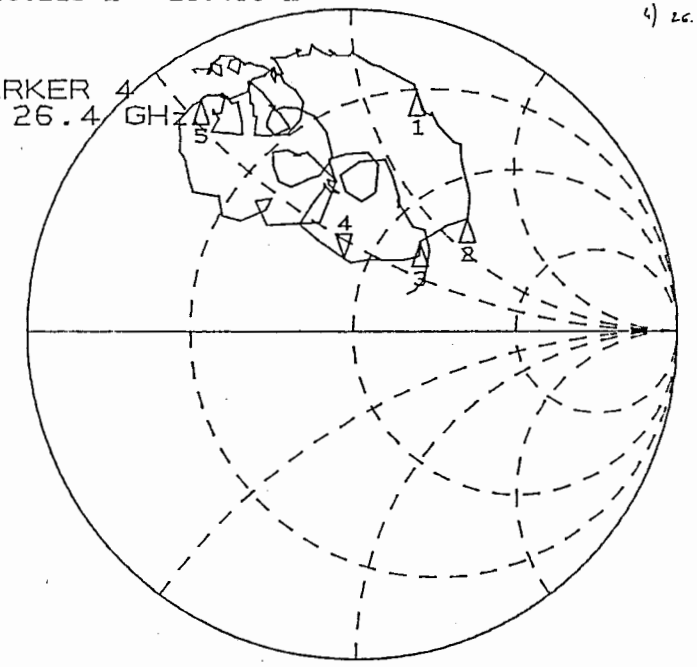

START 18.000000000 GHz
STOP 28.000000000 GHz

1) 25.6 GHz 17.3 62.45
2) 25.05 70.12 65.
26.15 62.75 39.045
4) 26.4 43.2 20.15

Wafer 2

2 cpslot 6b

1) 25.3Γ 69.7 78.31
2) 25.6Γ 106.6 Γ.
3) 26.0Γ 63.99 -13.Γ
4) 26.1Γ 41.6Γ -21.Γ

1.0 Units
200.0 mUnits/
70.676 Ω 78.469 Ω

ARKER 1
25.35 GHz

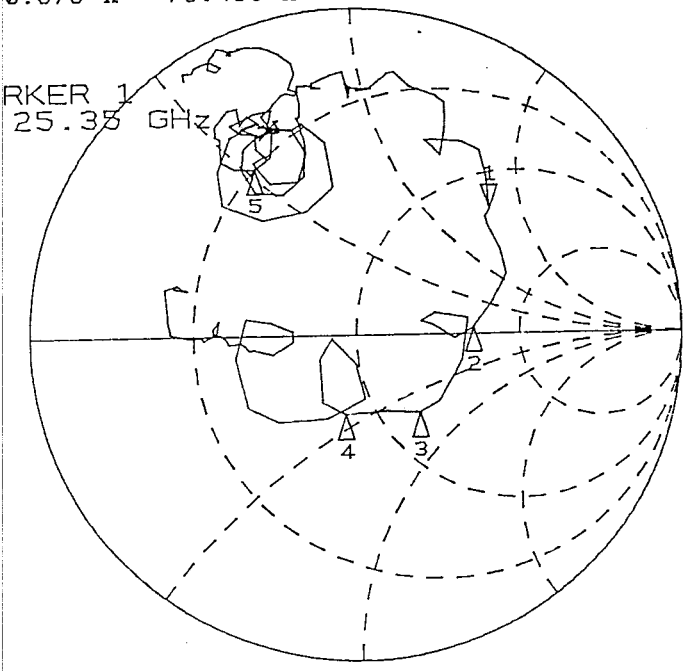

START 18.000000000 GHz
STOP 28.000000000 GHz

cpslot 6 Δn = 0.5 GHz

25 avg : 902 , 94
25.Γ 3 69.41 -21.4
26. 4 28.39 0
26.Γ Γ 51.98 34

1.0 Units
200.0 mUnits/
0.18 Ω 79.402 Ω

RKER 1
24.5 GHz

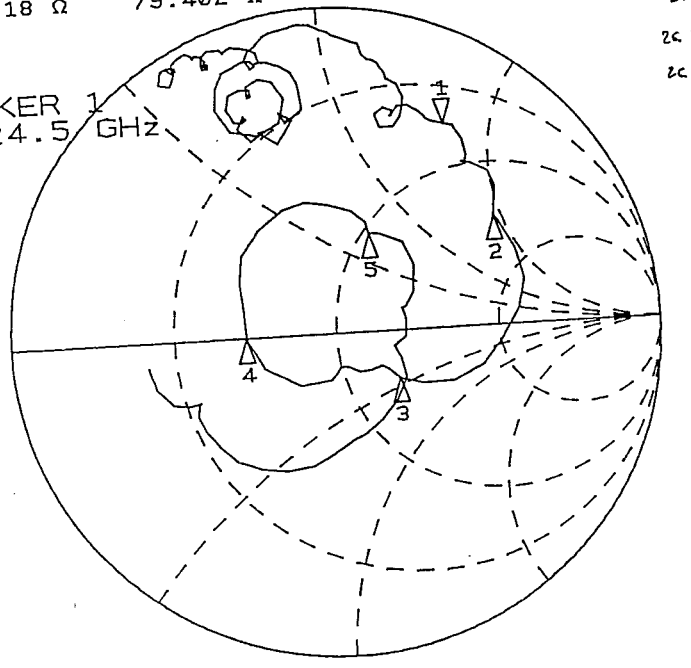

START 18.000000000 GHz
STOP 28.000000000 GHz

Wafer 2

2SQ5GT11

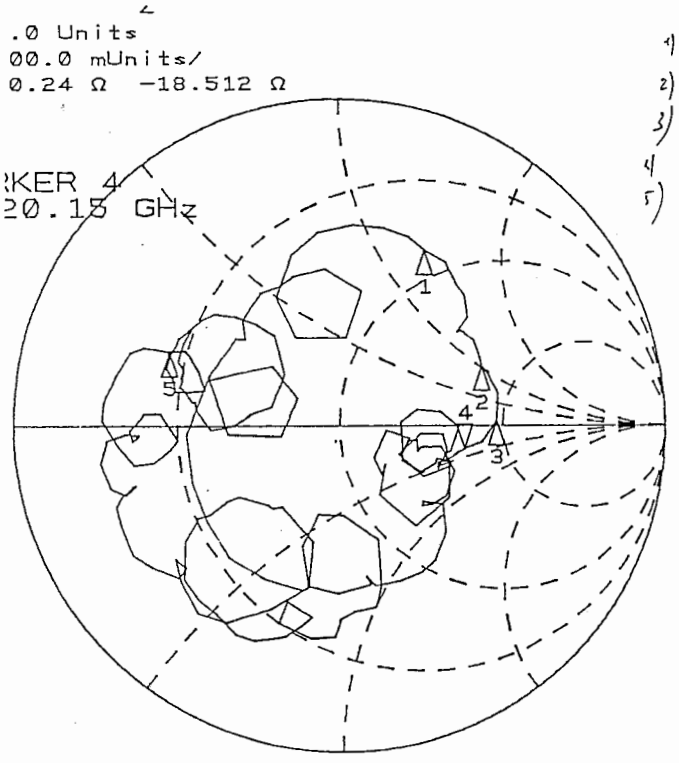

1)	19.4	39	65.2
2)	19.9	111.65	52.79
3)	20.05	144.14	05.602
4)	3.015	110.6	-18.21
5)	22.1	85.5	-42.66

SQ5GT11

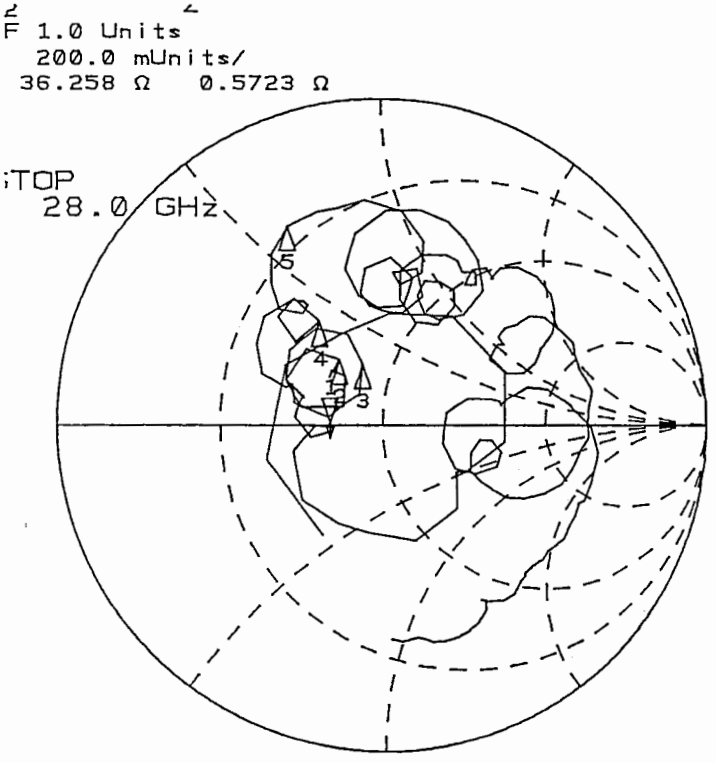

sqslot12

.0 Units
00.0 mUnits/
.41 Ω 16.396 Ω

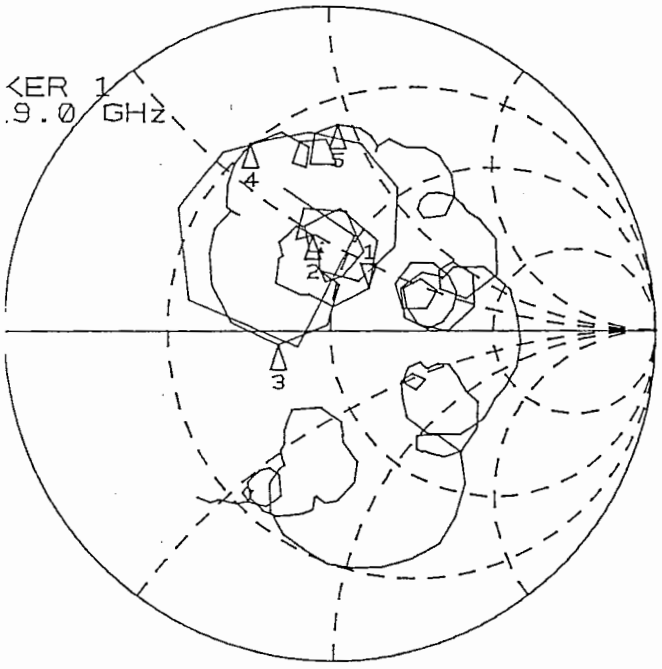

START 18.000000000 GHz
STOP 28.000000000 GHz

Wafer 2

2SQSLOT12

1.0 Units
200.0 mUnits/
01.82 Ω -68.102 Ω

1) 19.2 8.52 72.86
2) 19.65 181 53.90
3) 20. 101.82 -68.102

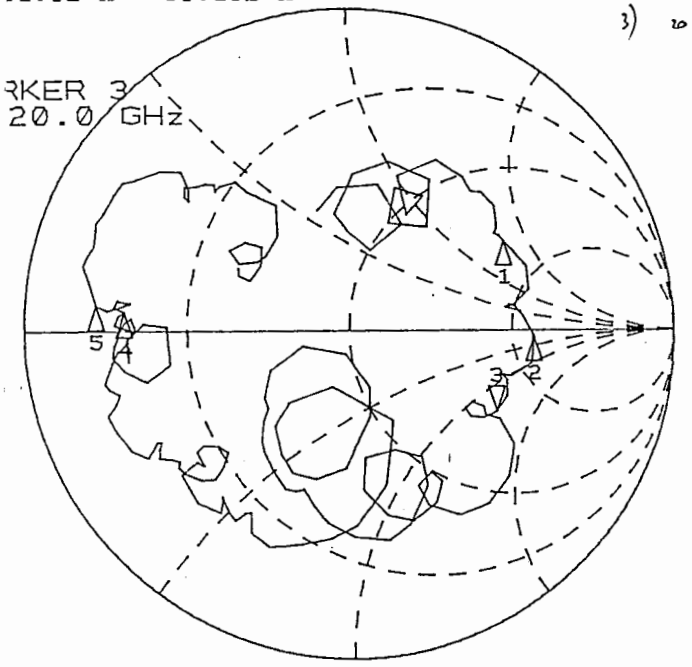

START 18.000000000 GHz
STOP 28.000000000 GHz

Wafer 2

sqslot21

..0 Units
:00.0 mUnits/
4287 Ω 18.885 Ω

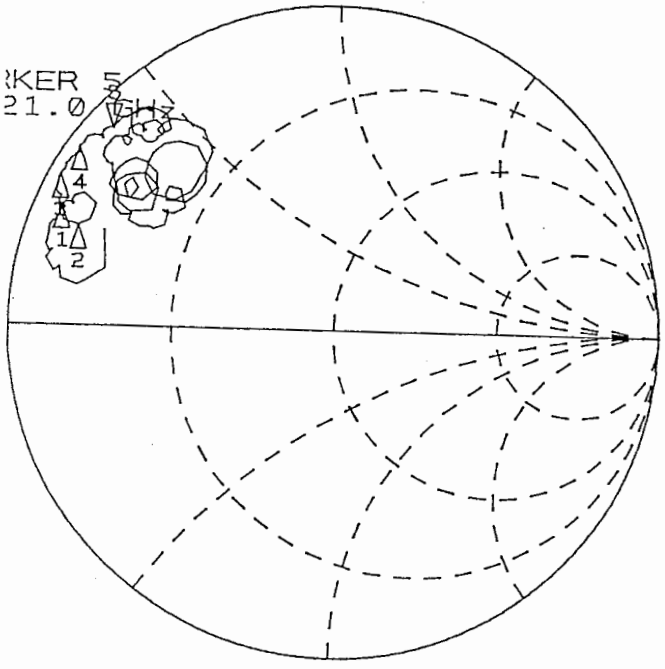

START 18.000000000 GHz
STOP 28.000000000 GHz

2 sqslot21

.0 Units
00.0 mUnits/
.934 Ω 8.6533 Ω

25.4	14.98	30.57
25.6	19.087	23.24
25.8	21.	14.5
25.9	12.8	8.8
25.95	8.29	10.27

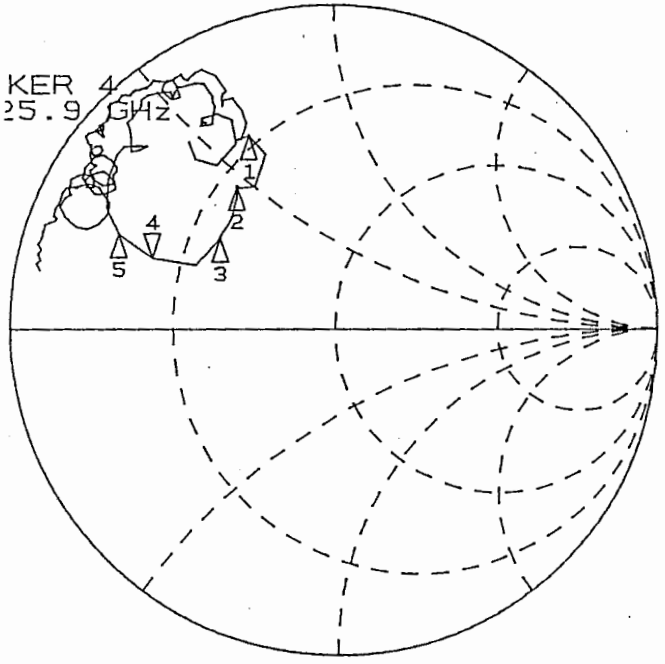

START 18.000000000 GHz
STOP 28.000000000 GHz

W2 SQSLOT 2-2

Wafer 2

1.0 Units
200.0 mUnits/
2.914 Ω 11.112 Ω

RKER 5
25.75 GHz

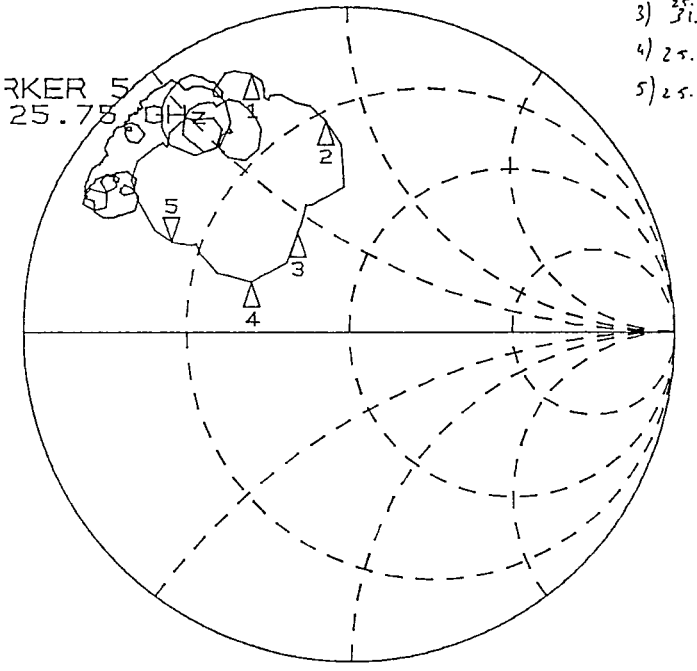

1)	24.65	6.22	36.35
2)	25.1	17.13	41.77
3)	25.5 31.19	21.092	
4)	25.5	25.99	8.89
5)	25.75	12.86	11.087

START 18.000000000 GHz
STOP 28.000000000 GHz

sqslot22

.0 Units
00.0 mUnits/
6431 Ω 13.426 Ω

KER 5
21.0 GHz

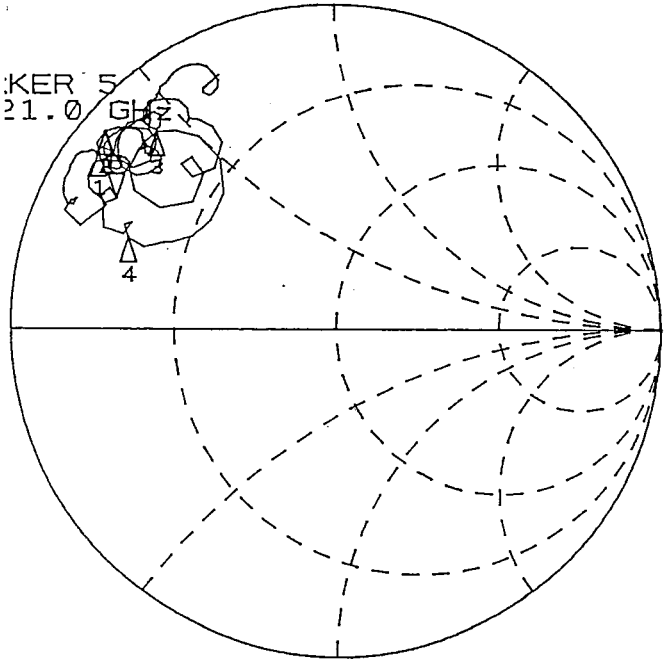

START 18.000000000 GHz
STOP 28.000000000 GHz

Appendix 3

Laser and photodiode data sheets

Or order via FAX: (415) 961-6072, 24-hours-a-day.

Photodetector/Receiver Selection Guide

Model Number	100X	101X, 101X-NT[1]	143X	141X	151X	1601, 1611	1801, 1811	1651	2001, 2011
Wavelength Range	400 to 900 nm	950 to 1650 nm	400 to 1650 nm	950 to 1650 nm	950 to 1650 nm	400 to 1100 nm 800 to 1800 nm	400 to 1100 nm 800 to 1800 nm	500 to 1100 nm	400 to 1100 nm 800 to 1800 nm
3-dB Bandwidth	60, (40)[2] GHz[3]	45, 30 GHz,	25 GHz	20 GHz	6 GHz	1 GHz	125 MHz	1 GHz	300 kHz
Rise Time [4]	6, (9)[2] ps	9, 14 ps	17 ps	20 ps	70 ps	400 ps	3 ns	400 ps	1.2 µs
Response × BW	300, (200)[2] $\frac{V}{W}$ GHz	450, 600 $\frac{V}{W}$ GHz	125 $\frac{V}{W}$ GHz	480 $\frac{V}{W}$ GHz	1800 $\frac{V}{W}$ GHz max	200 $\frac{V}{W}$ GHz	4000 $\frac{V}{W}$ GHz	40,000 $\frac{V}{W}$ GHz max	215 $\frac{V}{W}$ GHz max
Noise Equivalent Power	90 pW/√Hz	45, 15 pW/√Hz	90 pW/√Hz	15 pW/√Hz	40 pW/√Hz	14, 11 pW/√Hz	3.3, 2.5 pW/√Hz	0.5 pW/√Hz	0.25, 0.19 pW/√Hz
Peak Responsivity [5]	0.2 A/W	0.4 A/W	0.2 A/W	0.6 A/W	0.6 A/W	0.6, 0.8 A/W	0.6, 0.8 A/W	0.5 A/W	0.6, 0.8 A/W
Conversion Gain	5, (6.6)[2] V/W	10, 16 V/W	5 V/W	24 V/W	300 V/W	150, 200 V/W	2.4×10^4, 3.2×10^4 V/W	4×10^4 V/W	1.0×10^4, 1.4×10^4 V/W
Max Linear Power	5 mW	2.5 mW	25 mW	2 mW	2 mW	10 mW	75 µW[6]	1 mW	10 mW
Max Pulse Power	200 mW	100 mW	200 mW	100 mW	2 mW	10 mW	5 mW	1 mW	1 W
Optical Input	ST	ST or FC	Direct, ST, or FC	Direct, ST, or FC	Direct, ST, or FC	Direct, ST, or FC	Direct, ST, or FC	Direct	Direct, ST, or FC
Active Region Diameter	12 µm	12 µm	25 µm	25 µm	25 µm	0.4, 0.1 mm	0.9, 0.3 mm	0.2 mm	0.9, 0.3 mm
Power	9-V battery	9-V battery	9-V battery	9-V battery	use 0901 or equiv.	use 0901 or equiv.	use 0901 or equiv.	use 0901 or equiv.	(2) 9-V batteries
Case Style Options [7]	1, 2	1, 4	1, 4, 5	1, 4, 5	1, 4, 5	Specify optical input type.	Specify optical input type.	N/A	Specify optical input type.
Comments and Applications	Compatible with 1422 amplifier (p19). Fastest visible detector.	Compatible with 1422 amplifier (p19). Fastest IR detector.	Compatible with 1422 amplifier (p19). Covers Ti:Sapphire spectral range.	200-Ω termination. High sensitivity.	High-data rate fiber-optic communication.	Spectroscopy and phase sensitive detection.	Low-noise RF detection. Large RBW.	Laser range finding. Optical heterodyne.	Ideal for servo and sensor applications. Variable filter. Boards available.
Price Range [8]	$4,900–5,900	$5,900–6,500	$3,200–4,200	$3,800–4,900	$3,200–4,200	$1,150–1,250	$695, $795	$2,750	$750, $850

[1] NT denotes internal termination >50 Ω. (See discussion on page 7.)

[2] These specifications apply with case style 1.

[3] The 3-dB point for the 100X is in reference to its frequency response at 1 GHz.

[4] Rise time in picoseconds is approximately 400 ÷ Bandwidth in GHz.

[5] See pages 10–18 for spectral response data.

[6] For AC-coupled versions, the max. linear power is 10 mW. See page 11.

[7] When ordering, replace X with case style code; see below.

[8] See page 52–53 for specific pricing information.

Note: Specifications highlighted in blue refer to model numbers highlighted in blue

Detector Case Styles

Many of our photodetectors have several housing and connector options. Indicate your choice by replacing the X in the model number with the case-style number, listed below.

For the ST fiber connector, the reflection from the fiber-photodetector interface is -10 dB. For the FC connector, the fiber end has been angle-polished, reducing the back reflection to -35 dB.

Case-Style Number	1	2	4	5
Input Connector	SM - ST	SM - ST	SM - FC	Direct
Output Connector	K	V	K	K

SM–ST=Single Mode ST V=Wiltron V- connector

SM–FC=Single Mode FC K=Wiltron K-connector SMA compatible

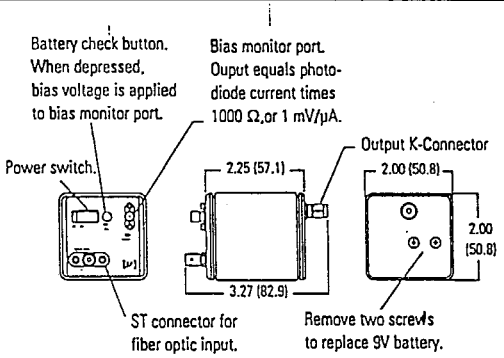

Case Styles 1, 2, & 4: These styles feature single-mode connectors for fiber-optic input.

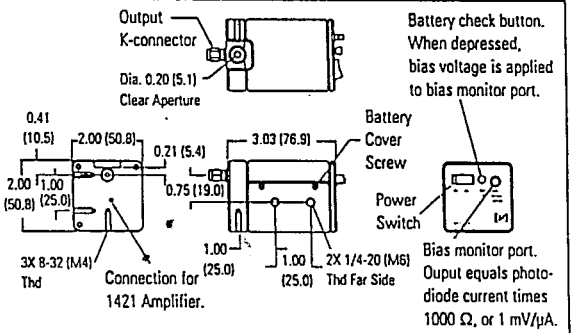

Case Style 5: This case style offers windowed input for direct illumination of the detector. Detector depth from window 0.21". Available with metric mounting holes; add (M) to the model number when ordering.

2.3 PERFORMANCE SPECIFICATIONS

Model	123-1319-010	123-1319-025	123-1319-40
Laser Gain Medium		Nd:YAG	
Wavelength		1319 nm	
CW Power Output	>10mW	>25mW	>40mW
Power Stability			
Amplitude Modulation		≤0.1% rms	
Relative Intensity Noise (RIN @ >10MHz)		-165 dB/Hz	
Long-term Power Stability		< ±5%	
Frequency Stability			
Linewidth		<5 kHz/msec	
Jitter		<75 kHz/sec	
Drift (constant temperature)		<50 MHz/hour	
Drift (due to temperature change)		<200 MHz/°C	
Broad Frequency Tuning			
Total Frequency Scanning Range		>30 GHz	
Continuous Tuning Range		>15 GHz	
Frequency Scanning Rate		>1 GHz/sec	
Fast Frequency Tuning Option (-F)			
Piezoelectric Tuning Coefficient		>1 MHz/Volt	
Response Bandwidth		≈100 kHz	
Guaranteed Tuning Range		±15 MHz	
Polarization (for PM fiber option only)		>25 dB	
Utility Requirements			
Voltage and [Current]		+5V [2.0 amp], +12V [0.1 amp], -12V [0.1 amp]	
Frequency		DC	
Total Power Consumption		8 W	
Environmental Requirements:			
Operating Temperature Range		10°C to 35°C	
Relative Humidity (non-condensing)		10% to 90%	
Storage Temperature Range		-10°C to 45°C	
Weight		1.1 kg (2.5 lb)	
Warm-up Time		15 minutes	